The Big Gun's Guide to Low-Band Propagation

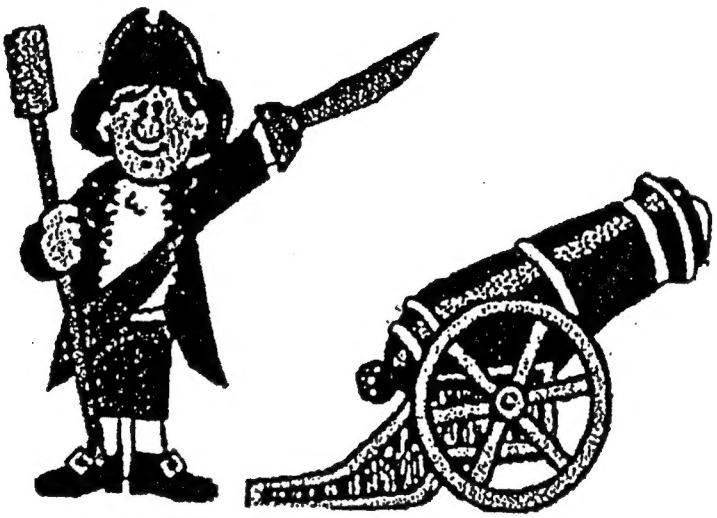

by Robert R. Brown, NM7M

The Big Gun's Guide to

Low-Band Propagation

by

Robert R. Brown, NM7M

April 2002

Frontpiece:
Thanks to 'Colonel' Lee Dawes, W7AFY
Fidalgo Island Artillery Company

Preface

In writing this book, I've tried to lay out what we know about the important things that happen in the ionosphere, between your antenna and that of the DX station you're pursuing, when you operate on the low-bands. And I must admit there are many things we don't know. In that regard, I also have to say that ignorance is not bliss; it is frustrating for both of us.

There seems to be a general consensus that DXing on the lower bands represents the last great challenge in Amateur Radio. But in many respects, it is "topsy turvy", being best at solar minimum while HF DXing is best at solar maximum. So the physics of the lower end of the radio spectrum here on earth is quite different than that at the high end; the low end is more demanding when it comes to the simplest DX accomplishments that can be realized so easily at the high end of the spectrum.

That is not to say that we can't do better. But as I see it, it is a matter of interest - spending a little more time thinking about what goes on and maybe even neglecting DXing from time to time. And it may not be all that hard as it appears that what we really lack is an understanding how the atmosphere affects DXing.

I say that as there is a "mob scene" scenario in effect which is really not fully understood nor appreciated. That scenario has to do with the fact that all the ionization we rely on for low-band propagation is really surrounded by strangers, neutral atoms and molecules, more than a million to one, and they are colliding at a tremendous rate. As a result, the ionization has to be carried along by the neutrals in their motions, just like in a mob scene.

So look at the sky and the clouds as they skud by; that sort of thing has to be happening to ionization at higher levels, where low-band signals fly. But if you still think the ionosphere we rely on is at rest and always parallel to the earth, I have a W2 friend who has a bridge for sale and he'd like to talk to you.

To be serious again, I'd like to raise the understanding of how low-band works and this book is aimed in that direction. But first, I have to review how propagation works, as you know it, and then march on to more complicated matters. So bear with me in the first pages of the book; I'll get to the point soon enough.

Anacortes, WA
April 2002

Acknowledgments

On the HF bands, I am deeply indebted to Sheldon Shallon, W6EL, for years of enjoyable QSOs on 20 meter SSB, discussing propagation and other matters. And I am indebted to my friend, Carl Luetzelschwab, K9LA, for all his help and kindly assuming my journalistic responsibilities.

And I wish to thank my Canadian friends for all they have done for me and Amateur Radio: Bob Eldridge, VE7BS, who first introduced me to the joys of Top Band; Cary Oler for a versatile propagation aid, PropLab Pro; Peter Oldfield for his superb program, DXAID; finally, Nick Hall-Patch, VE7DXR, and Bob Kavanagh, VE3OSZ, for their marvelous experimental work on dawn enhancements.

Others who have helped me in my work and this study include Drs. David S. Evans and Harold Leinbach of the Space Environment Center in Boulder and Professor T. J. Rosenberg of the University of Maryland. And I would be remiss if I didn't thank the members of the DXpeditions who provided low-band logs for my study - Bob Schmieder, KK6EK, Warren Hill, K7WX, Joerg Puchstein, DL8WPX and Garry Shapiro, NI6T. And a special thanks to Mike Bazley, VK6HD, and Steve Ireland, VK6VZ, for sharing 20 years of 160 meter logs.

Finally, my late wife, Mary Lou, NM7N SK, patiently suffered my enthusiasm for propagation studies and I am deeply saddened that she is no longer with me to share the joy of finishing this book.

Contents

Introduction -

In a way, the front cover for this book is symbolic of what I am writing about - the theory behind the advances of technology. To be more specific, "civilization" has progressed on two fronts - the methods of War and Communications. Thus, on one hand, our progress has involved slow advances from using huge slingshots to hurl stones at fortresses to the use of laser-guided projectiles on targets from moving tanks, and, on the other hand, rapid advances from spark transmitters on ULF to the use of HF and UHF to contact satellites in orbit.

While the atmosphere is the same for hurling stones and firing GPS-guided missiles, I'm sure the physics of "exterior ballistics" is different, depending on the speed, shape and mass of the projectiles. The same is true in the realm of RF - it is the same ionosphere but the physics depends on the radio frequency in relation to the inherent properties of the ionosphere - its plasma, collision and electron gyro-frequencies.

At present, I know there are many who are devoted to earlier days, riflemen who load and fire muskets of Colonial and Civil War vintages as well as cannoneers who shoot from artillery pieces like on the front cover. But they do that more for "appearances" than "effects", not loading shot in their muskets or cannons.

Amateur Radio is the same way, with low-band operators who ply their hobby in the range of earlier days, "200 meters and down". But while they use more modern equipment, they "fire for effect" in the ionosphere, hoping for DX way beyond their own horizons, even long-path more than half-way around the world.

For the riflemen in Colonial and Civil War dress, there is no need to worry about exterior ballistics - at most, they fire wadding, not bullets. Not so for the Amateur Radio operator; the physics of the ionosphere is of importance, really determining success or failure in the pursuit of DX, unless heed is paid to its meaning. While advances in hardware have helped to a great extent, low-band DXing is certainly no easy task.

Now one can ask why do things get so tough the lower bands? There is a legion of reasons - continental drift or demography, the politics of the Third-World and emerging nations, the effects of solar cycles, El Nino and other weather effects, and industrial growth - but the real reason comes down to one word - physics. The physics of propagation is ultimately responsible for all the challenges that face Big Guns on the low-bands and it is not all that forgiving, as you will see.

So this book, "The Big Gun's Guide to Low-Band Propagation", will deal with the physics of signals in an ionosphere that's in the dark hemisphere of the earth, immersed in the earth's magnetic field, and bombarded by the solar wind. Now that's quite a contrast to the high HF ionosphere that Little Pistols thrive on, largely controlled by EUV changes with solar cycles.

Not to take anything away from Little Pistols but the HF propagation they deal with is simple when compared with what Big Guns face on a daily basis on the lower bands. For one thing, the HF bands thrive on ionization at high altitudes and DX fortunes rise and fall with sunspot cycles. Not so on low-bands; there, propagation is at lower altitudes and there is more than enough ionization overhead for propagation on those bands, even at solar minimum. In point of fact, propagation is better on the low-bands when the sunspot count is the lowest, times of solar minimum.

And for HF signals, absorption and noise are not a serious problem while on the low-bands, they are often the entire problem. Finally, when it comes to propagation predictions, the HF bands are far simpler as they are under the influence of one strong, steady source of ionization, the sun high in the sky, while low- band operations are conducted in the hours of darkness when the day's ionization is slipping away, by recombination. To a large part, sunspot counts govern HF propagation predictions while the low-bands have no such ready parameter to rely on. As a result, the low-band operator faces far greater challenges.

It is fair to say that most Big Guns succeed admirably, but not because they "know it all"; they don't. Instead, they know enough, from their past experience and intuition, and are very determined in their efforts. The purpose of this book is to broaden and complete their knowledge so they can look back and understand all the obstacles they overcame in the pursuit of DX.

The Ionosphere -

1 - Fundamentals -

Even "newebies" on the HF bands know that the atmosphere is lightly ionized by solar photons in the UV range. But they cannot quickly come up with numbers or details on how the ionization is distributed. That's a lot harder but they have heard about the various regions or layers of the ionosphere: D-, E- and F. Beyond that, a "newbie" would know that the density of ionization in those regions varies from day to night, with the seasons, even with solar cycles. That being the case, **Figure 1** wouldn't come as a surprise.

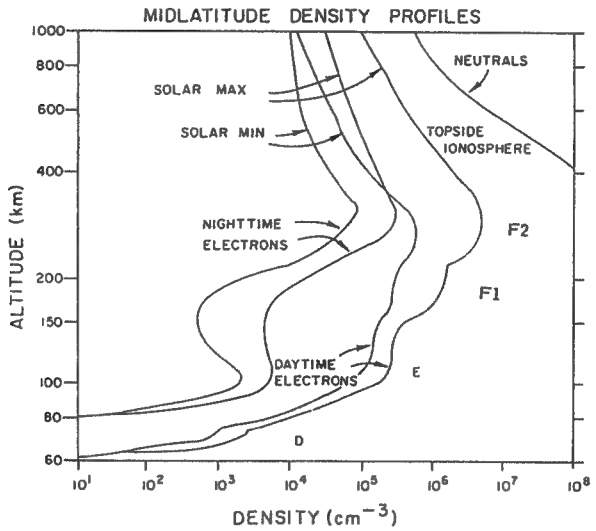

Figure 1 - Ionization profiles for ionospheric layers

That figure is for a mid-latitude location, perhaps something like Boulder, CO, and shows altitude and solar cycle variations of ionization in the various regions. But we have to go back to the beginning now and speak to the degree of ionization mentioned earlier. For that we need to give some features of the neutral atmosphere to compare with the ionosphere to gain our perspective, so look at mass and number densities of neutrals and ionization in relevant altitude ranges of the atmosphere and ionosphere:

Atmosphere (daytime)		Number (per cc)	Mass (gm/cc)
D-Layer	70-90 km	1E16-1E14	2E-08
E-Layer	95-140 km	1E12-1E11	2E-11 4E-12
F1-Layer	140-200 km	1E10-1E09	4E-12 3E-13
F2-Layer	200-400 km	1E09-1E08	3E-13 4E-15

That table shows how tenuous the atmosphere is at those heights

compared to standard sea level values: 2.8E+19 particles/cc and 1.293E-03 gm/cc. And the table below shows how lightly the atmosphere is ionized, with less than one ion pair (positive ion and electron) per million neutral atoms and molecules.

Ionosphere and Solar Cycles -

		Night		Day	
		Min/cc	Max/cc	Min/cc	Max/cc
D-Layer	70-90 km	10-100		100-1000	
E-Layer	95-140 km	1E03	6E03	1E05	2E05
F1-Layer	140-200 km	1E04	2E04	5E05	2E06
F2-Layer	200-400 km	1E05	3E05	6E05	6E06

But for completeness, we should include the basic composition of the atmosphere: Nitrogen 78.1%, Oxygen 20.9%, Argon 0.9%, Carbon dioxide 0.03%, Neon 0.002%, Helium 0.0005% and Water, variable, all at sea level. As will be seen later, those abundances will vary at altitudes above about 100 km but they represent the basic material from which the ionosphere is made by solar photons.

Having looked at **Figure 1** and the numbers in the two tables, the "newbie" might be a bit overwhelmed, trying to digest those magnitudes as well as when and where they would apply. But sooner or later, the static aspect of those numbers would give way to an obvious realization that the quantities involved also change with time: so winds blow, stirring up the local atmosphere, and also large-scale shifts of the atmosphere occur with the changes in global weather systems, and the composition of the atmosphere can be altered, witness the ozone pollution that is discussed so often. So there is a lot more to the atmosphere and ionosphere than meets the eye with just those elementary aspects.

And most obvious of all, from everyday experience, there is a variation in atmospheric temperature at ground level and intuition suggests that extends upward. So our "newbie" has to be shown how atmospheric temperature varies, from ground up to where signals are propagated. In that regard, experience shows the temperature rises, beginning with the troposphere that starts at ground level and goes to 12 km, then the stratosphere to 47 km, the mesosphere (which includes the lower D-region) to 85 km above, and into the higher temperatures of the thermosphere (which includes the top of the D-region as well as the E- and F-regions). That is shown in Figure 2, which also demonstrates that solar cycle variations occur at high altitudes, above what we think of as the ionosphere. That matter probably is beyond the experience but not the intuition of our "newbie".

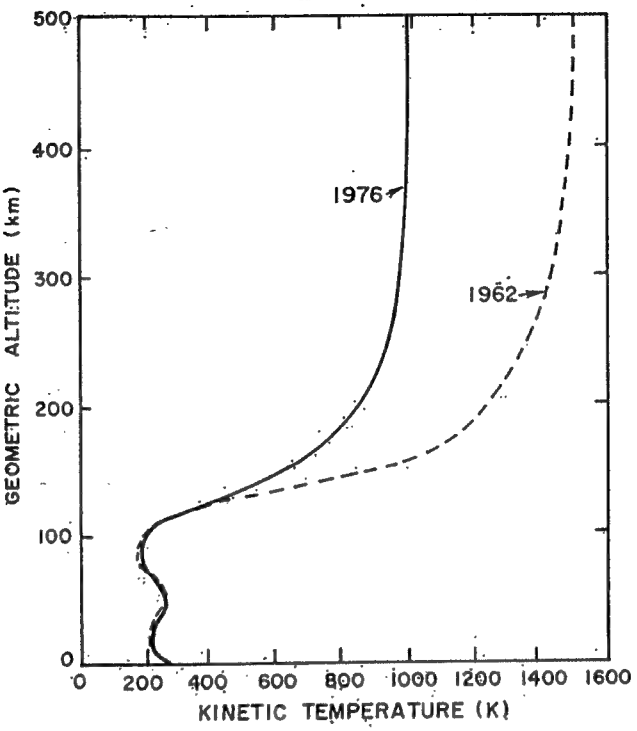

Figure 2 - Atmospheric temperature variation for low and high levels of solar activity.

That figure shows the temperatures of upper atmosphere and ionosphere as fairly insensitive to solar cycle variations of energy input from the sun. True, the thermodynamics of the atmosphere is determined by the radiant energy input from the sun but that is relatively steady, the Solar Constant (the radiation per unit area hitting the earth, 1,380 W/sq.mtr.), varying only a small fraction of a percent in the course of time.

In contrast to the visible part of the solar spectrum, our "newbie" knows from experience that the short-wavelength part of the sun's emissions, in the EUV and X-rays from active regions, is highly variable. The same is true of the long-wavelength part, radio emissions in the wavelength range from 10 cm (used in the daily reports on solar activity) to 10 meters (heard on HF bands during solar flares). Those variations are interesting but the basic properties of both the atmosphere and ionosphere, from physics and chemistry, are still determined by temperatures, of the neutral constituents Tn, positive ions Ti and electrons Te.

Below 100 km, those temperatures are essentially equal due to the high density of neutral constituents compared to ions and electrons and that neutrals are having collisions at a very high

rate in every direction, starting at 1E09 Hz at sea level. Our "newbie" probably probably wouldn't recognize the equipartition of energy at work but it brings us to a point which is extremely important as far as propagation is concerned - collisions and signal absorption.

2 - Collisions -

With something like 3E19 particles per cubic centimeter at the surface of the earth, its not too hard to understand that each atom or molecule occupies a volume less than 3.7E-07 cm across. In fact, a good figure for the size of an air molecule is an order of magnitude smaller, 3.6E-08 cm. But those particles make up a gas and are in constant, chaotic motion from colliding with each other. All the particles in the gas move with speeds that have the same average energy, about 450 meters/sec for N_2 and O_2. At that speed and the size given above, it is a simple matter to work out the mean distance or free path between collisions, an average of 8E-06 cm, and the average number of collisions, 5.5E+09/sec.

That was for neutral-neutral collisions and numbers like 6 those decrease as we go up into the atmosphere. But the number of neutrals overwhelm the positive ions and electrons by about a million-to-one, and, obviously, collide with them. So even though ions are out-numbered, ion-neutral collisions are very important, particularly since motions derived from the winds in the upper atmosphere can carry ions along with them, drastically altering the distribution of ionization, since electrons follow along due to electrostatic attraction to the positive ions.

Electrons are outnumbered too and collide with both positive ions and neuterals but the electron-neutral collision rate is the higher of the two, just because neutrals are present in greater abundance than positive ions. Of course, there is another reason why electron-neutral collisions are important - electromagnetic waves going through a region can drive electron motions to even greater speeds, greater energies; when those electrons collide with any neutral particles, the collisions are inelastic to some degree and energy picked up from the waves is transferred to the neutral particles. That energy heats the atmosphere ever so slightly and results in loss of wave intensity, signal absorption.

Re-radiation -

When it comes to propagation, our "newbie" doesn't ordinarily think about it but knows down deep that signals start as electrons on antenna wires are driven by currents from the transmitter at the operating frequency. Then electrons radiate electromagnetic

wavelets which combine to give a larger wave surface going out through the ionosphere. And the electric fields in the outgoing waves make ionospheric electrons in free space oscillate and re-radiate just like the electrons back on the antenna. But the positive ions in the ionosphere do not contribute to the outgoing wave as they are too massive to be accelerated to the rate needed for re-radiation.

Those waves, perhaps initially cylindrical from the antenna geometry, go over to plane waves at many wavelengths from the antenna, and the electric and magnetic fields across the wave surface are all in phase at a particular instant, as in **Figure 3:**

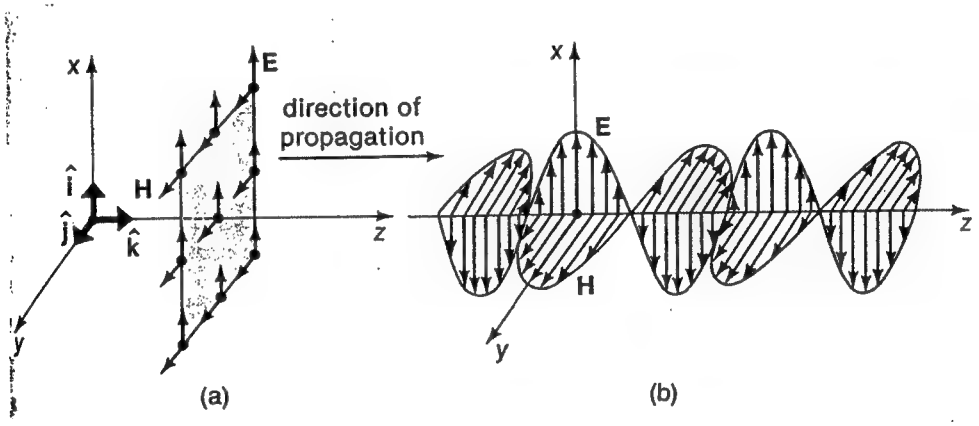

Figure 3 - (a) E- and H-vectors on a plane wavefront and (b) along a wave train at a given instant.

By all electrons re-radiating in phase, more wave surface is generated and advances at close to the speed of light, 3E08 m/sec. The plane wave surfaces are assumed to extend for many wavelengths across the wavefront and have been moving for many RF periods of wave oscillation. That is a way of saying that a mathematically ideal situation is being considered.

Now if the wave is going upward in an ionosphere where the electron density increases with height, as in **Figure 1**, the upper portions of the wavefront will be in regions of greater electron density than the lower portions. But the speed of travel of plane wavefronts in the ionosphere depends on electron density. Under those circumstances, the wave front from re-radiation by electrons in the more dense regions, at higher altitudes, will move faster than the wavefront from less dense portions, at lower altitudes.

That means the effect of a wavefront going into a region of

increasing electron density is to tip the wavefront forward and downward, more toward the earth. As is readily seen, that is true whether the wavefront is going up or down in the ionosphere and is the basic process of refraction, or bending, of wave paths in the ionosphere. Putting it succinctly, waves are refracted AWAY from regions of higher ionization and that applies in the vertical direction, where electron density in the ionosphere increases with height, or the horizontal direction, away from regions of greater ionization on the day-side of the terminator, separating sunlight and darkness. And if a wave is moving upward in the ionosphere, we can represent its path more conveniently by a directed line or ray that is perpendicular to the wave surface and points in the direction the wavefront is advancing in the ionosphere, as in **Figure 4:**

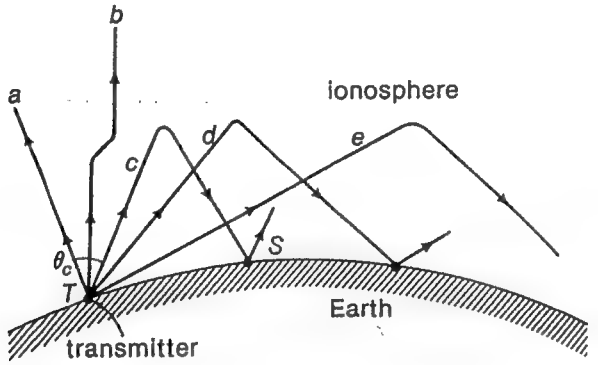

Figure 4 - A ray diagram for HF waves penetrating the ionosphere while MF waves are refracted back to earth on hops.

That figure brings up another matter, re-radiation or signal reflection from ground or other surfaces. That follows from the fact that any surface has some conducting properties and those electrons will be excited to re-radiate electromagnetic waves, just as in the ionosphere. As a result, there will be reflected waves leaving the surface as well as waves going into the surface.

The intensity of the reflected and transmitted waves depend on the properties, both conducting and dielectric, of the surface but the nature of the reflection varies, from diffuse to specular or mirror-like, depending on the roughness of the surface. Thus, diffuse reflection occurs when waves are incident on a rough surface and are scattered in many directions. And specular or mirror reflections occur off of smooth surfaces. As a practical matter, both types of reflections can take place on the oceans, covering almost 80% of the earth's surface, depending on how rough

the seas happen to be and the wavelength of the incident waves.

Those remarks deal with dense surfaces, either solid or liquid. Given that about 80% of the earth is covered by oceans, it is obvious that ocean reflections and scattering play an important role in propagation. But what about the atmosphere and ionosphere, they cover the entire earth above ground level and could perhaps contribute to scattered signals. That idea came to the fore during the Cold War when global communications became an urgent matter, particularly across the Arctic, where radio propagation is very unreliable due to magnetic and auroral disturbances.

That being the case, communications were carried out using scattering by plasma irregularities in the D-region due to natural turbulence in the ionosphere and their effects on the electron distribution at those altitudes. The method, scattering RF energy in all directions, was very inefficient because of the low signal strengths that resulted but because of the height of the D-region, it did put signals where they could not reach reliably by refraction in the ionosphere. The signal strength problem was simply overcome by the use of high power.

In Amateur Radio settings, power is limited by law but nevertheless, in the HF range, sideways ground scatter is well-known as a means of overcoming MUF failure on a path. Propagation on the HF bands can cover great distances due to low absorption rates but ground scatter is still possible for low-band signals; it will just not be as effective at large distances because of the greater absorption.

Ionospheric scatter and reflections are possible as well but the efficiency is even lower, limiting signals to short distances from the scattering region. But rapid echos on CW and multi-pathing on low-band RTTY are testimony to the reality of the effects.

This concludes a quick review of the fundamentals of low-band propagation, dealing first with the distribution of ionization, neutral constituents and the composition of what lies above us. Then there was the matter of collisions, between neutrals and positive ions as well as electrons. Also, the equality of their energies and temperatures was pointed out. Finally, the important matter of re-radiation of electromagnetic waves that results in the advancement of wavefronts in the ionosphere and on reflection from terrestrial surfaces.

Those are fundamental: now on to propagation in more detail.

Propagation -

Attenuation -

Our "newbie" knows about spatial attenuation of signals, how they weaken with distance according to the inverse-square law. But the world we all DX in is large, to say the least, and using the inverse-square law for intensity ratios with distances like 10,000 km or so will get us into handling BIG numbers. That is to be avoided at all costs and smaller numbers are used instead, from logarithms of the intensity ratios. So let's proceed, looking at how spatial attenuation takes its toll, in logarithmic terms, on our signals.

Now it is no mystery that if a kilowatt transmitter radiated by means of the mythical isotropic radiator in free space, signal intensity at 1 km from the transmitter would be 7.96E-5 W/sq.mtr. That signal intensity is in units of power per unit area but in propagation, signal intensities are expressed more often in terms of electric field strengths, the value of E in Volts/meter for waves that would have the same intensities. If one does the math, the E-field at 1 km from a 1 kW transmitter is 0.173 V/m or using a smaller unit, 1 microvolt/meter, one gets 173,000 uV/m.

Now large numerical factors are awkward to carry around and deal with so signal strengths and reductions from all causes, not just spatial attenuation, are expressed in decibels, a simple logarithmic way of comparing intensity ratios. By that token, if we used 1 uV/m as a standard intensity, the comparison at 1 km gives

Numerical Ratio = (173,000 uV/m)/(1 uVm) = 173,000

or

Ratio(in dB) = 20*log(Numerical Ratio) = 104.6 dB

Thus, at 1 km from a kW transmitter, the signal strength would be 104.6 dB greater than the standard unit of intensity. Then, going on, at a distance of 1,000 km, the signal is 1,000,000 times lower or 0.173 uV/m. So using the inverse-square law and comparing the signal intensities at those two distances, we have numerically

Ratio = (1 kW/(1 km)^2)/(1 kW/(1,000 km)^2) = 1,000,000

or in logarithmic terms:

Ratio(in dB) = 10*log(Numerical Ratio) = 10*6 = 60 dB

With that, the signals at 1,000 km are 104.6 + 60 or 164.6 dB above the standard signal, 1 uV/m, or 60 dB lower than at 1 km.

It should be pointed out that all this discussion had nothing to do with the operating band or wavelength of the transmitter. So in terms of the intensity standard, the signal strength above 1 uV/m at a distance R (large compared to 1 km) would be

$$SIG(\text{in dB}) = 104.6 + 10*\log(P) - 20*\log(R)$$

where P is the transmitter power in kW and R the distance in km. To that expression, one must make a correction for the fact the transmitter is really in a half-space, not free space; so with a perfect ground that reflects all downgoing signals back into the upper hemisphere, doubling the intensity, some 3 dB must be added.

At this point, the matter becomes frequency-dependent, with ionospheric losses and antenna gains entering into the discussion. Ionospheric losses are worked out from frequency-dependent aspects of collisions by ionospheric electrons with neutrals. But antenna gains pose more difficult problems because low-band antennas often involve compromises, for lack of space, and current distributions are not well-known or understood. That makes the use of antenna programs rather difficult. Ground losses from surface reflections should be added to the calculation too but they are simpler, more affected by wave polarization and surface properties than directly by frequency. That being the case, let's deal with that matter first.

Surface Reflections-

On the HF bands, ground losses are not much of a problem - wavelengths are short, antennas are relatively high, low radiation angles result and surface reflections are comparitively efficient. On low-bands, however, it is a different story - wavelengths are much longer, antennas are quite low, higher radiation angles are the result, with greater concerns about signal losses from surface reflections.

That concern is even greater than just from antenna heights as low-band signals penetrate less than HF signals into the ionosphere for a given radiation angle. That means shorter hops for low-band signals, more hops to cover a given distance and greater total loss from ground reflections.

To see what is involved, use is made of the formulas (Terman, 1945) derived for electromagnetic waves reflected off surfaces with both bound and free electrons. Those properties are given by dielectric constants and conductivities and representative values for typical surfaces encountered in DXing are given below:

Surface	Sigma	Epsilon
Ice Cap	0.0001	2.0
Sea Water	5.0	80.0
Ground	0.001	4.0

where Sigma is the conductivity in mhos/meter and Epsilon is the dielectric constant, a quantity without units.

As indicated above, antenna considerations play a greater part on low-bands, with a large fraction of short, vertical antennas in use but not without antennas with some horizontal structure, such as inverted-Vees, Marconi or L-antennas. Thus, on the low-bands, more attention is paid to reflections from both vertical and horizontal polarizations and less to reflections by unpolarized signals, as on the HF bands.

But ground surfaces encountered on paths are important even though sea water is a good reflector and covers almost 80% of the earth. To see that, consider a path from here in the Northwest to Egypt, in **Figure 5:**

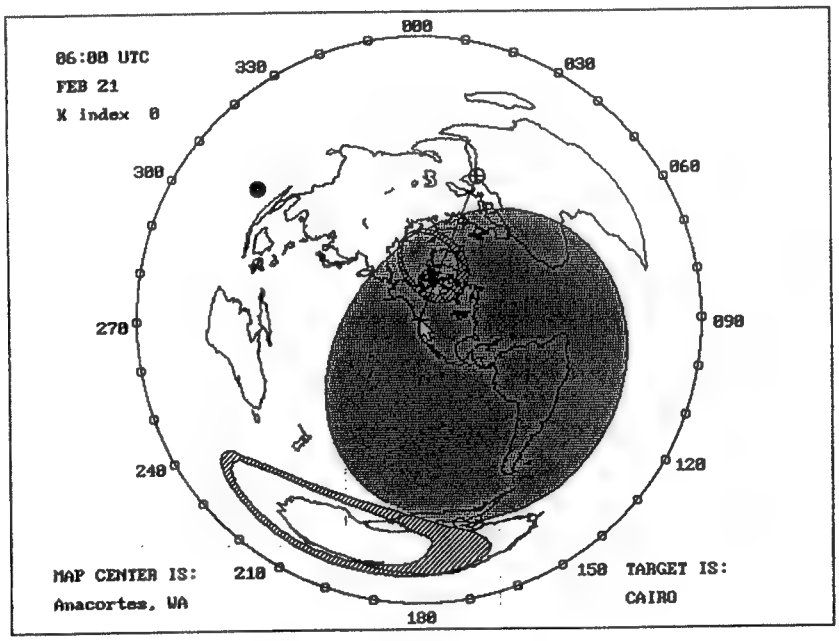

Figure 5 - Azimuthal Equidistant Map from the Northwest to Cairo.

That path goes across ground until it reaches the polar ice cap in northern Canada, then across the ice cap until it crosses the North Sea to reach Norway and ground again until reaching Egypt. Sea water makes up only a small portion of the path and less efficient

reflecting surfaces, ground and ice, are involved in a major way.

Consider **Figures 6 and 7,** showing the signal loss per reflection for horizontal and vertical polarizations on 1.8 MHz.

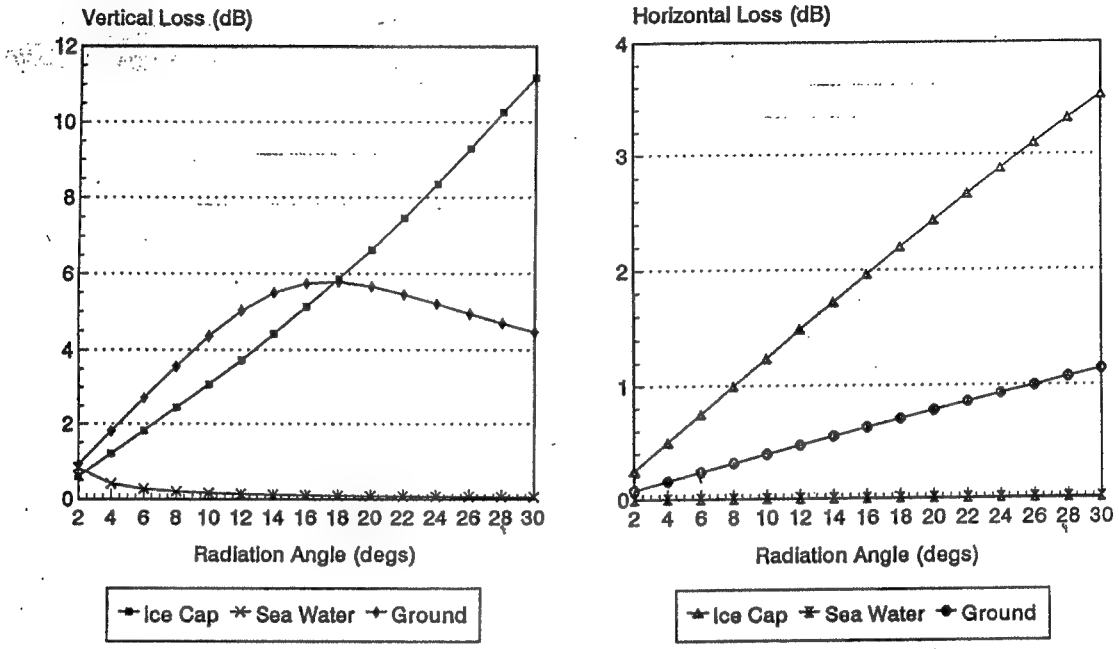

Figures 6 and 7 - Losses for vertically and horizontally polarized signals on 1.8 MHz.

Those shows very low loss per reflection from seawater, less than 1 dB for about 20% of the path. But for the remaining part, ground and ice cap, it is a different story - 3 to 6 dB for typical angles, 10-20 degrees, with vertical polarization and 1-2 dB for horizontal polarization.

It should be noted that the vertical loss for ice cap reflections goes through a maximum of 12.2 dB at 36 degrees, as compared to a maximum of 5.8 dB for ground reflections at 18 degrees. For horizontal polarization, losses just increase with angle.

It

It should be noted that surfaces are considered to be smooth and parallel to the earth's surface. In the absence of roughness and diffuse reflections, the angle of reflection is the same as the angle of incidence. Beyond that, for a given surface, reflection loss for horizontal polarization rises continuously in contrast to vertical polarization which goes through a maximum, as noted above.

The two polarizations reach a common loss for a radiation angle of 90 degrees (normal incidence), 6.8 dB for ice cap and 2.3 for ground.

At this point, one can start to look at propagation with some of the tools in hand, spatial attenuation and reflection losses. Spatial attenuation is independent of frequency so it can be written down at once, using typical DX distances as in **Figure 8:**

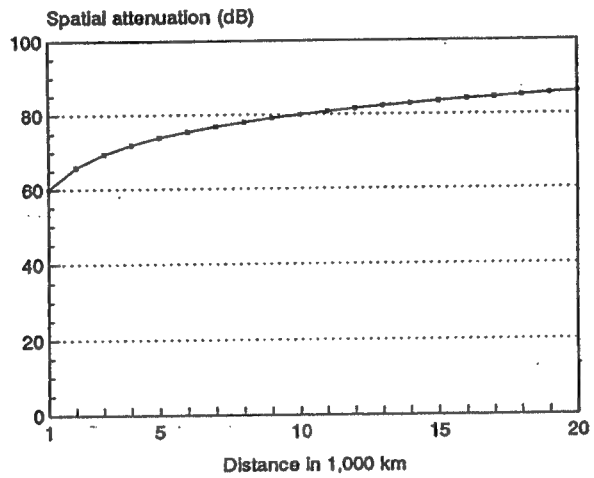

Figure 8 - Loss by spatial attenuation.

With the length of a path given, the next thing is to break it down into ground surfaces and then estimate that loss. To illustrate the method, consider a 15,000 km path on 1.8 MHz that is one-third ground, one-third ice cap and one-third sea water.

Assuming 1,250 km/hop and a radiation angle of about 15 degs for vertical polarization, there are 12 ground reflections to consider with about 5 dB loss per reflection on 8 of them. The losses for sea water reflections are negilgible, making a total reflection loss of about 40 dB and 124 dB when added to spatial attenuation. That's not much signal left to rise over the noise at the receiving end and ionospheric losses have not even been considered yet.

Before leaving the subject of surface reflections, it should be noted that loss of signal intenity is an important aspect of the propagation but not the only effect; the amplitude and phase of the reflected waves are shifted relative to the incoming wave and that varies with the reflecting surface, affecting the wave polarization on reflection.

Waves from a transmitting antenna have a geometry relative to the earth which depends on the antenna construction and direction of propagation. Thus, vertical antennas give rise to vertically polarized waves in all directions. On surface reflection, the wave amplitude will vary with surface and radiation angle as shown in **Figure 9.** And antennas with horizontal portions will give rise to horizontally polarized waves in some directions. On surface reflection reflection, the wave amplitude will vary in a different manner, as shown in **Figure 10.**

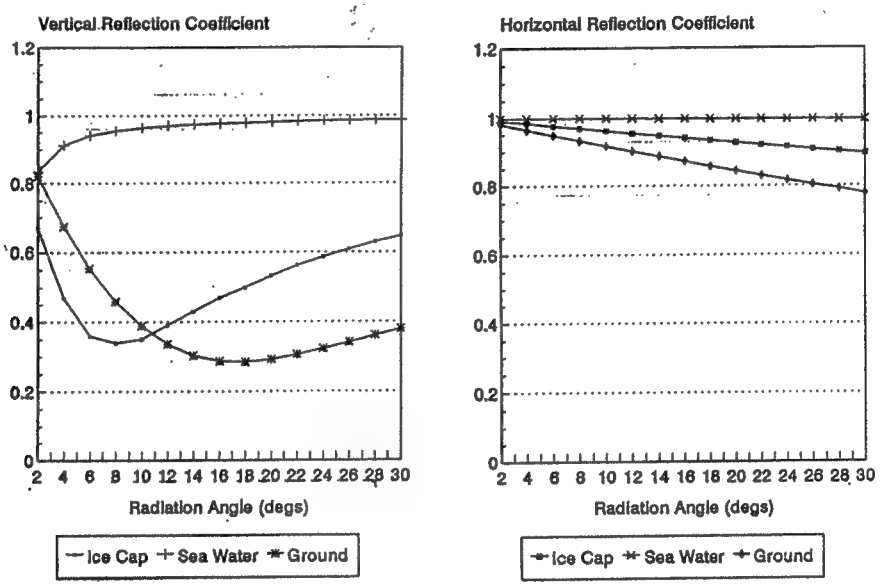

Figures 9 and 10 - Reflection coefficients for vertically and horizontally polarized signals on 1.8 MHz.

The amplitude minima for reflection of vertically polarized waves off of ice cap and ground surfaces are at the so-called "pseudo-Brewster angles" of the substances and coincide with the peak in reflection loss at the same radiation angles. Those features are well-known in optics as well as in the HF range and are discussed in the ARRL Antenna Book.

Of interest to low-band operation are the phase shifts of waves on reflection. Those are of no concern with vertical antennas as the polarization of the emissions is relatively pure. But antennas with significant horizontal structures will have mixed polarizations for waves away from their principal direction of radiation. Thus, both horizontal and vertical waves off the ends of a dipole (Krauss, 1988) or inverted-Vee could be reflected off a surface, with changes in amplitude, as shown in earlier **Figures 9 and 10.** In addition, the reflected waves will also undergo phase shifts, lagging the incident polarized waves as in **Figures 11 and 12.** The reflected wave will change then from having

two linearly polarized components in phase and take on an elliptically polarized aspect by ionospheric reflection alone, without any interaction with the earth's magnetic field. Such polarizations will be seen later to be important for low-band signals transmitted across the geomagnetic field.

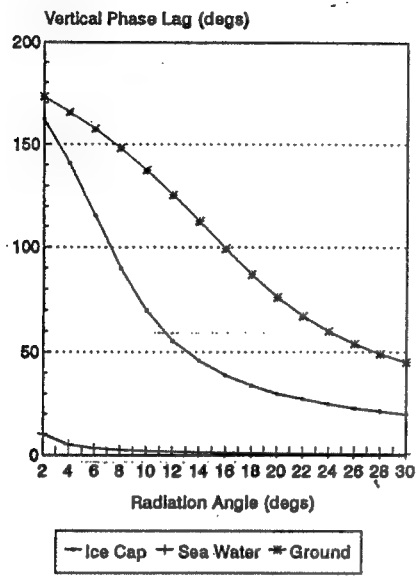

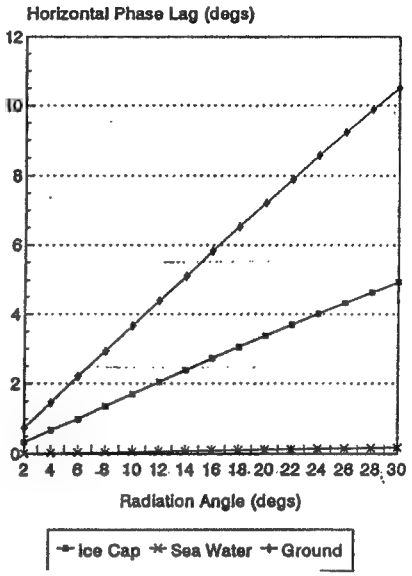

Figures 11 and 12 - Reflection phase lags for vertically and horizontally polarized signals on 1.8 MHz.

Turning now to other ionospheric losses, greater attention has to be paid to the mechanics of electron-neutral collisions, the distribution of neutral constituents and how losses vary with altitude when driven by RF waves.

Collision Loss -

As noted earlier, electrons driven by the passage RF waves undergo inelastic collisions with the constituents which surround them, thus transferring energy from the waves to the atmosphere. Since electron collisions are mainly with neutral constituents, the rate of collision loss depends on the altitude distribution of the neutrals as well as electrons and their motions. In general, the greatest collision loss takes place around the D-region and in that region, well-mixed compared to higher altitudes, electron energies are in equilibrium with those of neutral particles and only change slightly with solar activity, as shown earlier in **Figure 2**, or day-night transitions.

The collision rate at 100 km altitude is almost 0.1 MHz, varying about 25% between day and night but only a few percent

between solar maximum and minimuim (Rosenberg, 2000). The altitude variation decreases with the distribution of neutrals, as shown in **Figure 13**, for solar minimum, reaching about 100 MHz for the collision frequency at 50 km.

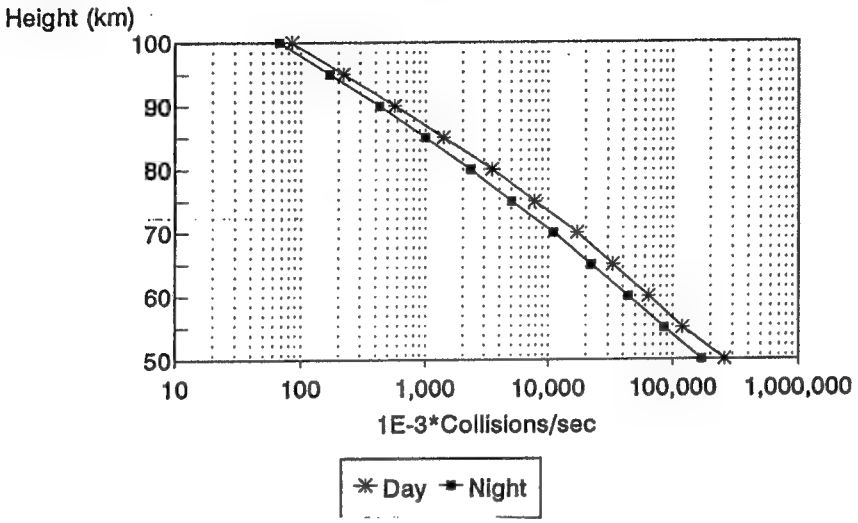

Figure 13 - Electron-neutral collision frequency profile for solar minimum.

The transfer of wave energy to the atmosphere takes place in two steps, when the electron gains energy from the wave and when it undergoes a collision with a neutral particle. Deep in the ionosphere where the electron-neutral collision frequency is high, RF waves have little opportunity to impart energy to the electrons before a collision takes place. So the absorption of wave energy is very small at low altitudes. On the other hand, at higher altitudes, an ionospheric electron undergoes many RF oscillations between collisions and thus re-radiates energy from the incident wave before finally making a collision, transferring energy to the atmosphere.

In between those extremes, the absorption of energy from the passing wave goes through a maximum, when the collision frequency of electrons and the wave frequency are comparable. To work out the details, a mechanical model is needed for particle motions, driven by RF waves but damped by collisions with neutrals. The simplest model, neglecting forces on electrons due to the presence of the geomagnetic field, shows the absorption loss varies as the inverse-square of the operating frequency, in the high HF range.

That result, when applied to the harmonically-related amateur

bands, shows the relative absorption frequency on a per-electron basis varies with band and altitude as shown in **Figure 14.** For practical use, the altitude distribution of electrons would be needed and the absorption rate in dB/km summed along the path. But the fact remains, absorption on 1.8 MHz would be very high and the only way around the problem is to operate at night, when the electron density is at its lowest.

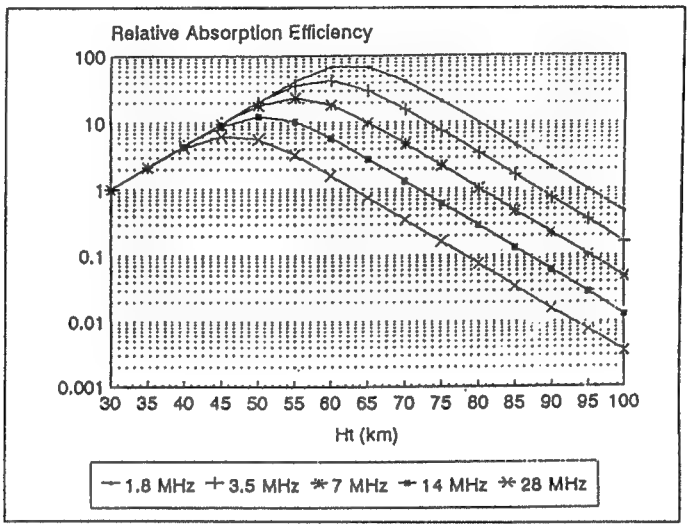

Figure 14 - Relative absorption efficiency per electron

Given the above, ionospheric absorption would be relatively high on 1.8 MHz with just a few electrons/cc around 65 km in the lower D-region but would require an electron density higher by about two orders of magnitude for a comparable effect around 100 km in the E-region. In geophysical terms, both extremes are possible, the first during bombardment of the ionosphere by solar protons after a solar flare and the second during auroral activity. Analytically, when the details are worked out for the HF case, ignoring effects from the geomagnetic field, the absorption loss (dB/km) on a wave path is given by

$$k = 4.6E\text{-}02 * N*Fcoll/((2*pi*Frf)^2 + Fcoll^2)$$

(Davies, 1989) and the total ionospheric absorption on a path is obtained by summing the effects along its entirety. The model for collision frequency in **Figure 14** would be used along with an electron density profile for the distribution along the path.

Clearly, absorption depends on the number of electrons that are encountered along a path. That is illustrated nicely by the

absorption observations made during solar proton events. Thus, 30 MHz receivers are used to monitor the galactic radio noise that penetrates the high-latitude ionosphere, as in **Figure 4**. That noise is absorbed when solar protons create ionization in the polar cap and the absorption in dB is found by comparing the record for a disturbed day with that of a quiet day.

The effect of a solar proton event on signals headed for the polar cap can be found by increasing the absorption observed on a vertical path by a factor of 3-4 for oblique propagation on a slant path, as in **Figure 4**, and another factor of 2 for signals ascending and descending through the ionization. Finally, the 20 absorption could be adjusted for the band in use by using the inverse-frequency approximation given above. For a typical 1 dB solar proton event, that gives 12 dB absorption or 2 S-units per hop in the polar cap on 14 MHz. On 1.8 MHz. the effect would be absolutely devastating!

Ionization -

At this point, some discussion of ionizing processes in the ionosphere is in order. The nature and composition of the target atmosphere has already been mentioned but more details are called for, the energy available in parts of the solar spectrum and the energy required to ionize the neutrals in the atmosphere.

In the solar spectrum, the energetic part lies in wavelengths below the violet end of the visible spectrum at 3000 Angstroms. Only a fraction of a percent of the energy in sun's radiation is down there but that's where ionization by the EUV part begins and continues with shorter wavelengths in the X-ray range. The EUV part of the solar spectrum ionizes neutrals in the F-region, "soft" X-rays below 1000 Angstroms can penetrate and ionize in the E-region while "hard" X-rays below 10 Angstroms can ionize down in the D-region. Any ionization below 60 km is due to energetic particles, cosmic rays either from the galaxy or the sun.

The full solar spectrum is incident on the top of the atmosphere and ionization of a constituent depends on penetration through the absorbing layers overhead and the energy required. In that regard, threshold energies and wavelengths needed to ionize the more important atmosphere constituents are listed below:

Species	Energy (eV)	Wavelength (A)
N_2	15.58	796
O_2	12.08	1026
NO	9.25	1340
O	13.61	911

Using the concept of photons, it is easy to show that a handy, easily-remembered approximation for the ionizing wavelength is given by

Wavelength (Angstroms) = 12340/Energy (eV)

The principal positive ions below 100 km get their start from ions of permanent constituents, diatomic nitrogen and oxygen molecular ions. The electrons released by photo-ionization may have little energy or there may be some excess energy and further ionizations can be produced by electron collisions. In any event, any electron motion gives rise to a force from the presence of the earth's magnetic field and instead of going off on a ballistic trajectory, the electron is "contained" locally. Thus, the geomagnetic field organizes the electron distribution, as seen from global ionospheric maps.

As an example, **Figure 15** shows a foF2 critical frequency map, a global map of the highest frequencies returned by the ionosphere in sounding experiments. The map is for 0600 UTC in March 1979, when the sun is on the equator at 90E longitude, and a smoothed sunspot count of 137, close to the maximum of Cycle 21.

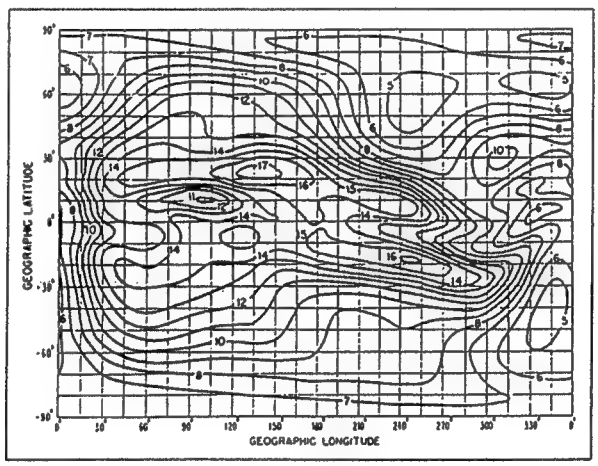

Figure 15 - Global map for foF2 at 0600 UTC in March 1979.

Examination of the map shows it is not symmetrical with respect to the equator, as it would be at the equinox if F-region ionization were controlled by the sun's radiation. Rather, the ionization is seen to be more symmetrical with the dip equator of the magnetic field which goes across the equator into the Southern Hemisphere.

Now consider the global foF2 for 0600 for March 1976 in Figure 16:

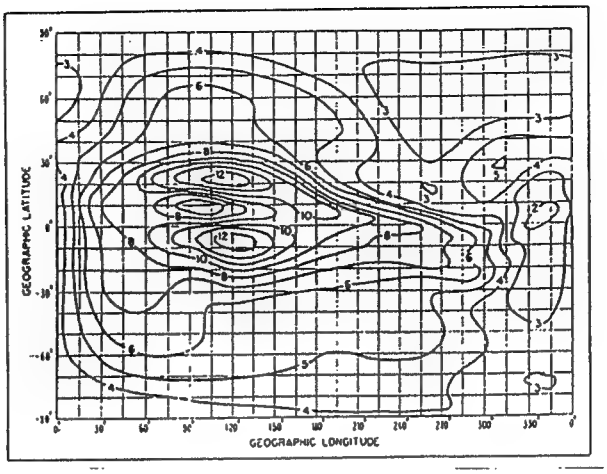

Figure 16 - Global map for foF2 at 0600 UTC in March 1976.

The same features are there, showing geomagnetic control of the ionosphere. But there is one feature of particular interest to low-band operators - none of the foF2 values anywhere in the world at solar minimum was less than 2 MHz. That means several things, depending on how you look at it: 160 meter signals were trapped in the ionosphere, unable to go out through the F-region into the galaxy overhead nor could 1.8 MHz galactic radio noise enter to be heard here on earth.

Put another way, that means MUFs are of no interest on 1.8 MHz as more than enough ionization is present overhead to support oblique propagation at typical angles, say up to 30 degrees above the horizon. That being the case, the ionospheric processes that really control 1.8 MHz propagation are absorption and noise.

Before getting to those new topics, let's finish what we started, ionization. First, let's consider what happens to the positive ions and electrons after the ionization process takes place. As a first guess, one would think the charged particles would collide with their neighbors, positive ions perhaps then recombining with electrons to form neutral structures again. That happens but instead of molecules, the ions dissociate into atoms:

$$N_2^+ + e^- \text{-----> } N + N$$
$$O_2^+ + e^- \text{-----> } O + O$$

instead of reforming by radiative processes:

$$N_2^+ + e^- \text{-----> } N_2 + \text{photon}$$
$$O_2^+ + e^- \text{-----> } O_2 + \text{photon}$$

and the molecules, N_2 and O_2, are reformed later from the atoms by going through a different chemistry cycle. Actually N_2^+ is not a major ion in the D-region below 100 km, in spite of being a major neutral constituent. The N_2^+ ion is formed by solar radiation but a more rapid process takes over, an ion-atom interchange

$$N_2^+ + O \text{ -----> } NO^+ + N$$

with an oxygen atom that was available from the dissociation of O2+. The NO^+ ion joins the O_2^+ ion as one of the major sources of electron recombination or loss in the lower ionosphere. There are many neutral chemistry and ion-chemistry processes going on throughout the ionosphere. For example, no mention has been made yet of the oxygen cycle which results in ozone being formed when oxygen molecules are dissociated by solar photons:

$$O_2 + \text{photon} \text{-----> } O + O \text{ (daytime)}$$
$$O + O_2 + N_2 \text{ -----> } O_3 + N_2 \text{ (day or night)}$$
$$O_3 + O \text{-----> } O_2 + O_2 \text{ (day or night)}$$
$$O_3 + \text{photon} \text{-----> } O_2 + O \text{ (dayutime)}$$

In the absence of sunlight to dissociate ozone and end atomic oxygen creation at night, the ozone in the atmosphere lingers til dawn when the cycle starts all over again. But ozone remaining at dawn is important to low-band operators, as may be seen from another process in the ionosphere, the formation of negative ions at night.

It turns out that ionospheric electrons not only recombine with the relatively small number of positive ions available but they may also become attached to some of the far more numerous neutral molecules, forming negative ions. That is of interest to low-band propagation as the negative ions are more massive than electrons and do not take part in the signal absorption process, energy transfer from RF waves to the atmosphere.

Electrons bound in negative ions are photo-detached at dawn but the energy required for the process is greater that found in photons in the visible part of the solar spectrum. The energy needed is not as great as the 10 eV or so for the photo-ionization processes for N_2 and O_2 but that part of the spectrum below 3000A is blocked by the ozone layer present before dawn. So detachment of electrons from negative ions does not start at sunrise but later, when the sun has risen above the ozone layer. That gives low-band DXers a break, as it were, by delaying the onset of heavy absorption (Brown, 1999) which ends DXing in the morning. The creation of negative ions is not a global benefit for low-band DXers as it varies, according to the presence of minor constituents

in the atmosphere (Brown, 1999) such as carbon dioxide, nitric oxide and water vapor. Positive ions go through a complicated ion chemistry in the lower ionosphere but they are of little importance when it comes to low-band propagation and will not be considered further.

The discussion of ionization up to this point has dealt with the lower ionosphere, below 100 km. When ray-tracing of low-band signals is considered, it will be seen that while absorption is determined at lower altitudes, propagation to great distances is controlled by the distribution of ionization at higher altitudes, above 100 km.

Around that altitude, there is a dramatic change in the composition and processes in the atmosphere and ionosphere, a transition from a well-mixed atmosphere to one where atoms and molecules are distributed vertically by gravity according to their atomic weights and where the ionization is more affected by the geomagnetic field than atmospheric motions.

So we have to look at the world above the D-region, into the E-region and lower F-region. The higher F-region is left to our friends who still operate on the HF bands.

More on Propagation -

Ray Paths -

Having touched on the fundamentals, it is now the time and place to begin treating the details of low-band propagation. To do so, we start first by using the ideas of refraction in the ionosphere. But instead of using wave fronts, ray paths will be used and the idea that they are bent or refracted downward when the electron density increases with altitude, as in **Figure 1.**

In the "flat earth" approximation, ray paths may be shown as in **Figure 17**, with the left side of the figure showing an example of vertical sounding of the ionosphere and the right side showing oblique propagation under the same ionospheric conditions. The right side shows a virtual reflection height A while the real maximum height of wave penetration is shown at B in the figure.

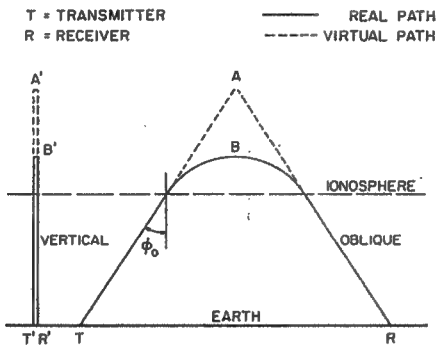

Figure 17 - Signal reflections for vertical (left) and oblique (right) propagation paths.

Looking at **Figure 17** with **Figure 1** in mind, and taking the simple case of day-time conditions at solar maximum, the ray path shows little refraction until it reaches the E-region at 110 km, where the electron density is 2E+05/cc; the signal reaches a peak altitude in the F-region at about 350 km, where the peak electron denasity is about 5E+06/cc. After that, the ray path is refracted downward and reaches the bottom of the ionosphere (and ground) at the same angles as on the ascending leg of the path.

If one went to the records of the ionosondes that probed the ionosphere on that occasion, the critical frequency foE for wave reflection back to earth at vertical incidence was 4.0 MHz at the 100 km level and at 350 km, it would have been 20.1 MHz. But night-time conditions at solar maximum would be different, with lower critical frequencies, 0.7 MHz at the E-region and 6.9 at the F-region peak.

But for low-band DXers, the preferred time is at solar minimum, with even lower night-time critical frequencies, 0.4 MHz for foE and 2.8 for foF2 using the curves for Boulder, CO in

Figure 1, and with less ionosperic absorption. But at oblique incidence on the bottom of the ionosphere, as shown in **Figure 17**, waves of frequency F enter into the ionosphere and are refracted as though they actually had a lower frequency, called the effective vertical frequency (Davies, 1989) or EVF and given by

$$EVF = F * \cos(\phi) \qquad \text{(Eqn. 3)}$$

where ϕ is the angle of incidence with the normal to the bottom of the ionosphere.

In the "flat earth" approximation, the angle of incidence at the bottom of the ionosphere is the same as the zenith angle of the ray at its time of launch. If, instead, we go to a curved earth and replace the zenith angle with the radiation angle relative to the horizon, we can calculate the EVF as a function of launch angle, as shown in **Figure 18:**

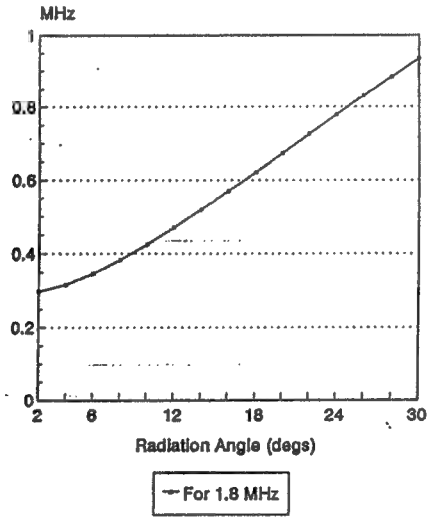

Figure 18 - Effective vertical frequency for 1.8 MHz signals as a function of horizontal radiation angle.

That figure is for 1.8 MHz signals and shows the EVF is 0.4 MHz or higher for radiation angles 10 degrees or more. Using that for paths at night, say from Boulder to London on 1.8 MHz, one can use propagation programs like IONCAP to look at the differences in path structure at angles above and below 10 degrees. Obviously, angles below 10 degrees result in E-hops, five of them below 100 km and

with lossy ground reflections, on the way to London while angles just above 10 degrees result in three F-hops, above 100 km and with less loss from the fewer ground reflections.

Programs like IONCAP use great-circle paths to connect the location of a transmitter to a receiver. The paths are broken down into E- and F-hops using layer heights derived from sounding studies. With a spherical earth and treating ground reflections as mirror-like, the angles of incidence and reflection are taken as equal, relative to a perpendicular to the ground surface, in accordance with Fresnel's Laws in optics. With a range of angles available, the geometry of the path is worked out by the program, the radiation angle chosen for the number of E- and F-hops.

Now the ionospheric layers are considered to be spherically symmetrical although their height above the earth may vary along a path, according to the results of ionospheric sounding. As a result, hop lengths will also vary along a path. In any event, for low-band DXing, it is desirable to have radiation penetrate the E-region and reach the lower F-region before being refracted back to ground.

That means that radiation angles above 10 degrees are the important ones in the radiation pattern of an antenna, especially at solar minimum. On the other hand, high angles above 25-30 degrees are not productive, only resulting in many short F-hops. To illustrate the point, for the case of 1.8 MHz signals heading from Boulder to London at night, consider the path on the Mercator projection in **Figure 19:**

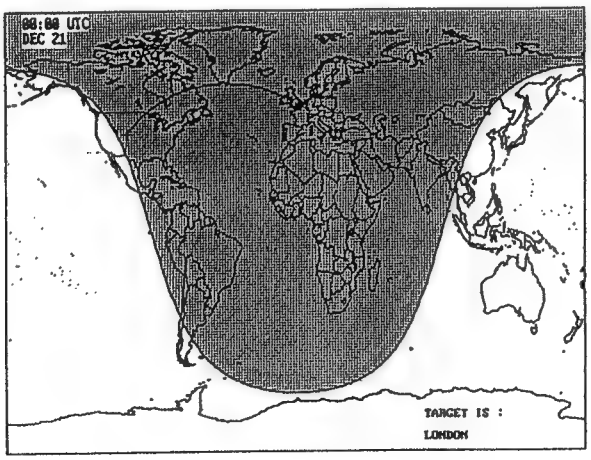

Figure 19 - Post-sunset Mercator path from Boulder to London.

About one-third of the path is over ground, one third over snow and ice and the last third is over the North Sea. For radiation angles of 25-30 degrees, the path involves 8-10 F-hops, instead of 3 F-hops just above 10 degrees. For sea water, the reflection losses are negligible but 5-10 dB/hop over ground and ice for vertical polarization, the polarization of choice for low-band DXers. That is to be compared to 4 dB/hop for three hops at the lower radiation ang7le.

At solar maximum, it was pointed out that the critical frequency foE at night at Boulder was 0.7 MHz; using the curve in **Figure 18** for that EVF, that raises the angular range so that lossy E-hops continue until radiation angles of about 20 degrees are reached. With vertical antennas, that increases reflection loss to about 5 dB/hop for 8-10 hops instead of 4 dB/hop for three hops at the lower level of solar activity.

The discussion above was for the surface reflections; still to be considered is the ionospheric loss for the traversals of the ionization in the D-region, as indicated in **Figure 14.** That is handled in different ways, depending on the propagation program. For example, programs like IONCAP make use of limited data, the critical frequencies and layer heights obtained from ionospheric sounding. The frequencies are obtained from the sounding records, frequency vs time, and the heights from time-of-flight features in the records.

The sounding records that go with **Figure 1** would show that E- and F-region reflections occurred at about 100 km and 300 km, at ionosonde frequencies of 0.7 MHz and 6.9 MHz for night at solar maximum, as discussed above. At radiation angles above 20 degs, 1.8 MHz signals would penetrate the E-region but certainly not go as high as the F-region peak at 300 km. The question then becomes where is the peak, something not given by ionosopnde records.

At this point, appeal must be made to ionospheric propagation theory. That deals not just how waves are returned from critical layers, the plateaus or peaks of electron density seen in **Figure 1** but with propagation through the entire distribution of ionization overhead. But to see the details, a hypothetical experiment must be performed.

So imagine going up into the ionosphere and grabbing a handful of plasma, with positive ions with one hand and electrons with the other hand. If they were pulled apart and then released, they would oscillate back and forth because of the electric force of attraction between them. That frequency of oscillation is called

the plasma frequency, Fp, and depends on the electron density:

$$Fp(MHz) = 9E-6*(N^{0.5}) \qquad \text{(Eqn. 4)}$$

where N is the electron density (number per cubic meter).

Now we consider the 1.8 MHz signals from an antenna at a 24 degs radiation angle; the EVF from **Figure 18** would be 0.8 MHz. Now propagation theory indicates 1.8 MHz signals rise obliquely until reaching an peak altitude where the local plasma frequency Fp is the same as the EVF. Now from Eqn. 4, a plasma frequency of 0.8 MHz corresponds to an electron density of 7.9E+09 per cu. mtr or an altitude just below 200 km in **Figure 1.**

So the simple aspects of the problem, from ionosonde results, are not enough to give answers that would yield a ray diagram, as in **Figure 20:**

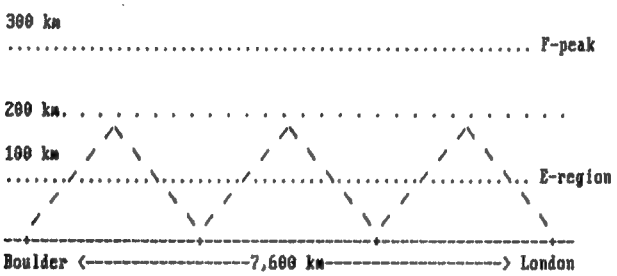

Figure 20 - Reflection path from Boulder to London.

That figure shows a reflection diagram for the ray path but the critical frequencies and reflection heights must be supplemented by information about the electron density profile. While the ray diagram showing reflections is simple and informative, it is not as detailed nor definitive as a ray path based on refraction in the ionosphere as a whole. That brings us to electron density maps and profiles, the product of work with incoherent scatter radars, sensitive to low levels of ionization and electromagnetic theory, based on Maxwell's Equations.

Ionospheric Models -

A good summary of earlier atmospheric and ionospheric models can be found in "The Handbook of Geophysics and Space Environment" published by the U.S. Air Force in 1985. Since that time, newer models have become available, the MSIS model of the atmosphere in

1986 and the Internation Reference Ionospheres (URSI and CCIR) 1990. The URSI and CCIR ionospheric models can be examined in the propagation aid, PropLab Pro (1996). Thus, foF2 global maps based on those models may be explored, as in **Figure 21:**

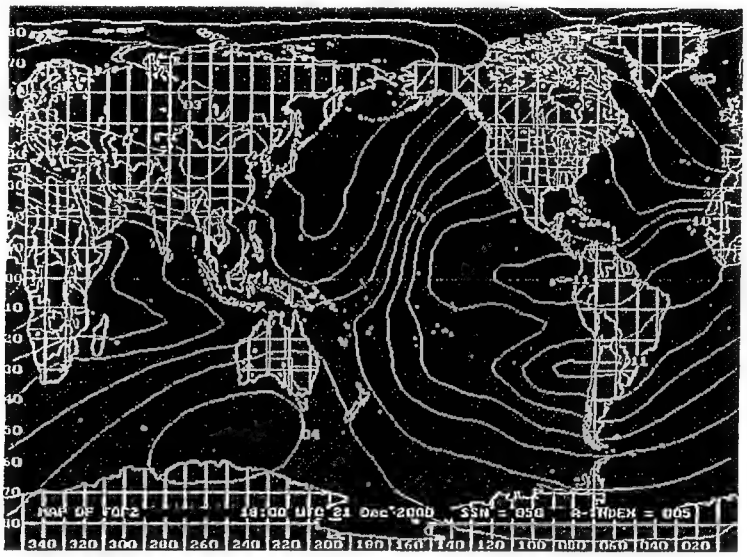

Figure 21 - Global foF2 map for the winter solstice at 1800 UTC.

That map is for 1800 UTC on the winter solstice, with foF2 iso-frequency contours spaced by 1 MHz; the highest contour, 11 MHz, is west of Peru, and lowest, 4 MHz, by Australia.

The Proplab program also gives maps for the height of the peak of the F-region, hmF2, as in **Figure 22:**

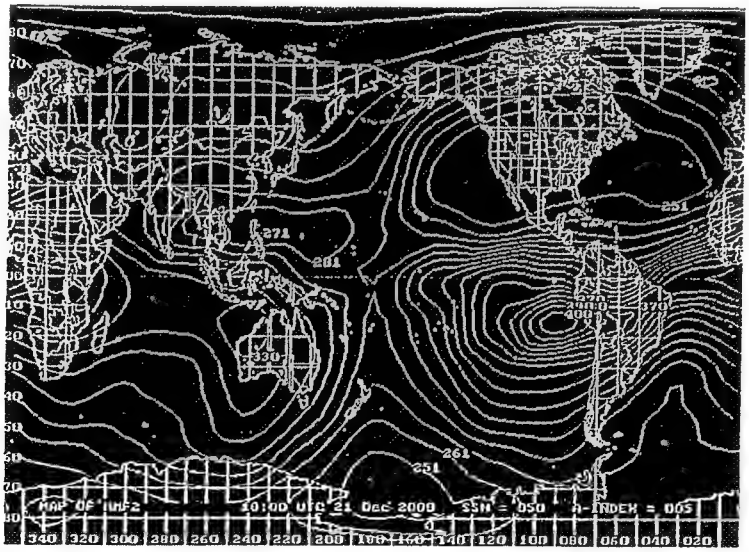

Figure 22 - Global hmF2 map for the winter solstice at 1800 UTC.

That figure shows the highest foF2 peak is 400 km at the sub-solar point off the coast of South America; across the equator, the peak height over North America is no more than 250 km.

That sort of information, along with the foF2 values, would be of value in working out details of MUFs on a HF path. But for low-band operations, MUFs from F-layer considerations are of no interest; signals never get that high in the ionosphere. But having them penetrate the E-region at about 105 km altitude is another matter. So the foE iso-frequency contours in the winter months are of great interest, especially their values in the dark part of the ionosphere.

Winter darkness begins with the fall equinox and reaches its fullest extent in the Northern Hemisphere at the winter solstice, about December 21. That was shown in **Figure 19**, when the path to England was considered just after sunset at Boulder, CO. Another time of interest is just before sunrise, as shown in **Figure 23**. Again, the figure is for the winter solstice but instead of around sunset, when darkness extends to DX in the east, dawn opens up to DX in the west, in the Orient. In that figure, the path is from Boulder to Tokyo, about 1,900 km longer than the path to London in **Figure 19.**

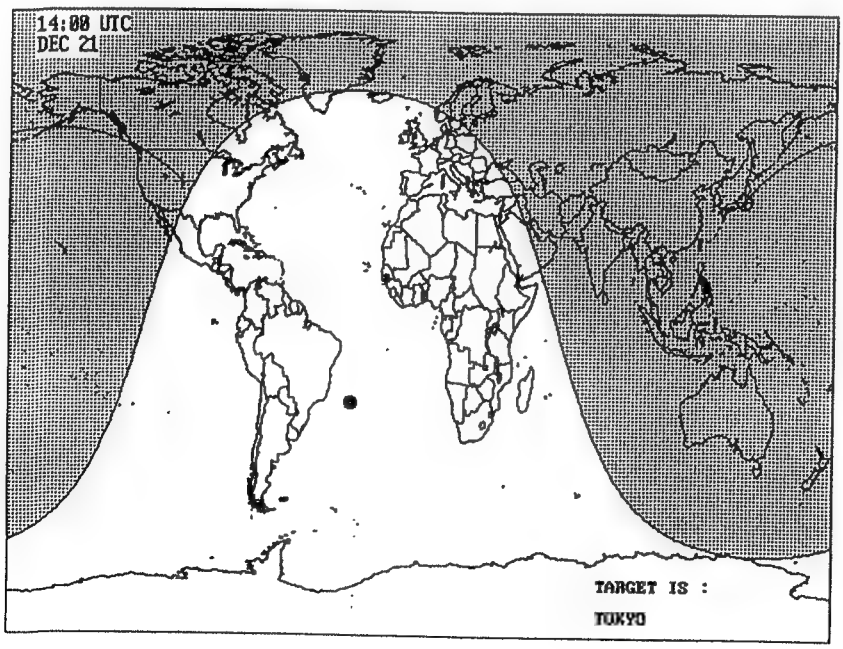

Figure 23 - Pre-sunrise Mercator path from Boulder to Tokyo.

Because of the high rate of ionospheric absorption of low-band signals, particularly on 1.8 MHz, possible paths to the east or west are limited to locations within the dark hemisphere and operations have to be worked out around that limitation, from equinox to equinox. Exceptions do exist, as will be seen, and those prove to be very interesting to low-band DXers. More on that later.

Returning to ionospheric maps, **Figure 24** shows iso-frequency contours for the E-region:

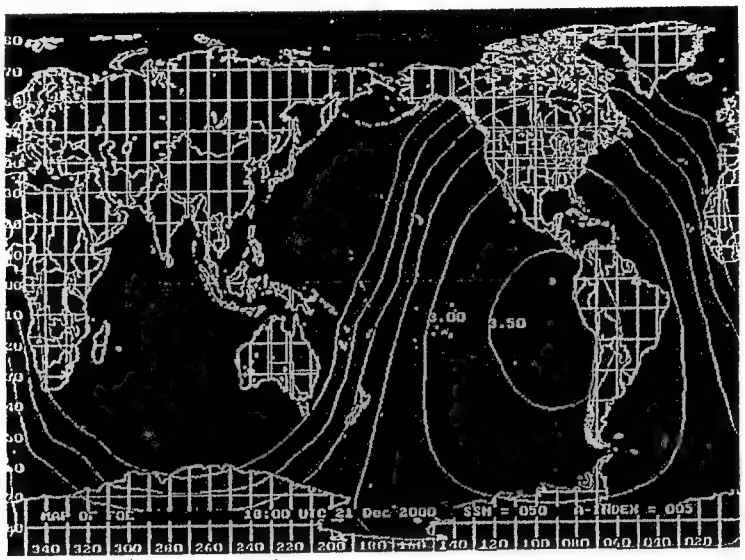

Figure 24 - Global foE map for the winter solstice at 1800 UTC.

Again, this is for the winter solstice at 1800 UTC. The highest foE iso-frequency contour is 3.5 MHz and surrounds the sub-solar point at 23.5 S lat, 90 W long. In both **Figures 21 and 23**, night-time ionization conditions prevail in the left-hand halves of the figures, from 0 long to 180 long. Note the latitude and longitude divisions in those figures are in 10 degree steps, seen at the left and bottom of the maps.

The full description of ionospheric conditions at a given time and place is given by the electron density profile from the F-region peak down to the bottom of the D-region. For the path from Boulder to London, a day-time profile (1800 UTC) at the winter solstice is given in **Figure 25**. That figure shows a slow increase in electron density above the E-region at 100 km, then the F-region peak around 250 km, as was indicated in the height data in **Figure 22**.

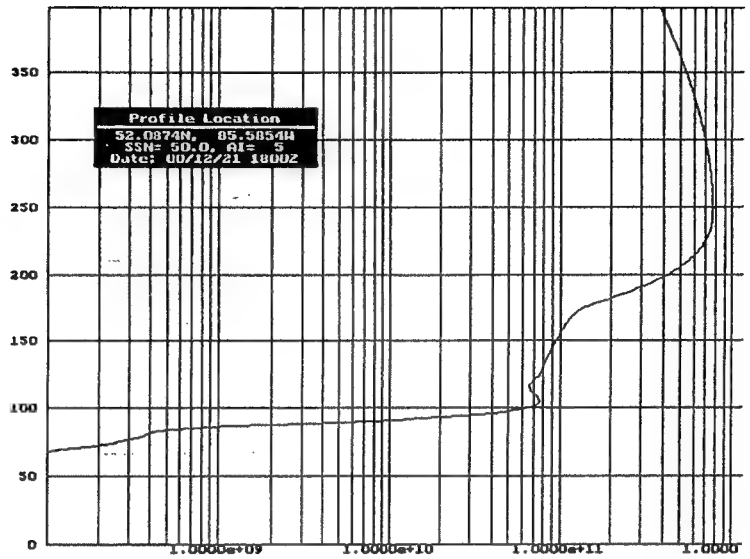

Figure 25 - Day-time electron density profile at 52N, 85W for the winter solstice at 1800 UTC.

At night, when the powerful solar source of ionization goes to zero, the electron density profile is entirely different, as shown in **Figure 26.** Then an electron density valley appears just above the E-region peak, the depth of the valley being about 25% of the nearby peak.

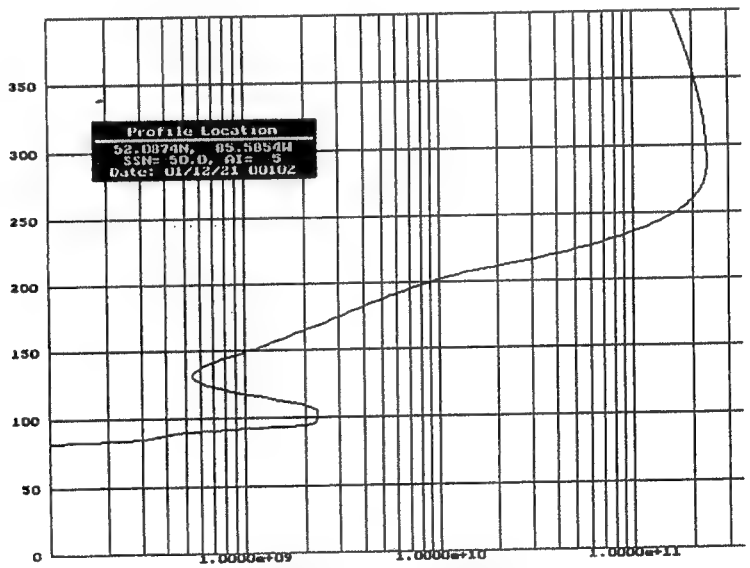

Figure 26 - Night-time electron density profile at 52N, 85W for the winter solstice at 0000 UTC.

In the absence of strong sunlight, ionization in the valley is supported be weak sources of ionization - EUV in starlight, stellar X-rays and solar UV scattered into the dark hemisphere by the

atmosphere, the geocorona. The sources from the galaxy are steady in time but the stronger source, scattered solar photons, will vary with solar activity. So even in the dark, ionospheric absorption will continue, albeit weakly.

Fluctuations in Critical Frequencies -

Beyond that, the critical frequencies obtained from vertical soundings are highly variable, monthly median (50%) values varying by 20-40% during quiet times (Bilitza, 2001) and even more during magnetic storms. That is seen by going to the database in the IONCAP program. But vertical soundings are of less interest to DXers than predictions for oblique paths, say Boulder to London.

For predictions, the "control point" method is used; that involves breaking a path down into hops and using the critical frequencies from soundings at the first and last hops. The question then becomes "what is the lowest frequency returned at the two ends of the path at a given time?" That is obtained from the critical frequencies at the mid-points of the first and last hops by increasing the vertical values by about a factor of 3 to values appropriate for propagation at an angle with the horizon.

Using median (50%) values, the lowest of the two values at a given hour gives the maximum usable frequency or MUF for 15 days of the month. If the other decile values of the sounding records were used, say the 10% and 90% values, the predictions would give the FOT (optimum frequency of transmission) for 90% of the time and the HPF (highest possible frequency) for 10% of the time. Thus, **Figure 27** shows the range of foF2 critical frequencies for the Boulder-London path, as considered before:

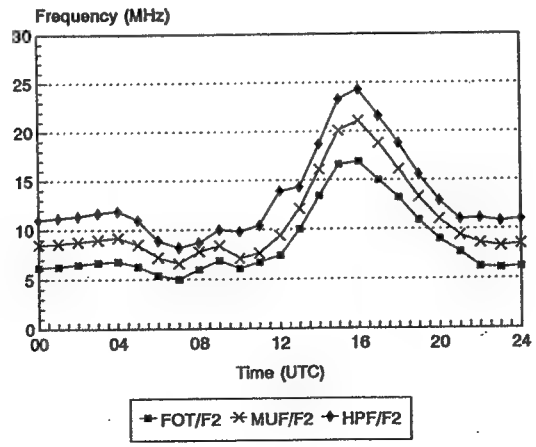

Figure 27 - FOT/F2, MUF/F2 and HPF/F2 for Boulder-London path.

That figure shows the spread in F-region critical frequencies, FOT to HPF, which are responsible for differences in communication, one day to the next on a HF band like 14 MHz. Thus, 14 MHz signals could start to get through around 11 UTC, have a solid communication link from 14 UTC to 18 UTC and fading out by 20 UTC.

For low-band operators, the spread in E-region frequencies are far more important and **Figure 28** shows the situation for the Boulder- London path:

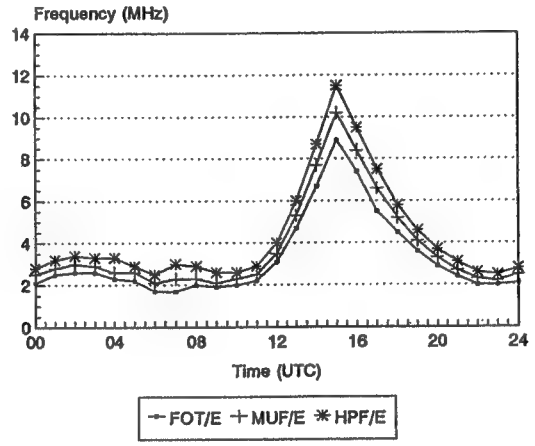

Figure 28 - FOT/E, MUF/E and HPF/E for Boulder-London path.

But the operating frequency is 1.8 MHz so the path appears open for 24 hours a day. That statement deals with the refraction of signals, not their strength. As remarked earlier, there is more than enough ionization overhead to assure 1.8 MHz propagation; signal strength will disappear from absorption when the sun rises on the E-region.

In looking at those two figures, it should be noted that the curves for the E-region variation are more symmetrical in time than those for the F-region. In particular, the curves for the E- region decay faster than those in the F-region, as would be expected from solar control with the sun's zenith angle. The F- region decays slower at sunset because of its lower density, different ionic composition and electron-ion recombination rates in the two regions as well as greater geomagnetic control in the F-region.

For the low-band DXer, statistical fluctuations in critical frequencies can be very important to propagation even though MUFs are of no concern. To see this, a typical spread could be like at 0600 UTC in **Figure 28**, when the FOT, MUF, HPF values are 1.7, 2.1 and 2.5 MHz, or 2.1 MHz +/-20% during the month. For a given radiation angle from an antenna, the EVF in **Figure 18** is fixed in

value. So a 20% variation in the critical frequency at the E-region level could make the difference between a ray path reaching into the lower F-region for a long hop or being shunted back to ground for a lossy E-hop.

An interesting aspect of low-band propagation and E-region critical frequencies has to do with their variations along a path, due to irregularities in the ionosphere of non-solar origin. By and large, those are unpredictable but are known to occur. As a result, a ray path may get into the valley region in **Figure 29** at one point on the path because of an irregularity. But, farther along the path, it may not be able to get out of the valley as its EVF is too low to penetrate the E-region, now with a higher critical frequency than before.

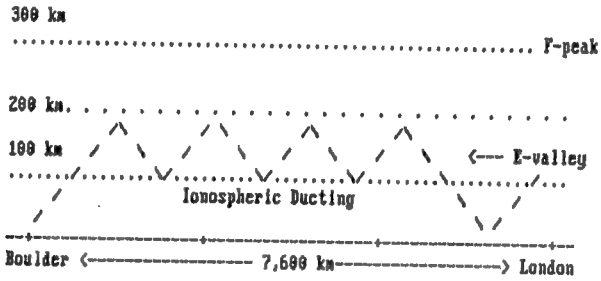

Figure 29 - Ionospheric ducting, Boulder-London path.

In short, the ray is trapped in the valley. That can lead to ionospheric ducting, a mode of propagation which is very efficient as the rays are elevated, going great distances without transits of the D-region and ground reflections, until returning back to ground level by another irregularity.

There is another form of ducting of magneto-ionic origin but that will not be discussed until the effects of the earth's field have been considered. The origin of the two types of ducting are different even though they are found in dawn enhancements of DX signals. But in the ionospheric case, the dawn is at the transmitter while in the magneto-ionic case, it is at the receiver.
Examples of both types will be given later in the discussion.

Ray-Tracing -

With maps of critical frequencies and electron density profiles available, like in **Figures 25 and 26**, the next step is to introduce ray-tracing, to show paths in more realistic terms and detail. For that, it is necessary to Snell's Law for wave refraction in optics and cast it in a form appropriate for electromagnetic waves.

Before using Snell's Law, it is important to understand the implicit limitations of the analytical method. Thus, at the outset it is assumed that the electron density in the ionospheric region under consideration varies smoothly over a space that extends more than a wavelength in all directions. So the method does not apply to small, turbulent regions nor to possible small- scale scattering regions that are rough, uneven and might give rise to diffuse reflection. Those are all propagation modes in their own right but not the gradual, slowly-varying process of refraction covered by Snell's Law and the results of smooth refraction should not be used for those circumstances.

In geometrical optics, Snell's Law deals with the change in direction of a ray as it passes from one medium to another, The media are characterized by indices of refraction, the ratio of the speed of light, c, in a vacumn to that in the material, v:

$$n = c/v \qquad \text{Eqn. 5}$$

So Snell's Law states that

$$n_1 * \sin(\theta_1) = n_2 * \sin(\theta_2) = \text{constant} \qquad \text{Eqn. 6}$$

for the incident and refracted rays going across an interface, where the theta is the angle with the normal to the surface in going from one medium to another, as in **Figure 30:**

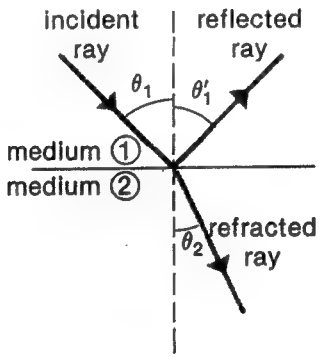

Figure 30 - Incident, reflected and refracted rays at the interface of two media.

That was for a plane surface and is quite simple. For the ionospheric case, where the surfaces are curved and at a height above ground, the geometry is more involved. In that case, the ionosphere may be layered in thin shells and rays traced through by refraction, shell by shell. An even better approach is to go to the methods of calculus and trace the path using numerical

along the path.

In any event, in order to study wave refraction in the ionosphere, an expression will be needed for the index of refraction n of the ionosphere. That requires a model of how the ionosphere is made up, electrons and neutrals, and use of the wave equation of Maxwell. That will not be done here in any detail; rather, it is left as an exercise to those interested in the physics of the matter and who have a good book on electromagnetic theory at the college level. But the method will be discussed, including its limitations.

First, it must be understood there is a difference between wave trains and wave pulses. In electromagnetic theory, wave trains go on forever, steady and without any information to be obtained from them; on the other hand, wave pulses are brief, interrupted wave trains and, by the nature of their formation or grouping, may convey information or intelligence, e.g., dots and dashes. Distinction is made between the speed of the two, wave or group velocity. The same is true of their indices of refraction, wave index and group index.

For the simplest model of the ionosphere, free electrons with a number density which varies with height, as in **Figure 25**, the wave index of refraction at a given height is given by:

$$n = (1 - (F_p/F)^2)^{1/2} \qquad \text{Eqn. 7}$$

where F_p is the plasma frequency at that height, related to the electron density N by Eqn. 4, and F is the operating frequency. That index is less than 1 so the wave speed v is greater than c, the speed of light. That is not a violation of the Special Theory of Relativity as it deals only with an infinite wave train, a mathematical construct and not physical reality. It can be shown that the group speed, that which is involved in transmitting real information, is less than c, as it should be.

The wave index is useful, however, and in geometrical optics, it is used to determine the refractive properties of materials. In ionospheric problems, it gives meaningful results about wave refraction without getting into details as to how wave groups are formed. In that regard, I used the above expression along with a differential form for Snell's Law when I programmed some ray-tracing back in '95. That was to explore the method and get some ray-traces to use in my Little Pistol book. It was largely for the HF range, 14 and 21 MHz, as in **Figures 31 and 32**, and used varying radiation angles from 5 to 90 degrees, in 5 degree steps.

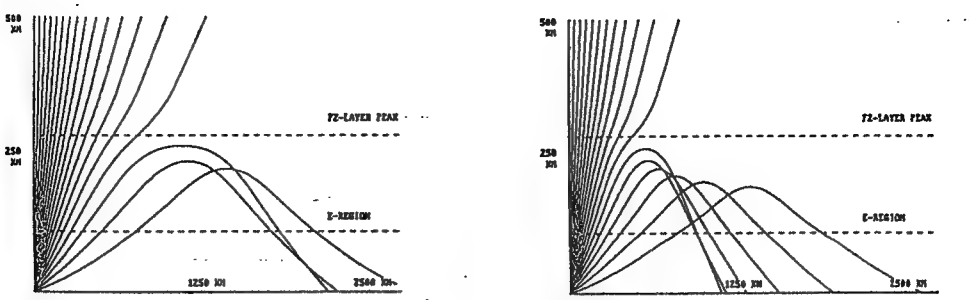

Figures 31 and 32 - Ray-tracings for 14 and 21 MHz signals, with rays going from 5 to 90 degrees in 5 degree steps.

Those figures are for around dawn, when the E-region critical frequency was 2.5 MHz and the F-region critical frequency was 8 MHz. The figures show the familiar skip and focusing found in the HF range as well as give the range for F-hops, 1250-2500 km. Skip results because high angle rays penetrate the F-region instead of being returned to points close to the location of the transmitter. On 160 meters, there is no such skip as all rays are returned from the ionosphere overhead, no matter how high the radiation angle.

Longer hops are possible in the HF range when the radiation angle at launch is such as to have the refracted ray pass close to the bottom of the F2-layer, shown by the 5,000 km hop in **Figure 33**:

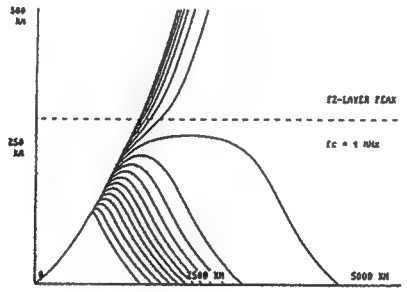

Figure 33 - Ray-tracings for HF signals, with the frequency going from 2 to 20 MHz in 2 MHz steps.

That is called a Pedersen Ray and the figure is for night-time conditions, but being for HF signals, it is different than the ionospheric ducting in **Figure 29**, involving 160 meter signals in the electron density valley above the E-region.

Another example of a longer HF hop is found when a ray just penetrates a layer at an angle ABOVE the Pedersen Ray. Thus, a long E-F hop may result, even several in a row to give signal ducting, without intermediate ground reflections or lossy D-region transits. This is shown in **Figure 34**, below:

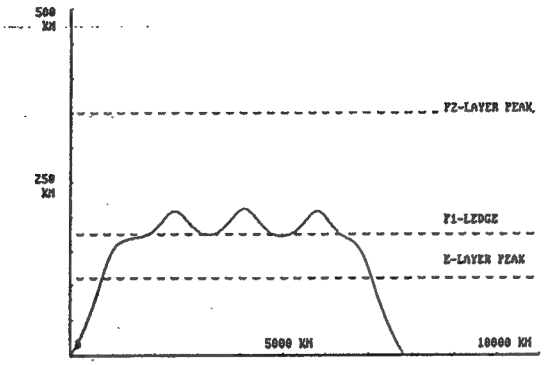

Figure 34 - Another example of ionospheric ducting.

It should be noted that all the ray-tracings shown so far were in two dimensions, in the vertical plane and along the ground projection of the ray. In those cases, the refraction results from the vertical gradient of electron density in the plane of the great-circle path. But that is somewhat unrealistic as other types of gradients exist too, making the ray-tracing matter one in that is in three dimenions. That can be included in calculations if a horizontal gradient is added to the problem, ionization that is greater on one side of the path than the other, with results as in **Figures 35 and 36:**

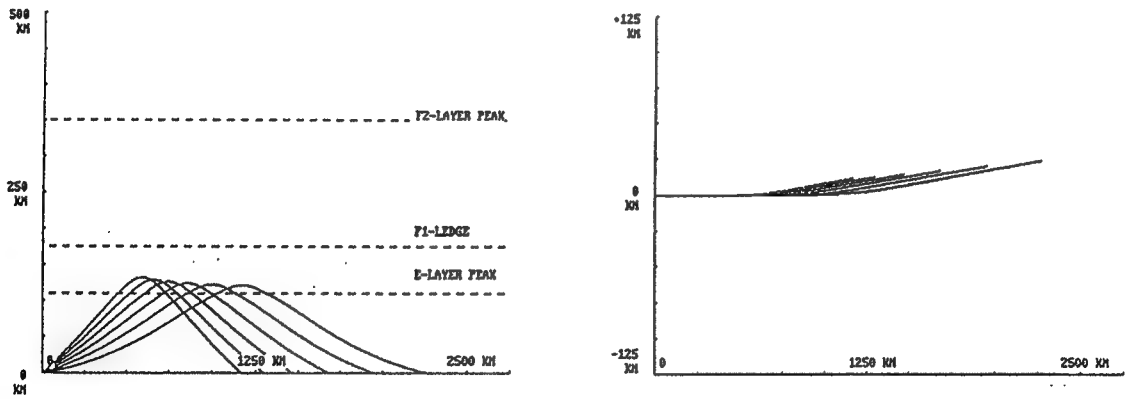

Figure 35 and 36 - Paths of non-great circle propagation projected on the vertical plane and the earth's surface.

The transverse gradient in ionization refracts the ray path away from the region of higher ionization. **Figure 35** shows the ray trace of the non-great circle hops projected onto the vertical plane while **Figure 36** show the projections of the sideways deviations of the non-great circle paths on the earth's surface.

The ray-tracings in **Figures 31-36** are from my personal HF calculations but serve as good models for low-band calculations. The programs were meant to show physical effects and were not for specific paths or dates and times. Those may be obtained from the PropLab program (Oler, 1996) by entering the coordinates for the terminii of the path, date and time as well as a sunspot number. Then the ray-tracing program in PropLab picks out the appropriate ionospheric profiles along the path and does the whole refraction calculation in small steps, finally plotting up the result.

The earlier calculations involved the same method but only used the RF frequency and the plasma frequency or electron density along the path. For that approximation in two dimensions, polar coordinates r and 0 in **Figure 37,** theory shows the change in path direction dθ in a short distance ds due to refraction varies with the vertical gradient dN/dr of the electron density and the inverse-square of the frequency F:

$$d\theta = \text{const} * (-dN/dr)/F^2 * ds \qquad \text{Eqn. 8}$$

For dN/dr>0 in the ionosphere, i.e., electron density N increasing with height r, the ray is refracted downward, dθ<0, whether on ascending or descending legs of the path:

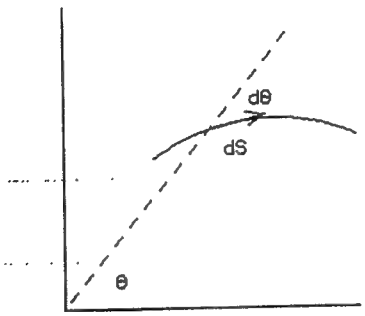

Figure 37 - Illustration of infinitesmal steps in angle and distance along a path.

Beyond that, the inverse-square dependence on the frequency means that refraction changes are larger at lower frequencies. That has particular meaning for horizontal refraction or path skewing due to horizontal gradients in ionization, as found around the sunrise

terminator.

So for the 10 meter band, great-circle paths serve as a good approximation to radio paths as horizontal gradients give rise to only small deviations from their direction. On the other hand, for the 160 meter band, a given gradient would produce deviations in direction which are more than 250 times greater. Thus, the ionization gradients around the sunrise/sunset line give rise to large skewing of paths but out in the vast darkness of night, paths do continue along great-circle directions.

Returning to features of the PropLab program, still in two dimensions, it should be noted that the path deviation d0 radians per km of distance ds in Eqn 8 as well as the rate of absorption dB per km distance ds in Eqn. 1 include the collision frequency, Fcoll, and ray tracing in PropLab shows absorption along a path. Thus, **Figure 38**, is a PropLab ray-tracing for the Boulder-London path on 1.8 MHz and with a 13 degree radiation angle. The figure shows an "X" on the trace, just short of the 6,000 km mark. That indicates the distance at which the 1.8 MHz signal has suffered 100 dB absorption or loss in signal strength.

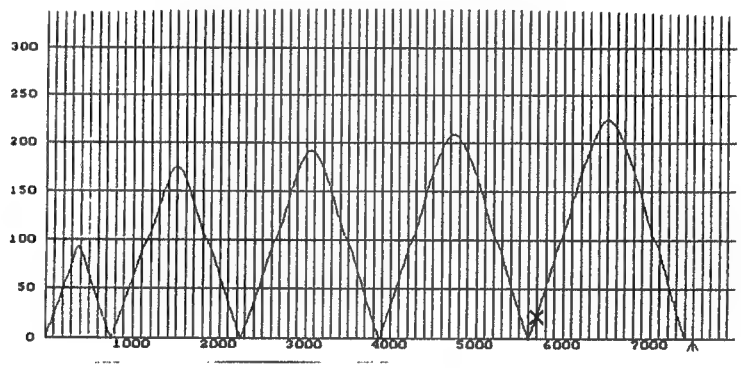

Figure 38 - A PropLab ray-tracing for 1.8 MHz signals for Boulder-London at the winter solstice.

The figure is also interesting for the fact that the electron density profiles chosen by the program for the Boulder-London path yield an E-hop at the outset but all the F-hops are limited in height to about 200 km.

At a lower radiation angle, 6 degrees, the program shows E-hops out to almost 5,000 km and then a long E-F hop from a Pedersen ray incident on the E-region, as in **Figure 39.** That possibility was raised in connection with **Figure 34.** In the present instance, the PropLab program changed electron density profiles along the path and around 0000 UTC the E-layer critical frequency at the end of the path became so low that the radiation angle was close to a Pedersen ray and the long E-F hop resulted.

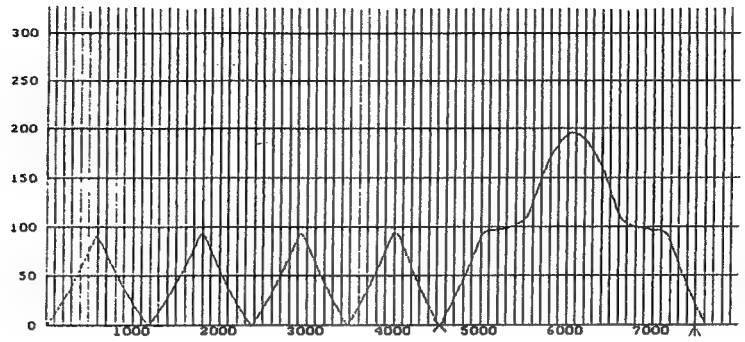

Figure 39 - Low-angle E-hops on 1.8 MHz, followed by a long E-F hop, on the path from Boulder to London.

Other frequencies in the low-part of the spectrum include 3.5 and 7.0 MHz. So we can look at ray-tracings on the path from Boulder to London under the same circumstances, only raising the frequency. Thus, **Figure 40** shows a ray-trace for 3.5 MHz but the radiation angle has been increased to 18 degrees. In contrast to **Figures 38 and 39,** it is seen that 3.5 MHz signals reach higher into the ionosphere, above 200 km to 250 km. But this is a long way from the radiation angles and F-region heights in use at the top of the HF spectrum.

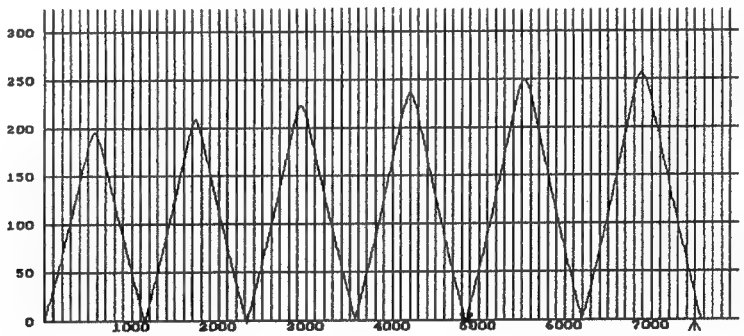

Figure 40 - Ray-trace for 3.5 MHz signals, Boulder to London, at a radiation angle of 18 degrees.

Going to 7.0 MHz and the same radiation angle, **Figure 41** shows that the angle is too steep or the EVF is too high for the ionosphere as the signal escapes, penetrating the F2-region and going off to Infinity, just like in **Figures 31 and 32.**

Of course, an antenna's radiation pattern contains many low angle rays so this does not rule out signals getting from Boulder to London, just a different mode will be involved.

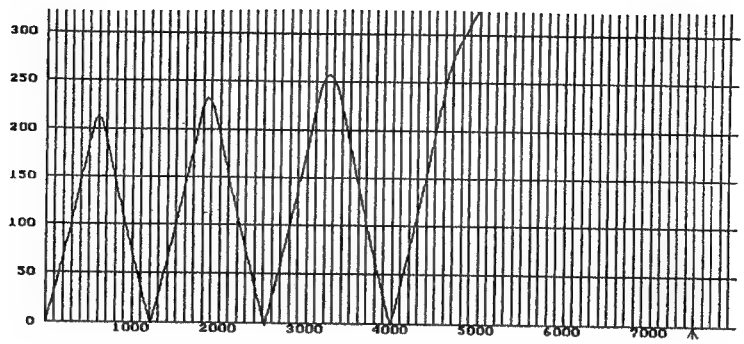

Figure 41 - Ray-trace for 7.0 MHz signals, Boulder to London, at a radiation angle of 18 degrees.

As noted earlier, there is more than enough ionization in the F2-region overhead to support 1.8 MHz propagation and, by and large, those signals are trapped in the ionosphere. Not so for higher frequencies, like the 7 MHz signal in **Figure 42**. But there are other meanings to that statement, e.g., that galactic radio noise on 7 MHz may enter the lower ionosphere at night. That is shown in **Figure 42**, where an "iris" exists, with low-angle 7 MHz signals trapped at night but high-angle signals are free to cross the F-region peak, going either way, to or from the galaxy. 44

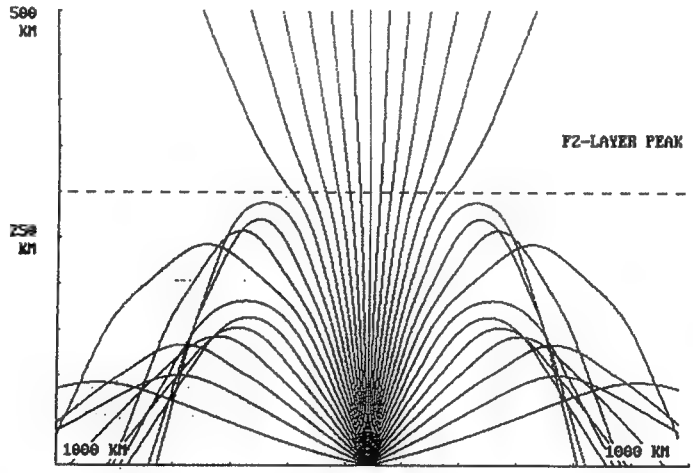

Figure 42 - Ray-tracing for 7.0 MHz with an "iris" of rays penetrating the F-peak, 5-90 degs in 5 deg steps.

The iris closes for 7 MHz signals in the day but is open for higher frequencies and bursts of solar radio noise get through from time to time, with the occurrence of solar flares. Galactic radio noise, say around 30 MHz, does get through the F-region, day or night, but is not a problem like solar noise can be.

But going back to 1.8 MHz, those signals are trapped in the lower ionosphere but the same is true for atmospheric and man-made noise

on that frequency. Noise propagates and is absorbed like any other signal. In any event, atmospheric noise and can be a limiting factor, especially for DXpeditions going to the tropics.

With regard to atmospheric noise, CCIR maps show the noise power on 1 MHz and have to be corrected for frequency by using the spectrum (Davies, 1989) in **Figure 43.** That shows decile values for the noise power and a cut-off in the range 20-30 MHz:

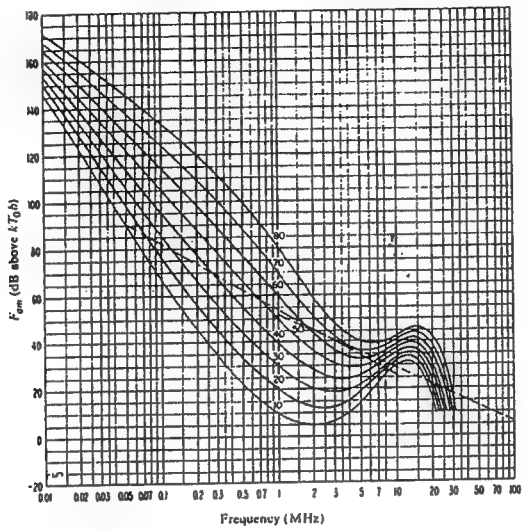

Figure 43 - Atmospheric noise power in decile units, as a function of frequency.

The curves in **Figure 43** show considerable variability about the average (50%) decile value near 1.8 MHz. The same is true of man-made noise but not being a natural phenomena, it has wider, unpredictable variations.

As a practical matter, in the morning a West Coast DXer may expderience QRM and atmospheric QRN from the East Coast while working into Asia or Oceania but as the sun rises, it is less of a problem, due to absorption. The East Coast DXer, working into Europe, does not enjoy the same advantage; noise and signals from the east fade out together as the sun rises while QRM and QRN from the west continue. But local man-made noise goes on forever.

Finally, It should be noted that galactic radio noise, while not strong enough to be problem for receivers of low-band DXers, may serve a valuable purpose in the study of ionospheric disturbances. In that regard, solar flares may emit high-energy particles, protons, which reach the earth and deposit heavy ionization on DX paths that cross the high-latitude ionosphere. The presence of such events can be detected by monitoring galactic noise at polar latitudes for absorption effects. This will be discussed in more detail in connection with the various types of disturbances.

Magneto-ionic Theory -

Geomagnetism -

The earth's magnetic field has been studied for centuries - on land, at sea, with rockets, satellites and spacecraft. So the strength of the field, its spatial distribution, time-variations and anomalies are all well-known. But there are several models of the field, depending on what is taken as the location for the origin of the coordinate system.

Thus, the simplest model is the centered-dipole approximation where the origin is at the center of the earth and the dipole moment M and axis are chosen to get the best fit of the field with that of a dipole. At the present time, the dipole moment is 7.8E+22 M.K.S. and the magnetic axis is tilted about 10.7 degrees from the earth's axis, with the north geomagnetic pole located at 79.3N, 72.0W; here in the Northwest, the total field is 52,000 nT.

Lines of longitude and latitude are used with the dipole model, the prime meridian located by a line of longitude which passes through the geomagnetic poles and the geographic South Pole. The magnetic equator is perpendicular to the dipole axis and the equatorial plane passes through the center of the earth. The PropLab program gives a map for the lines of latitude and longitude in the centered-dipole approximation but that data is more appropriate for the farther reaches of the ionosphere that extend above the F-region peak than the lower heights where low- band signals are propagated.

Another approximation uses dip pole coordinates, from the locations of constant dip of a compass on the surface of the earth. In that system, the magnetic poles have more meaning, locations where the compass needle is perpendicular to the earth's surface. But since the field varies slowly with time, it is expected the poles will wander, as in **Figure 43:**

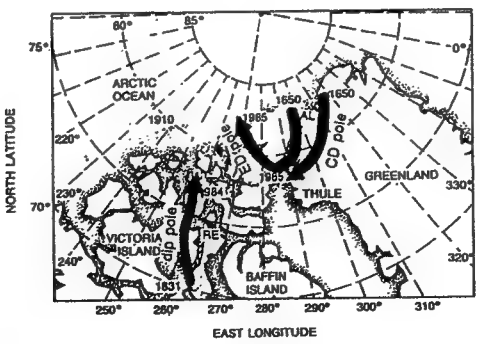

Figure 43 - Pole-wandering of the centered-dipole (CD), eccentric dipole (ED) and dip pole, up to 1985.

That figure shows the historic wandering of the poles but for our purposes, use will be made of the current geomagnetic data closer to the earth found in the International Geomagnetic Reference Field (IGRF, 1995), available on disk from the National Geophysical Data Center. For Boulder, the starting point of our path to London, the IGRF gives:

North = +21,106 nT
Vertical = +50,106 nT
Total = 54,370 nT

The horizontal component of the field is taken as positive if it points northward and the vertical component is taken as positive if it points down toward the earth, as in the Northern Hemisphere. Thus, the field at Boulder points northward and down into the earth at an angle of 22.8 degrees from the vertical, giving the components listed above.

At that altitude the ionospheric electrons are in rapid motion, making about 68,000 collisions/second with neutrals, according to the collision frequency profile in **Figure 13.** But with electrons in motion in the earth's field, magnetic forces come into play and the electrons spiral around the field lines at a high rate, 1,520,000 cycles per second. Thus, in time, the field affects electron motions more than collisions and should be included in the discussion of propagation. That is particularly the case as the electron gyro-frequency, as it is called, is close to low-band frequencies, especially 1.8 MHz on the 160 meter band.

Frequencies -

At this point, the propagation problem deals with four frequencies - the radio frequency F and three others that are characteristic of the ionosphere - the plasma frequency Fp, the collision frequency Fc and now the electron gyro-frequency Fg. At the top of the HF bands, only the plasma frequency is important as the frequency F is considerably greater than the collision and electron gyro-frequencies. On the low-bands, however, all the frequencies are important and affect propagation. Thus, in treating electron motions under the influence of the low-band signals, the electron's equation of motion must be expanded from one where the incident plane wave exerts the only force of interest to where both collisions and magnetic forces are also included:

Driving force = e*E
Collision force = -m*Fcoll*V
Magnetic force = e*(V x B)

the bold-faced variables - incident field E, velocity V and magnetic field B - being vector quantities, with components in the right-handed coordinate system shown in **Figure 44:**

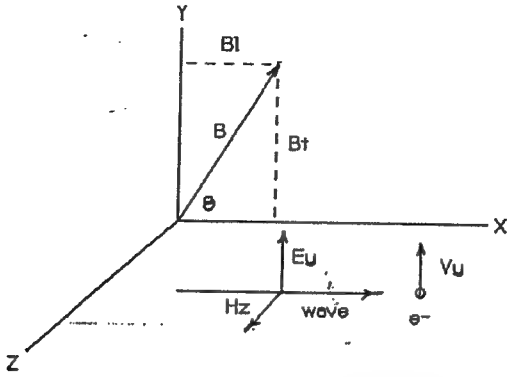

Figure 44 - Rectangular coordinate system, showing the vector components of some relevant variables.

When those forces are entered in an electron's equation of motion, the problem is then to find the mechanical motions that ensue and the polarization of the radiation produced. That is no easy task and is found in treatises on the subject (Ratcliffe, 1955). Here, only the principal results will be given and illustrative examples of how the theory bears on low-band propagation.

The general result is the ionosphere supports propagation of simple linearly polarized waves in the HF region but at low-band frequencies, the effect of the geomagnetic field on ionospheric electrons is to change that to elliptically polarized waves. So the vectorial nature of waves is changed from the E- or H-vectors oscillating in a plane as they advance, in **Figure 3,** to rotating around the direction of propagation, as with circular polarization in **Figure 45:**

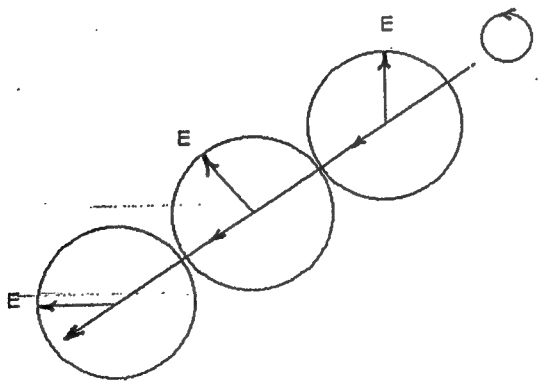

Figure 45 - Diagram showing the rotation of the E-vector in the advance of a right-hand, circularly polarized wave.

That figure for circular polarization shows a constant E-vector rotating in a right-hand sense as a low-band signal advances along the path, top-right to bottom-left in the figure.

Elliptical polarization is shown in **Figure 46**, a varying E-vector rotating in a right-hand sense as it advances. Note that the E-vector is a maximum in the direction of the semi-major axis of the ellipse and a minimum in the direction of the semi-minor axis. The orientation of the ellipse is fixed in this figure.

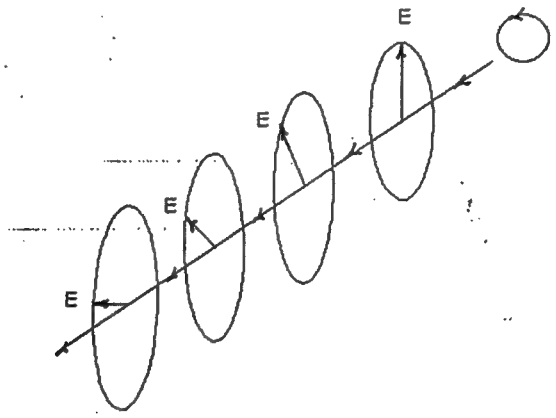

Figure 46 - Diagram showing the rotation of the E-vector in the advance of an right-hand, elliptically polarized wave.

The H-vectors are omitted for clarity in those two figures. The H-vector goes around its own circle in **Figure 45** but the H-vector's ellipse for the situation in **Figure 46** is rotated by 90 degrees relative to that for the E-vector.

Low-band antennas emit polarized radiation, say with E-fields in the vertical direction from the classic quarter-wave vertical monopole and in the horizontal direction broadside to a horizontal dipole. The question then is how the earth's field affects the entry of the radiation into the ionosphere. For that, we consider two extreme cases, at the north dip pole, the location where the field is vertical, and the magnetic dip equator, locations on the earth where the field is horizontal, with a dip of zero with the compass pointing north.

Consider RF being radiated by a vertical antenna at the dip pole. The RF is advancing perpendicular to the magnetic field but the wave's E-field is vertical, driving ionospheric electrons in the same direction. The magnetic field does not exert any force on the electrons, just like the field was not there, as their motions are parallel to the field. In magneto-ionic propagation, vertical waves in a mode like that are called Ordinary or O-waves and wave energy is coupled efficiently into the ionosphere.

With a horizontal antenna at the dip pole, the E-field that advances perpendicular to the magnetic field has great difficulty in propagating signals further by driving ionospheric electrons into motion. That is the case as the magnetic force severely limits the amplitude of electron motion that develops when the E-field drives electrons in motion perpendicular to the magnetic field. That mode, with the E-field polarized perpendicular to the msgnetic field, is called the Extra-ordinary or X-mode and in that extreme, energy is not coupled into the ionosphere.

Now let's turn to the dip equator and consider radiation from a horizontal dipole, the antenna orientated in the magnetic N-S direction. For E-W propagation, the situation is just like at the dip pole with a vertical antenna as the E-field from the dipole is parallel to the horizontal magnetic field and couples efficiently into the electron motions in the ionosphere as an O-mode. By the same token, E-W propagation with a vertical monopole at the dip equator is like a horizontal antenna at the dip pole and does not couple efficiently into electron motions as an X-mode.

Now consider N-S propagation at the dip equator where the geomagnetic field is horizontal, pointing north. With that axial symmetry, linearly polarized E-fields from vertical monopoles and horizontal dipoles would be expected to behave the same when it comes to RF energy sent horizontally into the ionosphere. But there is a difference.

With the magnetic field pointing north, ionospheric electrons spiral around the field lines in a clock-wise direction, looking north in the field direction. Now a linearly polarized wave of amplitude E may be shown to be equivalent in a vectorial sense to two circularly polarized waves of amplitude E/2 which rotate in opposite directons, as in **Figure 47:**

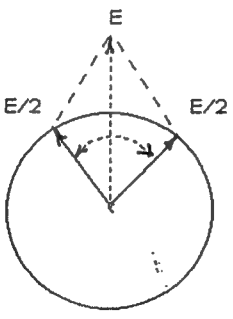

Figure 47 - Diagram showing the equivalence of a linear-polarized wave of amplitude E and two circularly polarized waves of amplitude E/2 rotating in opposite directions.

Sending linearly-polarixed signals to the north, along the field direction, magneto-ionic theory shows the clock-wise component of the wave, rotating like the ionospheric electron, propagates poorly as an X-wave while the counter-clockwise component suffers much less absorption as an O-wave.

That point will be discussed in more detail in connection with power coupling when low-band signals enter and leave the ionosphere; for the moment, suffice it to say that on long DX contacts, the X-mode is heavily absorbed and only half the effectively radiated power (ERP) propagates as an O-wave in the direction of the field, with either horizontal or vertical antennas at the dip equator. In the magnetic E-W direction, a high, horizontal antenna at the equator is very effective in the O-mode while a vertical antenna is a poor choice for propagation in the E-W direction.

These same ideas may be applied at other latitudes where propagation of vertically polarized signals puts the radiation angle from the antenna in a direction such that the E-field is essentially parallel to the local magnetic field. Boulder, CO is a case in point. As noted earlier, the magnetic field at Boulder points northward and down into the earth at an angle of 22.8 degs from the vertical; thus, at a radiation angle of about 23 degs, signals going northward would be coupled efficiently into the ionosphere. Other locations where this would apply may be see in a global map showing magnetic dip, as in **Figure 48:**

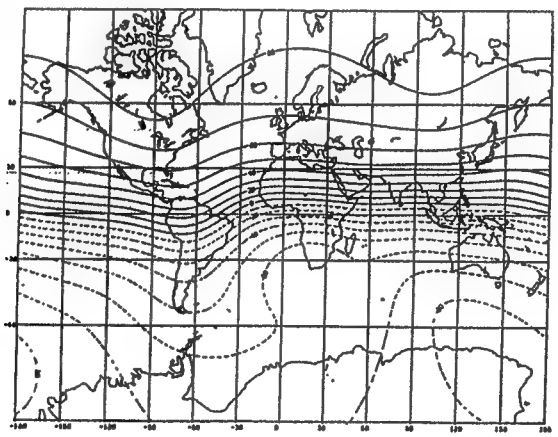

Figure 48 - Global map of latitudes for locations with constant magnetic dip with respect to the horizontal direction.

More general directions -

The discussion so far considered extreme simplifications, signals transmitted horizontally at one of the earth's dip poles and at the dip equator. For linearly-polarized waves from vertical monopoles and horizontal dipoles, it was shown that those signals were coupled efficiently into the ionosphere so long as the E-fields radiated were parallel to the local magnetic field. That was the case for a vertical monopople at the dip pole and for a horizontal dipole oriented N-S at the dip equator. But for either a monopole or a dipole sending signals horizontally along the field direction at the dip equator, it was another matter. At that point, circular polarization came into the picture.

Now if one goes back to elementary geometry, circles and straight lines are simply extreme variations of the ellipse, as in **Figure 49:**

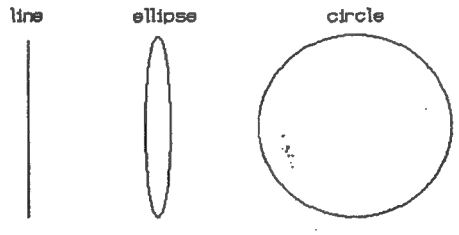

Figure 49 - Various forms of the ellipse.

And so it is with magneto-ionic propagation; linearly-polarized and circularly polarized waves are extreme variations of the more general form of propagation that is supported in the earth's magnetic field, elliptical polarization. In short, it depends on the direction of wave propagation relative to the magnetic field.

Thus, go to the coordinate system in **Figure 44** to look at more general cases. For a linearly-polarized signal going the x-direction, the wave propagated in the ionosphere when the field is nearly vertical (Bl<<B) now has some elliptical polarization, as in **Figure 50.** Instead of waves perpendicular or transverse to the field, as in a polar situation discussed earlier, this is quasi-transverse or QT-propagation in the language of magneto- ionic propagation. In a similar fashion, the wave propagated when the field is nearly horizontal (Bt<<B) now has less circular polarization, as in **Figure 51.** Instead of waves along the field, as at the dip equator, this is termed quasi-longitudinal or QL-propagation.

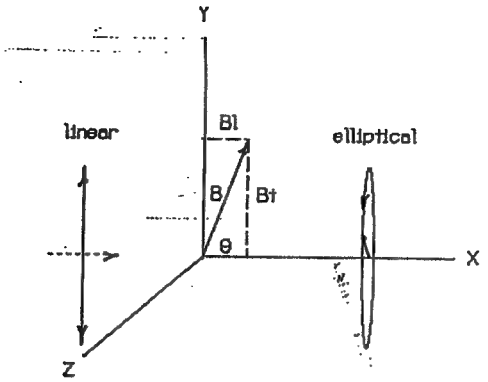

Figure 50 - Elliptical polarization from quasi-transverse (QT) propagation (Bl<<B).

and

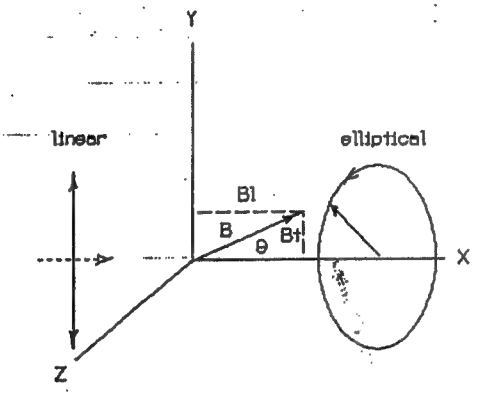

Figure 51 - Near-circular polarization from quasi-longitudinal (QL) propagation (Bt<<B).

to illustrate the two cases.

For propagation of low-band signals from point A to point B, the propagation of signals can be broken down intro three parts: getting signals into the ionosphere at point A, magneto-ionic propagation in the ionosphere from A to B and then getting signals out of the ionosphere at point B. The "A to B" part is really very complicated as the field strength and direction will change constantly along the path, making any calculation or ray-tracing a daunting task for computers. But it is done, using models for the magnetic field (IGRF) and the ionosphere (IRI). Within the limits of the models, some insights are obtained.

55

But the theory, proper, leads to some interesting conclusions about magneto-ionic effects on absorption and refraction. For example, the theoretical expression for absorption, in dB/km along a path, becomes more complicated as the frequency is lowered, from

the HF range, 21 to 28 MHz, to the transition range, 10 to 18 MHz, and down to the low-band range, 1.8 to 7 MHz. Thus, for the HF case, it starts at

$$K = const*N*Fcoll/(2*pi*Frf)^2$$

then goes to

$$K= const*N*Fcoll/((2*pi*Frf)^2 + Fcoll^2)$$

for the transition bands, and

$$K = const*N*coll/((2*pi*Frf +/- 2*pi*Fbl)^2 + Fcoll^2)$$

for the low-bands, where

$$Fbl = Fb* \cos(\theta) = (e*B/m)* \cos(\theta)$$

and Fb is the electron gyro-frequency around the magnetic field. That motion around the field line was alluded to earlier, just to indicate the geomagnetic field might play a role in propagation. But now it is seen to play a major role, as a "resonance" factor in absorption, like in LCR circuits:

$$((2*pi*Frf +/- 2*pi*Fbl)^2 + Fcoll^2)$$

with the "+" sign for O-waves and the "-" sign for X-waves. So for a given direction relative to the field, the magneto-ionic aborption differs according to mode, with greater absorption for the X-mode, with the - sign, than in the O-mode, with the + sign. This is seen in the X/O absorption ratio in **Figure 52:**

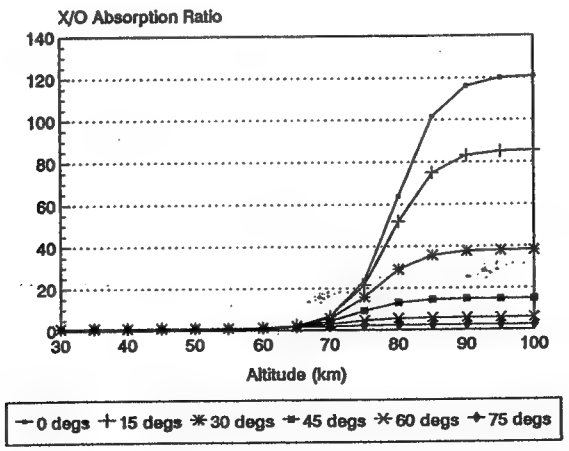

Figure 52 - Extra-ordinary/Ordinary absorption ratio in dB/km as a function of the angle between the direction of propagation and the magnetic field.

That figure is based on 1.8 MHz for the radio frequency, using 1.5 MHz for the gyro-frequency and the night-time collision frequency profile in **Figure 13**. The angles are for the direction of propagation relative to the field direction. Thus, 0 degrees is for longitudinal propagation along the field lines, as for low angles at the dip equator, and higher angles go toward 90 degrees and transverse propagation, as with a vertical antenna at the dip poles. At that angle, the E-field of the wave is parallel to the magnetic field and electron motions and absorption are just as though the field was not there, with an X/O ratio of unity.

The large X/O ratio at other angles results from the difference part of the denominator, and that has the greatest effect at locations with field intensities like Boulder, CO (54,370 nT) which served as the case in point. The global map of magnetic intensity in **Figure 53** would help in that regard.

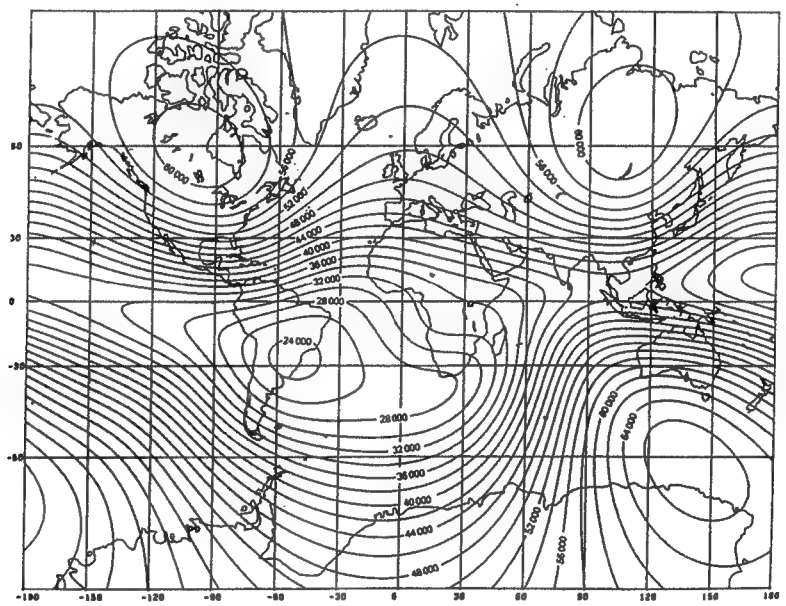

Figure 53 - Global map of magnetic field strength (in nano-Teslas)

On the other hand, the X/O ratio at low latitudes would be smaller at sites in the magnetic anomaly in the South Atlantic region, seen clearly in that figure. In any event, the high X/O ratio on 1.8 MHz indicates a rapid loss of propagation in the X-mode and for long-haul DX contacts, the radiated power in the X-mode is lost so quickly as not to be effective in making DX contacts.

Finally, magneto-ionic effects are smaller at frequencies greater than the electron gyro-frequency. Thus, the X/O ratio for longitudinal propagation (0 degs) on 3.5 MHz is 6.25 and 2.40 on 7.0 MHz, respectively, in contrast to over 100 on 1.8 MHz.

Power coupling -

At this point, power coupling of signals in and out of the ionosphere should be considered to complete the discussion. In that regard, magneto-ionic theory gives the limiting polarization of waves relative to the local field as they enter or leave the bottom of the ionosphere at some angle. That is compared with the polarization of the radiation pattern of the antenna in use and the power transfer or coupling, much like with the Law of Malus in the optics of polarized light, is calculated. This technique was developed by Phillips and Knight in 1965 and applied then to the propagation in the broadcast band; later, it was applied (Brown, 1998) to DX contesting on 1.8 MHz.

Power coupling is much like insertion loss in RF power transfer situations and the results of more general magneto-ionic theory give all the simple results discussed earlier at latitudes like Boulder as well as the dip pole and the dip equator. Thus, for Omaha, NE, where the magnetic dip is 69.6 degs, the O-wave power coupling of a vertical antenna at 20 degrees radiation angle is shown in **Figure 54**.

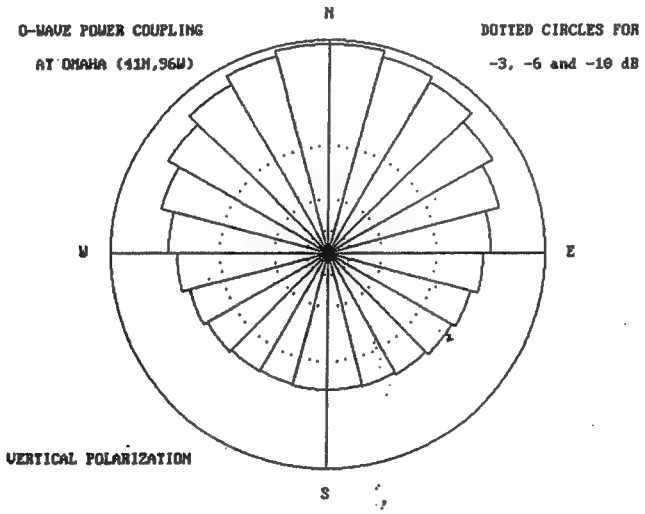

Figure 54 - 1.8 MHz O-wave power coupling in dB at Omaha, NE.

That shows a high power coupling between the antenna and ionosphere in the northern direction, much like at Boulder. The more general theory of Phillips and Knight also gives power coupling at other headings of the vertical antenna.

Another example of interest (Brown, 1998) is for the low latitude of Togo (7S, 1E) where the earth's field is almost horizontal in the N-S direction. With a vertical antenna, a large insertion loss or low power coupling would be expected for O-waves

in the E-W direction, as discussed earlier. In addition, in the N-S direction, X-mode power is eventually lost or dissipated by absorption and the power coupling is down 3 dB in that direction, as in **Figure 55:**

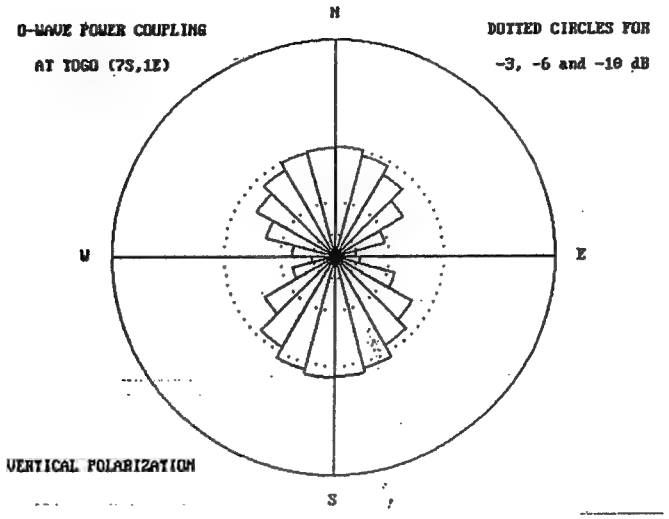

Figure 55 - Power coupling for a vertical at Togo (7S,.1E)

But a high, horizontal dipole in the N-S direction should couple efficiently into the ionosphere at that low-latitude and the high power coupling for E-W propagation with a horizontal dipole is shown in **Figure 56:**

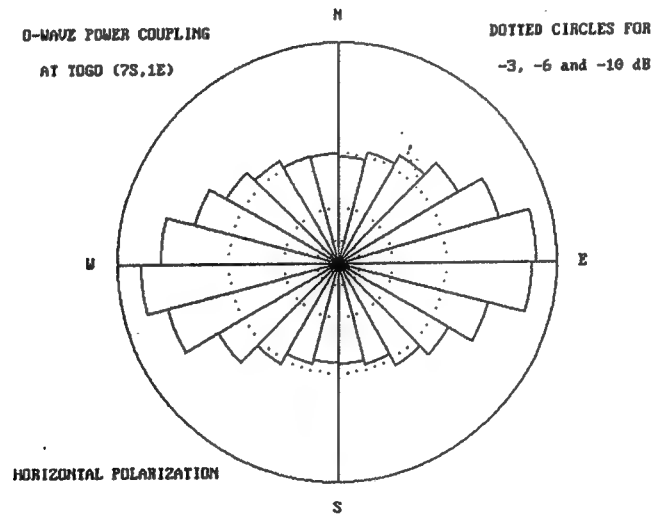

Figure 56 - Power coupling for different orientations of a dipole

Magneto-ionic Ray-tracing -

Ray-tracing gets more involved as the number of features of an ionospheric model are expanded. Thus, ray-tracing is two dimensional so long as the electron density is the only factor, varying in a plane, as in **Figure 57:**

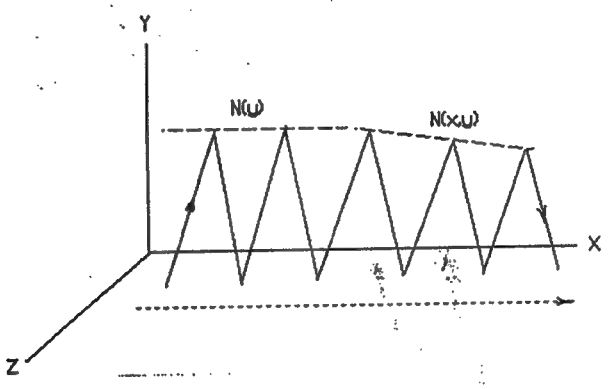

Figure 57 - The effect of different electron density contours.

In that figure, the electron density contour having a plasma frequency equal to the EVF of the path is horizontal when the density varies only with height, N(y), but is shown tilting downward when it varies with height and distance along the path, N(x,y). That affects the length of the hops and reflection angles along the path.

If the electron density varies out of the plane, N(x,y,z), as was the case in **Figures 35 and 36,** then the ray-trace becomes one in three dimensions and depends very much on the nature and extent of the transverse gradient in electron density. Some ionospheric structures are quite extensive and continuous in space and time, like the strong ionization gradient across the terminator, the sunrise/sunset line. Others may be brief and highly variable, as with ionization in auroral displays.

As noted earlier, wave refraction depends on the features of the wave index of refraction. Ray-tracing involves finding the path of the ray, normal to the wave front, and is a mathematical problem very much like particle dynamics, say for the motion of a spacecraft. So equations of motion (Budden, 1966) for the ray look like thoe of a particle and are solved numerically, step by step, through the ionosphere, using the path bending that results from the spatial variation of the index of refraction.

The index of refraction (Davies, 1989) becomes more involved, just as the absorption coefficient noted earlier, as the frequency is lowered from the HF range to the low-bands. At low-band frequencies, the magnetic force on ionospheric electrons is not always in the plane of the ray path, meaning that the ray path will be in three dimensions due to that magneto-ionic effect. But unlike the transverse electron density gradient responsible for the refraction shown in **Figures 35 and 36**, the magnetic force on electrons is relatively constant and wide ranging, like the extent of the magnetic field. As a result, when magneto-ionic effects are included in ray-tracing programs like PropLab, their spatial extent can be quite large.

This may be seen in **Figures 58 and 59**, 3-D ray-traces for the 1.8 MHz path from Tokyo to Seattle. **Figure 58** is for a "no field" condition in the ray tracing program (PropLab) and shows six hops into the lower F-region.

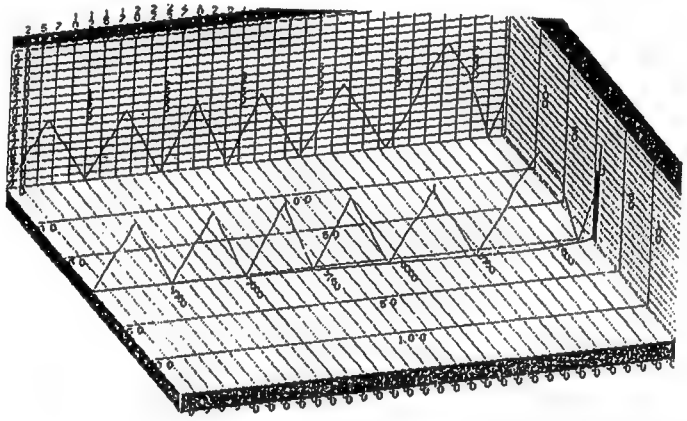

Figure 58 - Tokyo-Seattle ray-trace for "no field" condition.

Figure 59 is for exactly the same path and conditions but it was for a "with field" condition:

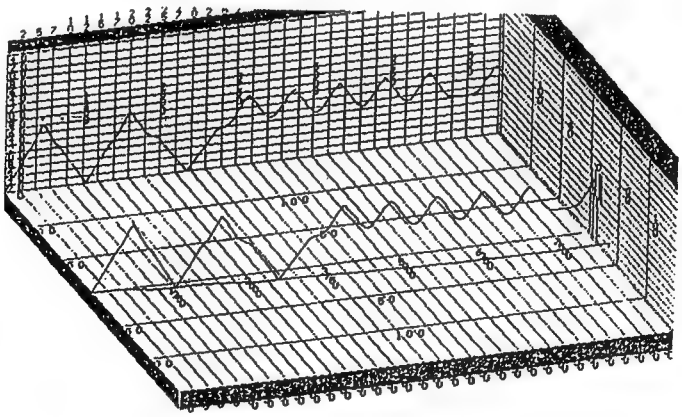

Figure 59 - Tokyo-Seattle ray-trace for "with field" condition.

and shows two F-hops followed by the sudden emergence of ducting. That is a major result for magneto-ionic propagation as it points to an efficient means of propagation, without losses from intermediate reflections off of ground or transits of the D-region.

Those figures have ranges marked out horizontally in 2,500 km intervals and laterally in 50 km divisions. Note the trace on the ground surface; for the "no field" case, there is a slight lateral deviation or skewing, away from the greater ionization in the west due to the effects of weak sunlight after sunset. But the "with field" case shows somewhat greater skewing to the east, due to the effects of the earth's field.

Now amateur radio installations for the 1.8 MHz band do not have antennas that are sufficient to observe or measure effects from elliptical polarization due to the earth's field. Thus, we get information on the effects from other directions, indirect in that they involve other services or simply theoretical in origin.

A good example of "other services" comes from the monitoring of broadcast stations. In that regard, Nick Hall-Patch, VE7DXR, used signals from a Korean BC station (Hall-Patch, 2000) to study dawn enhancements of low-band signals. That effect involved the increases in signal strength just before dawn on a W-->E path. That is a time when a strong DECREASE in signal strength would be expected from the rising sun yet a signal INCREASE is observed, quite often, as in **Figure 60:**

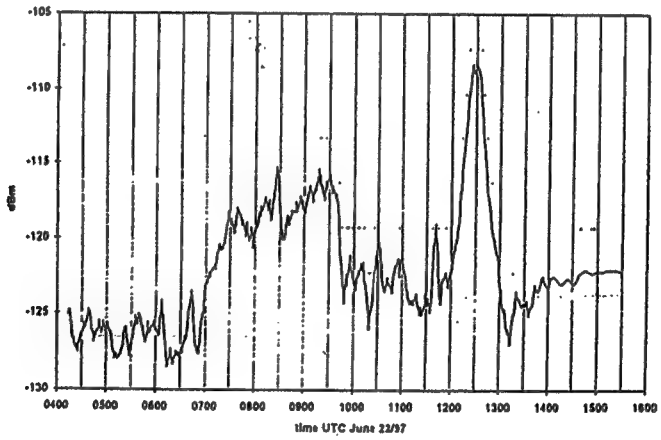

Figure 60 - Dawn enhancement of Korean broadcast station HLZ on 1613 KHz at 1230 UTC on June 22, 1997.

The explanation is that part of the signal from the transmitter was ducted at the outset, leaving earth-ionosphere hops to provide the initial signal at the receiver. But at dawn, the ionosphere over the receiver is tilted down at sunrise and sends the ducted signal

downward to add its strength to the earth-ionosphere hops. Another form of dawn enhancement is confined largely to the region near the transmitter (Kavanagh et al, 2002), due to brief ionospheric ducting or long E-F hops there. That was shown to be the case as the increase in signal strength was observed simultaneously on paths to widely separated sites, Ottawa and Victoria, but at dawn near the transmitter. The Victoria signal record in **Figure 61** is nearly identical to the trace observed at Ottawa, some 3,000 km distant.

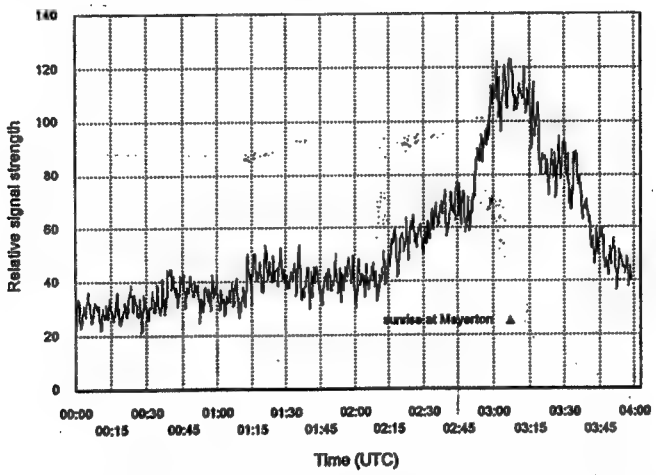

Figure 61 - Dawn enhancement of South African station on 3.32 MHz at 0312 UTC on December 5, 2001.

The path in **Figure 59** shows a "mode conversion", in VLF jargon, where earth-ionosphere hops change over to ducted hops. Considering that ducting is more efficient than with hops from ground reflections, mode conversion adds an element of ambiguity when it comes to interpreting DX contacts.

Take a contact made by VK6HD in Western Australia with VP9AD in Bermuda. What mode(s) were involved in that 19,000+ km path? That contact was in January of 1996, near solar minimum, and when the input parameters were adjusted appropriately for the PropLab program, the low-angle path turned out to begin and end with E-hops but was divided almost equally with 9,000 km of earth-ionosphere hops and 9,000 km of ducting, as shown in **Figure 62:**

In addition to showing a possible hop structure for that contact, the PropLab program calculates the ionospheric absorption along the path. That is shown in **Figure 63,** with effects from E-hops at the start and end of the path but absorption that is rougly linear during the earth-ionosphere portion, 5.6 dB/1,000 km, and the ducted portion, 2.0 dB/1,000 km.

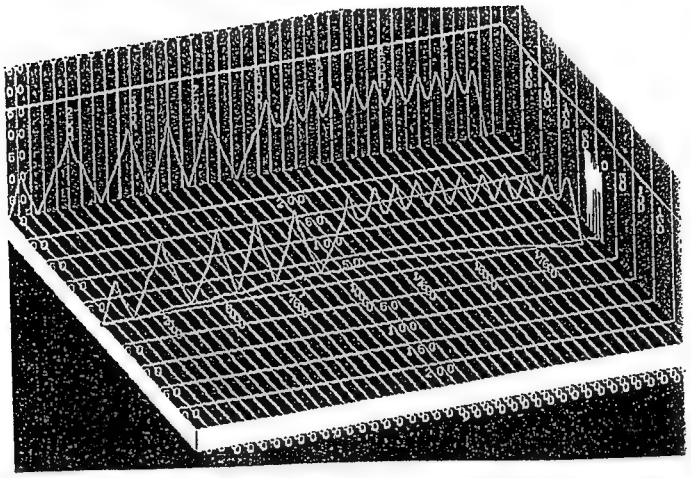

Figure 62 - Ray-tracing of VK6HD-VP9AD contact on 1.8 MHz.

and for Figure 63:

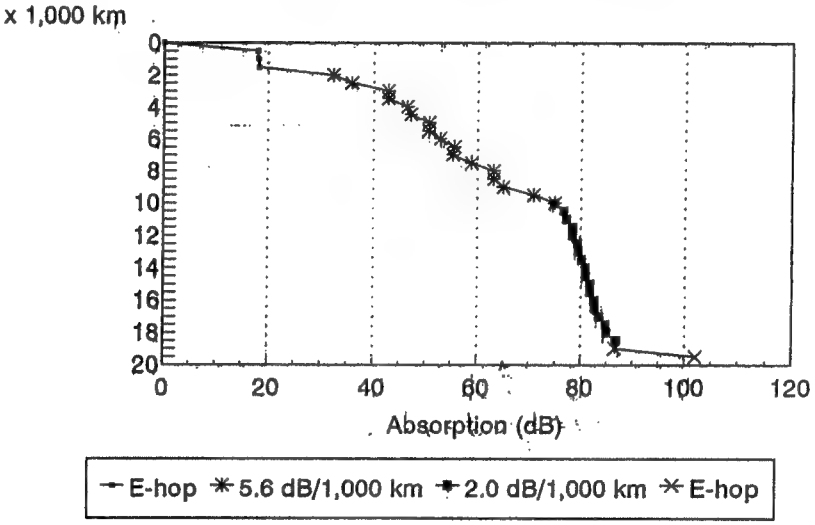

Figure 63 - Signal absorption for VK6HD-VP9AD contact.

The PropLab program is very useful, say in estimating signal absorption rates as above, and got its start with the work of scientists in the Central Radio Propagation Laboratory (CRPL) in Boulder, CO in the mid-70s. Like IONCAP, it was reduced in size, from main frame proportions to fitting on desk top computers. But given the caveat about ionospheric variability, any result from it must be viewed with interest, but also with caution.

In simple terms, ionospheric models are averages, at best, and can vary by 20-40%. Models of the geomagnetic field are averages too, but also represent "fits" to specific models and coordinate systems. So all in all, the low-band DXer should understand that

even the best models in propagation programs and aids like PropLab use average data and all calculated results must be viewed in that light, subject to variations about the average.

Of greater importance are well-documented observations, the careful work of VE7DXR and VE3OSZ on dawn enhancements being good examples. To that should be added short-term logs of numerous DXpeditions and long-term contacts with a given station, complete with summaries of the geophysical conditions at the times.

With intense, global interest in the VK0IR DXpedition to Heard Island, interesting aspects of low-band propagation were revealed from the contacts both made and not made with VK0IR. Thus, the striking role of absorption was shown by the complete lack of 1.8 MHz contacts with operators in a "dead region" that covered about 40% of the USA, during hours of the sunlight at Heard Island, shown in **Figure 64:**

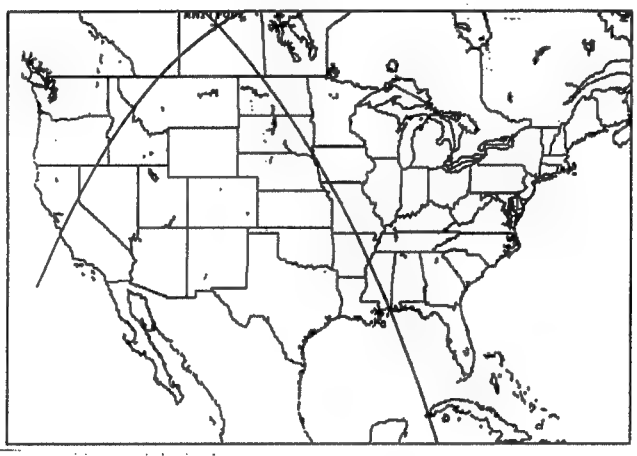

Figure 64 - Dead zone for 1.8 MHz signals from VK0IR.

That region began to open up for 3.5 MHz operators and was wide open to 7 MHz operators, due to decreasing absorption with increasing frequency.

A similar demonstration of the power of absorption is shown with the low-band phenomena of equinoctial path switching on 1.8 MHz (Ireland et al, 2002) where sunlight reaching one polar cap absorbs signals and the operating path then switches to the other polar cap at the time of an equinox. That was found to be the case for locations which differ in longitude by about 180 degrees, like VK6HD in Western Australia and VE1ZZ in Nova Scotia. A long series of contacts over 20 years time showed the path went over the northern polar cap from September to March, then as short- path, and switched to over the southern polar cap from March to September, then as long-path.

Disturbances -

Quiet day ionosphere -

Low-band propagation is best in the quiet times of night during solar minimum conditions. Then the sources of ionization are sufficient but weak and generally steady in time - stellar EUV and Xrays, galactic cosmic rays and solar EUV scattered into the dark hemisphere by the high atmosphere, the geocorona. Exceptions are rare, such as the intense gamma ray outburst from a stellar object, a "magnetar" (Inan, personal communication), that produced a striking absorption event on a number of VLF circuits in mid-1998.

The galactic cosmic ray background flux is modulated downward by a few percent due to solar activity, thus actually aiding the propagation conditions on low-bands. Beyond that, there are times of strong solar activity during which magnetic structures rooted on the sun can sweep past the earth, deflecting galactic cosmic rays away from the earth's orbit; those effects vary slowly, lasting about 10 days and can reach the 10-15% level (Brown, 1957). In addition, solar flares send shock waves through the interplanetary field which can produce similar effects of sudden onset, Forbush decreases in cosmic ray intensity, for a few days.

Those sources of ionization in the dark hemisphere reach the lower ionosphere; the source of ionization for the high ionosphere is the sun, from slowly recombining ionization remaining when EUV and Xrays from active regions disappear after sunset. As is well-known, active regions come and go with solar activity so they will influence the level of ionization during night-time in that way. In that regard, the most important effect of solar activity is the filling of the night-time valley above the E-region with some ionization, shown in **Figure 1**. In effect, that would reduce the probability of ducting by signals in that region.

Ionospheric disturbances -

Disturbances of low-band propagation due to the sun can be prompt, Xray photons from solar flares or high energy solar particles from flare outbursts, or delayed in their arrival, magnetic storms and aurora that follow coronal mass ejections (CME). The latter may take a day or so before affecting the earth due to the long time-of flight of the solar wind from th sun to the earth. On the other hand, Xrays and high energy particles travel with the speed of light, or close to it, and give rise to effects on signal strength within minutes of their occurrence on the sun.

Aside from its other roles in low-band propagation, the

geomagnetic field plays a major part in deflecting some solar cosmic rays away from the earth and others into the dark hemisphere.

In any event, solar cosmic rays, accelerated at the sun in the course of a solar flare, represent serious disturbing factors for low-band propagation. Those particles, massive compared to electrons responsible for the aurora, deposit their ionization deep in the ionosphere, where large absorption effects result.
If the particle spectra are known, calculations can be made using energy loss by ionization along their trajectories to find the electron density that results and the ionospheric absorption.

That much information is usually not available; instead, an estimate of the absorption may be in hand for some polar station. Solar proton events usually cover the polar caps so the data, say from McMurdo Station in Antarctica, can be used to find the effect on low-band signals going across either polar cap.

Solar proton events -

As an example, a solar proton event was reported (Rosenberg, private communication) at McMurdo Station in Antarctica in January of 2002. The solar protons had full access to McMurdo by coming down the steep magnetic lines of force. The >10 MeV flux proton at the NOAA satellite peaked around 90 p.f.u. (proton flux units) at 00-06 UTC on January 10, 2002 and data showed galactic radio noise on 30 MHz was attenuated by 1.3 dB on going through the ionosphere.

That was due to the ionization produced by the solar protons in the D-region. But for oblique propagation of signals across the polar cap, that should then be increased by a factor of 3 or so, to take into account the greater amount of ionization that was encountered by signals on a slant path, and another factor of 2 for a full hop. Finally, since absorption varies roughly as the square of the wavelength, there is another factor of 256 to bring the calculation down from 10 meters to 160 meters. That makes a total of about 2,000 dB, a huge absorption effect.

That calculation was for McMurdo Station in Antarctica, a location at which the ionosphere is fully illuminated in January. On the other hand, for the North Pole and other polar latitudes where 160 meter signals can really travel in darkness, the total absorption effect is smaller by a factor of 4-5 because some ionospheric electrons can become attached to molecules to form negative ions and those, being so heavy, are removed from the absorption process. Be that as it may, it is seen even a small flux of solar protons can still produce huge absorption effects.

Beyond the direct ionization solar protons produce in the atmosphere, there is also a secondary effect, nuclear reactions in the atmosphere (Bhavsar, 1962), that adds to the ionization affecting low-band signals. The nuclear reactions of energetic solar protons with N and O nuclei produce MeV nuclear gamma rays that penetrate much deeper and ionize down where the electron-neutral collision frequency is quite high. Those same reactions are considered a hazard to commercial aviation at high altitudes, like the Concorde's polar flights across the Atlantic Ocean.

The passage of charged particles through the atmosphere gives rise not only to ionization and ionospheric absorption but also to excitation of atoms and molecules, resulting in optical emissions. The emissions from solar proton events, the polar glow aurora, are very weak when compared to that from auroral events and observed only in remote sites, like Antarctica, that are well-removed from the lights of civilization. And it has been observed during Cycle 19 by Sandford (1961, 1962) in the 3914A emissions of ionized molecular nitrogen and the polar glow aurora was found to behave, in time and extent, like polar cap absorption due to protons.

But theoretical calculations of emission rates from proton spectra (Brown, 1964) fall short of the observations by about an order of magnitude. That was understandable at the time as there were uncertainties in the optical calibrations as well as the ionospheric rate coefficients used in the calculations. With the end of Cycle 19, very intense proton events have become rare and interest in polar glow aurora has essentially come to an end.

Finally, the duration of solar proton events must be mentioned to indicate the length of time signals are disrupted on the low-bands by the absorption that results. Those events can be of rapid onset, as seen in the record of an impulsive event that was observed by the GEOS 8 satellite, in **Figure 65:**

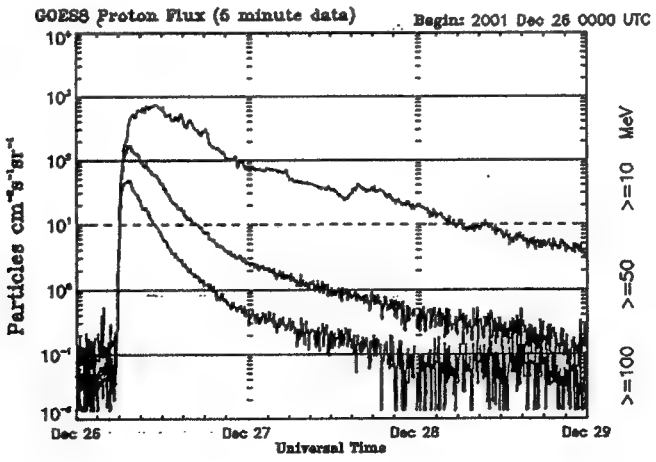

Figure 65 - The particle fluxes in an impulsive proton event.

That event shows a rapid onset for protons of all energies, from >10 MeV to >100 Mev, indicating a sudden acceleration in the flare process. But its duration is due, in part, to particle diffusion in the fields at the sun and the interplanetary field as well, with higher energy protons diffusing away more rapidly than low energy protons, as expected.

By way of contrast, look at the slow-rising proton fluxes in **Figure 66;** those took a day to reach full intensity. That is typical of proton events on the east limb of the sun, protons taking hours to diffuse across the interplanetary field before escaping into the far reaches of the solar system:

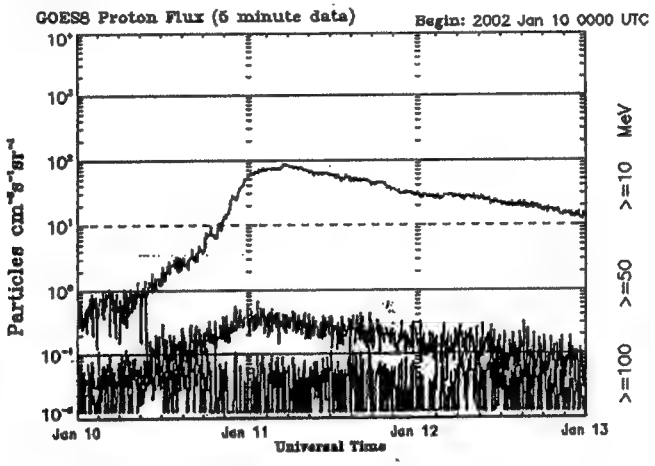

Figure 66 - The particle fluxes in a gradual proton event.

Those figures show the proton flux, as recorded at satellite altitude. But the low-band DXer is dealing with their ionospheric effects; what do those look like, when solar protons meet the ionosphere? A good example is found in the record of the August 22-25 event of 1958, one of the events in Cycle 19, shown in **Figure 69:**

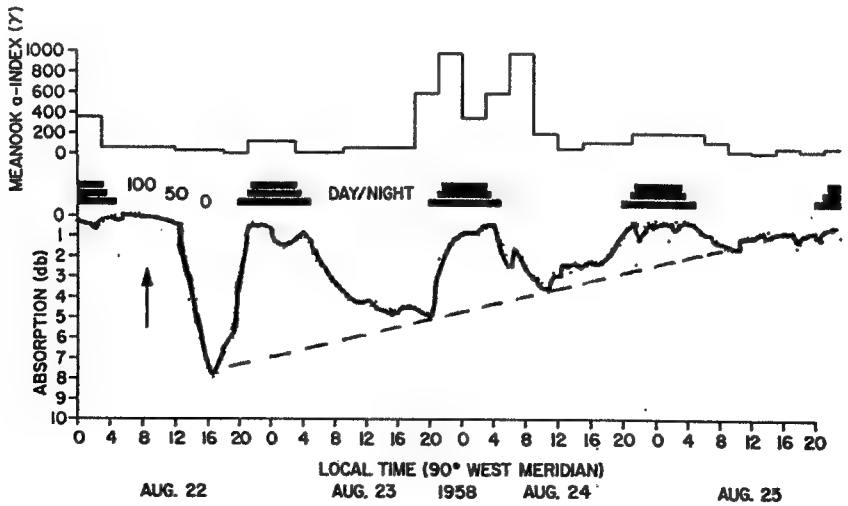

Figure 67 - Ionospheric absorption (down) in a proton event.

That event took place in daylight, around 08 L.T. at Churchill, Canada (59N, 94W); the ionospheric absorption began at 12 L.T, and peaked at about 8 dB absorption on 30 MHz at 16 L.T. After that, the proton flux declined, as in **Figure 65**, but the absorption curve showed strong night-time recoveries. Those times are shown by black horizontal bars representing darkness at ground level, 50 km km and 100 km. The reduction in absorption is due to negative ion formation in the D-region, as mentioned earlier in connection with the calculation based on the Mc Murdo data for January 2002.

At the top of the figure is shown the horizontal magnetic activity that ensued, with a strong disturbance starting around 18 L.T. on August 23, about 34 hours after the flare that probably initiated the event. That is fairly typical for strong flare events and the night of August 23-24 probably had bright auroral displays and intense, rapid ionospheric absorption variations from energetic electrons precipitating on the ionosphere. The absorption records for solar proton events were obtained from riometers (Relative Ionospheric Opacity METERs), 30 MHz radio receivers with 3-element Yagi antennas directed upward, either vertically or along the earth's axis of rotation. Those record both quiet-day and disturbed levels of cosmic radio noise to determine the amount absorption produced by the ionization.

But riometry has moved in other directions, with antenna arrays as large as 8x8 Turnstiles pointed upward at various sites in the Arctic and Antarctic. Those arrays record whatever shows up overhead, solar proton or auroral in origin. With the multiple antenna systems, the arrays can see structure in the ionization, albeit with only coarse spatial resolution. The hope is to combine multiple riometer records with those of multi-beam photometers that view the same region. This will be discussed later in connnection with the spatial structure of auroral absorption regions. But nowadays the number of individual instruments still in operation is much smaller, but in key locations like Thule AFB in Greenland and McMurdo Station in Antarctica. Their data goes to NOAA in Boulder and is used in solar/terrestrial activity reports. But in their day, around the IGY in '57, riometers proved their worth by providing latitude profiles of solar proton events across the polar cap.

The theory at the time, due to the famous Norwegian auroral physicist, Stoermer, was based on particle motions in the dipole model of the earth's field and pointed to a large variation in magnetic cut-off energies and absorption across the polar cap during proton events. None was found and that showed the dipole model needed correction. That was the first step toward the current model of the magnetosphere, with field lines compressed by the solar wind on the sunward side and trailing back, away from the

earth, in the other direction.

Other monitoring functions for protons are now handled by solid-state detectors on NOAA's satellites. The energy ranges change from time to time but the general idea is to look at protons with energies >10 MeV, which can penetrate to ionospheric heights, and protons with energies >100 MeV, which reach balloon altitudes.

Beyond that, there are a few detectors which record ground level events (GLE). Those involve relativistic particles in the Gev range and by themselves, produce little in the way of ionospheric disturbance because of their low rate of ionizatiion in the absorbing region. There are a few of those events per solar cycle and if the flux is high enough, secondary protons and gamma rays from nuclear reactions may give rise to absorption.

It should be noted that the more intense solar proton events can affect atmospheric composition, notably the oxygen-ozone cycle in the lower atmosphere. Thus, a depletion of atmospheric ozone was noted in the 50-70 km range after intense proton events in '69 and '72; also, NASA satellites, looking down on the ozone distribution, have noted ozone depletions with proton events in late '89. In that regard, ozone variations are important as ozone aids low-band propagation because of the shielding from photo- detachment that it offers to negative ions in the hour around dawn.

Normally, the discussion of ionospheric processes down in the D-region does not consider transport since ion lifetimes are relatively short. But with long-duration proton bombardment, as implied by absorption records, say in **Figure 67**, that may be important to the discussion. Certainly, continuing auroral activity in winter months gives rise to the production, transport and retention of NO in the dark polar cap, pointing to atmospheric motions as another factor to be considered in our discussion.

In another respect, atmospheric motions are important as the ion-neutral collision rate is so high in the lower ionosphere that the ionized population is carried along with the neutral wind. Since electrons are pulled along by electrostatic attraction, the distribution of electrons which determines ionospheric refraction is affected by neutral winds too. So one can expect the tilts or inclination of ionospheric regions to be affected by winds.
And any sort of turbulence in the wind would also serve to reduce the scale-size of atmospheric regions. So when it comes to the coherent motions and re-radiation of electrons, winds could affect not only their effectiveness on DX paths but also the direction or inclination of low-band signals. In a nutshell, propagation paths would be much spottier than in quieter atmospheric conditions.

Magnetic storms and aurora-

Magnetic observations -

The earth's field has been studied for over a hundred years, keeping records of how its components vary in magnitude and time at each location. The field components typically are for the northern direction, X, to the east (Y) and down into the ground, Z, and variations are expressed in nano-Teslas, nT. Variations are indexed every three hours using maximum deviations, positive or negative, from quiet conditions.

Magnetic activity is described by six categories, from quiet to severe storm, and the activity at each station is given with 3 hour K-indices, from 0 to 9. Each station has its own minimum value for severe storm conditions, depending on latitude, and the K-indices are adjusted accordingly so that all stations report on the same quasi-logarithmic scale, 0 to 9. Those Kk-values are converted to an ak scale, reaching 400, as in **Figure 68**, and the 8 ak-values are averaged to give one value, Ak, for the day.

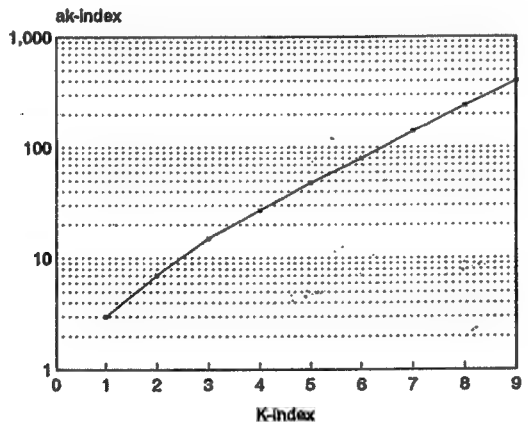

Figure 68 - Relation between the K-index and the ak-index.

In terms of the 24-hour A-index, magnetic activity is described as follows:

Category	A index range	typical values
Quiet:	0< A < 08	usually no K indices > 2.
Unsettled:	08< A < 16	usually no K indices > 3.
Active:	16< A < 30	a few K indices of 4.
Minor storm:	30< A < 50	K indices mostly 4 and 5.
Major storm:	50< A < 100	some K indices 6 or greater.
Severe storm:	100< A	some K indices 7 or greater.

Data from the NOAA magnetic observatory at Boulder, CO is broadcast at 18 minutes after every hour by WWV on 2.5, 5, 10, 15 and 20 MHz. That broadcast gives the latest 3-hour K-index from the Boulder magnetometer, an estimate of the current A-index, the category for the current magnetic activity as well as the current estimate for the 10.7 cm solar flux.

In addition to radio broadcasts, the Internet provides other forms of magnetic data. One of the most useful ones is from the Geological Survey of Canada. They operate 12 magnetic stations across Canada, from coast to coast and into the Arctic. Three years of data from the stations are in archives and the chart recordings in 1-minute intervals for each of the elements in nT, say X, Y, and Z, may be called up quickly.

Beyond those sources of data, there is another network which summarizes magnetic observations on a planetary basis. Thus, the Kp network made up by a dozen stations in the northern hemisphere, from Canada to Germany in **Figure 69**, report planetary averages, Kp and Ap, every two weeks via the Internet.

Figure 69 - Sites in the global Kp network.

Those stations, plus another two in the southern hemisphere, give a measure of the magnetic activity at latitudes near the auroral zone, in response to the energy input from the solar wind.

Since aurora occur during significant magnetic activity, records from high latitude magnetometers, say the Canadian network or Kp stations, may be logged to look for recurrence tendencies and, thus, predict aurora or magnetic activity. That assumes a degree of stability of solar streams as the sun rotates, with a 27 day period. Some success has been achieved with that method,

helping low-band DXers find quiet times for contacts across high latitudes, without disturbances from auroral ionization.

Geomagnetic statistics -

While magnetic and auroral quiet are desired conditions for low-band DXing across high latitudes, magnetic storminess can affect paths across lower latitudes, and more so for major or the severe storms with high values of Ap. In that regard, the integral distribution for the number of storms over five recent solar cycles, Cycle 17 from '32 to Cycle 21 from '87, is shown in **Figure 70:**

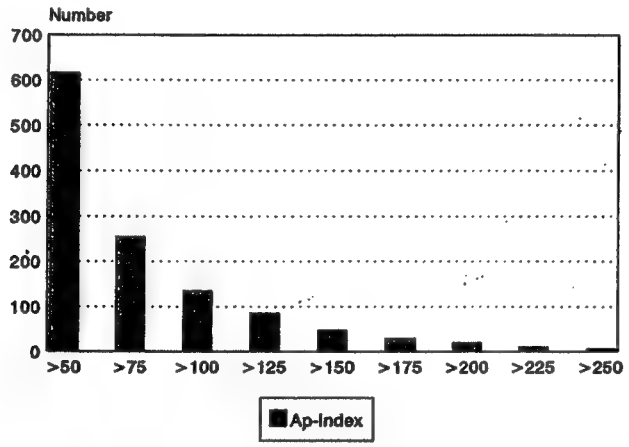

Figure 70 - Number distribution of Ap indices, '32 - '87.

That shows 600+ storms in 55 years or about 1 major storm a month averaged over the period. That may seem like a high figure but the period includes Cycle 19, the most active cycle in the history of solar/terrestrial studies.

The degree of disruption depends on operating frequency. Physically, magnetic storminess reduces ionospheric electron content in the F-region, particularly on high latitude paths. So HF work is disturbed the most from MUFs being lowered. It may last for a day when Kp is around 50 but for storms with Kp greater than 100, it is a major disruption on HF frequencies and has some negative effects on the low-bands too. From Kp greater than 150, ionization electron released from the Van Allen belt begins to appear at mid-latitudes, affecting paths that were immune before.

Those are occurrence statistics, more a matter of record than of any physical significance. But going to seasonal statistics is another matter, showing more features of the dynamics of magnetic activity, how and why the earth's field responds to the solar wind to create magnetic storminess. For that, we have to look at the new model of the earth's field, shown in **Figure 71:**

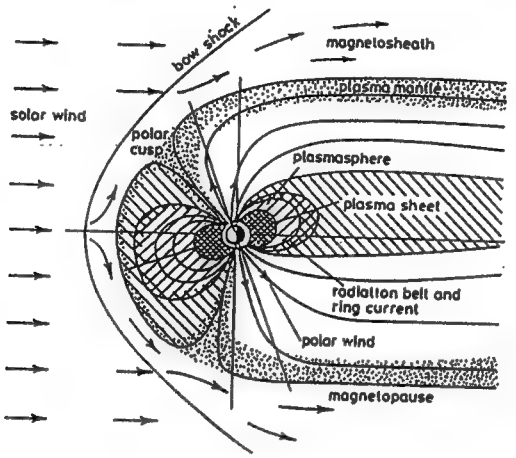

Figure 71 - The new model for the earth's field.

That figure shows the new topology of the magnetosphere, far different that that of the classical dipole - with field lines compressed in the direction of the incident solar wind and trailing away on the side away from the sun. That configuration stays with the earth as it rotates each day. But the magnetic axis precesses around the spin axis and the spin axis is inclined 23.5 degrees throughout the year from the direction perpendicular to the orbital plane, as in **Figure 72:**

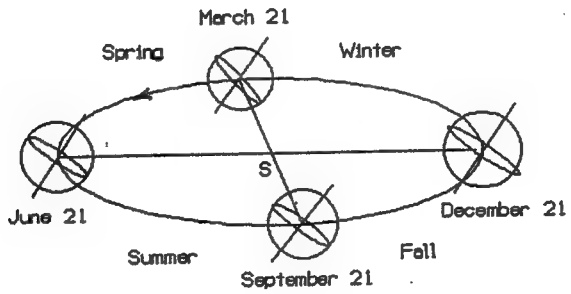

Figure 72 - Seasonal changes in the earth-sun relationship.

Now we consider the seasonal variation of magnetic storminess in **Figure 73.** That figure shows data from 1475 storms over a period of 124 years, from 1868 to 1992:

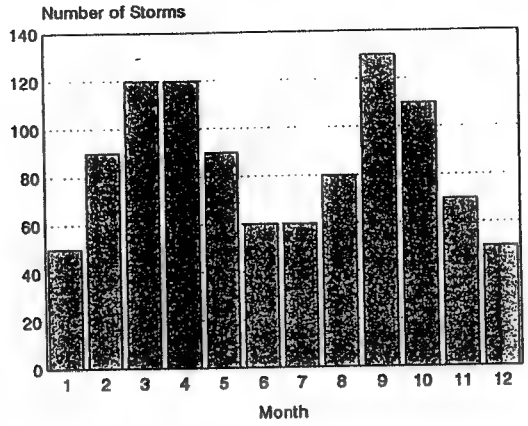

Figure 73 - Magnetic storm distribution by months, 1868-1992.

The data is averaged over 10 solar cycles, Cycle 13 to 22, and shows storms are most likely at the equinoxes, when the solar wind hits the magnetosphere head-on, and least likely at the solstices, when the solar wind hits glancing blows on the hemisphere leaning toward the sun. But magnetic storms do occur throughout the year due to the impact of the solar wind.

Geomagnetic processes -

The current thinking among magnetospheric specialists is a bit complicated but hear it out: the solar wind is made up of protons and electrons, with a density of 5-10 particles/cc, and moves away from the sun at an average speed of 400 km/sec. It carries part of the solar magnetic field along, "frozen" into the plasma because of its high conductivity. When it reaches the front of the magnetosphere, the interaction that follows depends on the direction of the field relative to that of the earth.

The earth's field out in the front of the magnetosphere comes up from the southern hemisphere, crosses the equatorial plane and goes back into the northern hemisphere, just like the distorted dipole field lines in **Figure 71.** If the field carried by the solar wind points north, the same way the earth's field points, nothing happens. But if that field points south, then the two field lines may become "connected" and the field in the solar wind can carry the terrestrial field line back into the magnetotail. That process takes F-region electrons spiraling around the field

lines back into the tail, lowering the electron content of field lines at high latitudes and MUFs for HF propagastion across the region.

At the front of the magnetosphere, the solar wind particles undergo charge separation because of the force on them by the earth's field. That gives rise to electric field across the magnetosphere which is "mapped" back into the magnetotail by the highly conducting plasma in the region. That electric field builds up, finally releasing energy by driving magnetospheric electrons down the field lines, into the high atmosphere where they create ionization and excite atom and molecules to radiate, the optical aurora.

The cross-tail electric field is mapped, in turn, down the field lines to the ionization created by the energetic electrons that excite the aurora; that gives rise to an ionospheric current, the auroral electrojet, recorded by magnetometers on the ground, as in **Figure 74:**

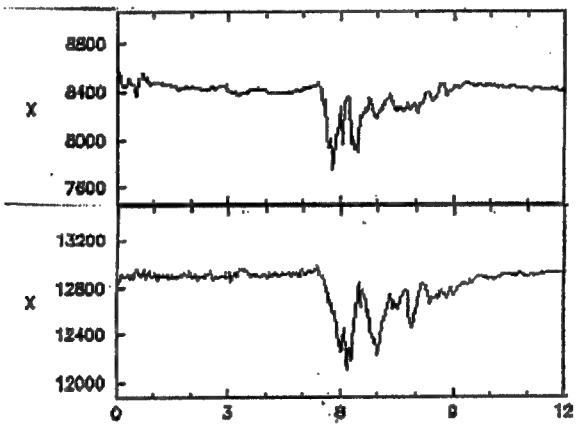

Figure 74 - X-component variations, Churchill (upper) and Meanook (lower). Units are nT.

That figure shows the northward, X-disturbance at Ft. Churchill (upper), and Meanook (lower) in Canada on April 1, 2001. On that date a strong solar wind disturbance gave rise to magnetic storm activity that resulted in an Ap value of 190. The magnetogram traces shown in the figure are but part of the Canadian records.

The X-disturbance at Churchill was −700 nT below baseline while that at Meanook was -600 nT. The same type of disturbance, called a "negative bay" (after the shape of a coastline) was noted as far west as Victoria (-100 nT), east at St. Johns, NF (-100 nT) and north as Baker Lake (-400 nT).

With the large changes in the northward, X-direction, there also were smaller changes in the eastward, Y direction, say the order of 100 NT. As a result, the greater X-disturbance means the electrojet current system was in the E-W direction. But an E-W current system, embedded in the auroral ionization around 100 km, produces changes in the field in the downward, Z-direction. Those changes were +500 nT at Churchill and -500 nT at Meanook; that places the current system between the two stations, as shown in **Figure 75:**

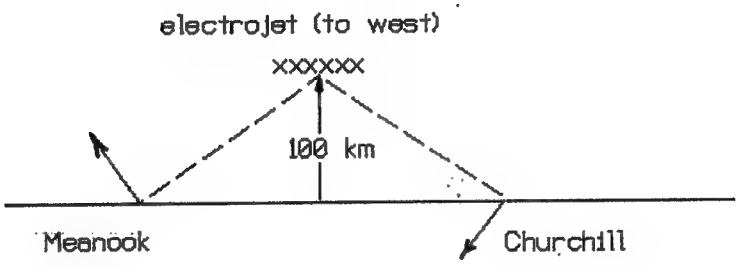

Figure 75 - Magnetic disturbances from a westward electrojet.

That figure has a westward-flowing electrojet at 100 km altitude and shows its disturbance field at Churchill and Meanook. The signs of the Z-disturbance, down at Churchill and up at Meanook, indicate that the current system lies between the two, as shown.

Electrojet currents are not fixed in latitude and their motions can be estimated from the changes in the Z-disturbance. Thus, times like 0900 UTC, when the change in the Z record on the Churchill magnetogram went to zero, correspond to motions that placed the center of the current system overhead.

Auroral absorption

As indicated earlier, the effects at ionospheric altitudes result from the incoming flux of energetic auroral electrons. That includes ionization which absorbs low-band signals crossing high latitudes. Typically, 30 MHz riometers are used to monitor galactic radio noise at high latitudes and can detect absorption due to any auroral ionization which falls within their antenna patterns. The auroral ionization extends over several tens of degrees of longitude and five degrees or so, depending on the level of disturbance. Riometer antennas are typically 3-element Yagis, pointing upward, and they have antenna patterns at the 100 km level which reach -3 dB at about 100 km from their center.

Riometer records were obtained from several Canadian sites during the April 1 event. Those were part of an instrument chain that monitored activity along a longitude line through Churchill. An estimate of the riometer patterns for Churchill (70 N. mag. lat.), Gillam (67 N. mag. lat.) and Island Lake (65 N. mag. lat.) ios given in **Figure 76:**

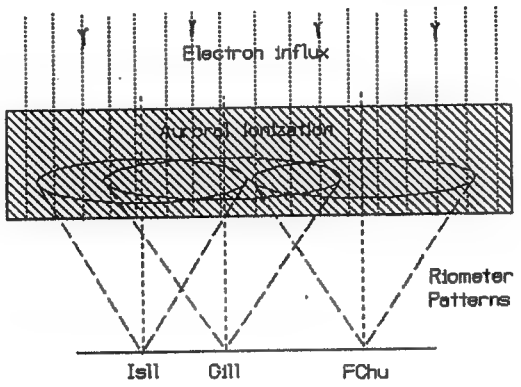

Figure 76 - Auroral ionization relative to riometer antennas.

That figure is a gross over-simplification, showing a uniform block of auroral ionization as well as a vertical electron influx. The electron density profile in that region should go through a peak around 120 km and then drop to low values below 100 km and the electron influx should be spiraling around the field lines at the local dip angle, close to 80 degrees from the vertical direction.

Moreover, the electron influx should be structured in space, showing the rayed forms that are characteristic of the dynamic activity of the aurora around local midnight. That type of activity can be seen in the absorption records from the three riometers, spiky downward excursions in the chart records with increases of absorption, reaching 3-4 dB on 30 MHz at the most southern riometer site, Island Lake, in **Figure 77:**

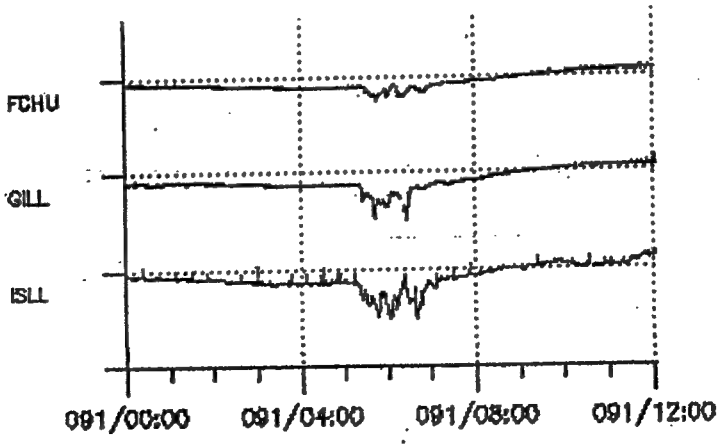

Figure 77 - Absorption records along a N-S riometer chain.

And the records show some spatial structure and movement of the precipitation regions as the absorption begins later at Ft. Churchill; moreover, the peaks in absorption are not coincident in time on the records.

But those records were obtained with broad-beam riomteters. The actual structure of absorption regions is obtained by using imaging riometers, at somewhat higher frequency and with multiple antennas. In that regard, the University of Marylnd has operated (Rosenberg et al, 1991) imaging riometers for ionospheric studies (IRIS) at a number of high latitude sites for a number of years. While the configurations vary from place to place, a 64-element circularly-polarized crossed dipole array on 38.2 MHz has been in operation at the South Pole (-74.2 mag.lat). Signals from the 64-element array are phased to produce 49 independent beams, shown in **Figure 78**, and those are sampled by 7 riometer receivers.

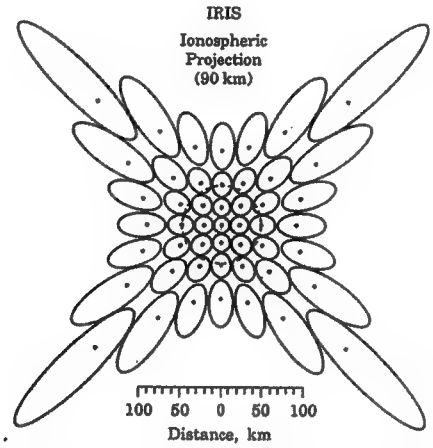

Figure 78 - Projection of the IRIS antenna pattern at 90 km.

The use of broad-beam antennas with riometers does not admit the study of the spatial distribution of ionization in the absorption region nor its motions. With imaging riometers, that shortcoming of the method is removed and, when oriented relative to the earth's field, motions and spatial distributions determined within the resolution of the antenna elements and the riometer sensitivity.

An example of the results of the imaging technique are given in connection with the auroral absorption event at the South Pole in **Figure 79**. That figure shows broad-beam observations on three frequencies and would ordinarily be interpreted as the result of a large precipitation region which either developed and decayed overhead or moved across the fields of view of the broad-beam antennas of the riometers.

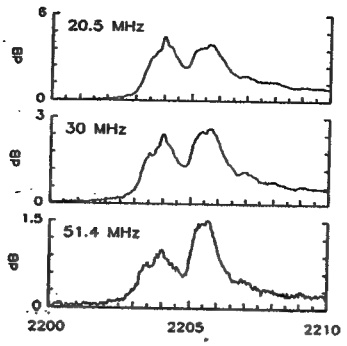

Figure 79 - Absorption records from broad-bean riometers.

By way of contrast, **Figure 80** shows the absorption region moving across the field of view of the imaging riometer:

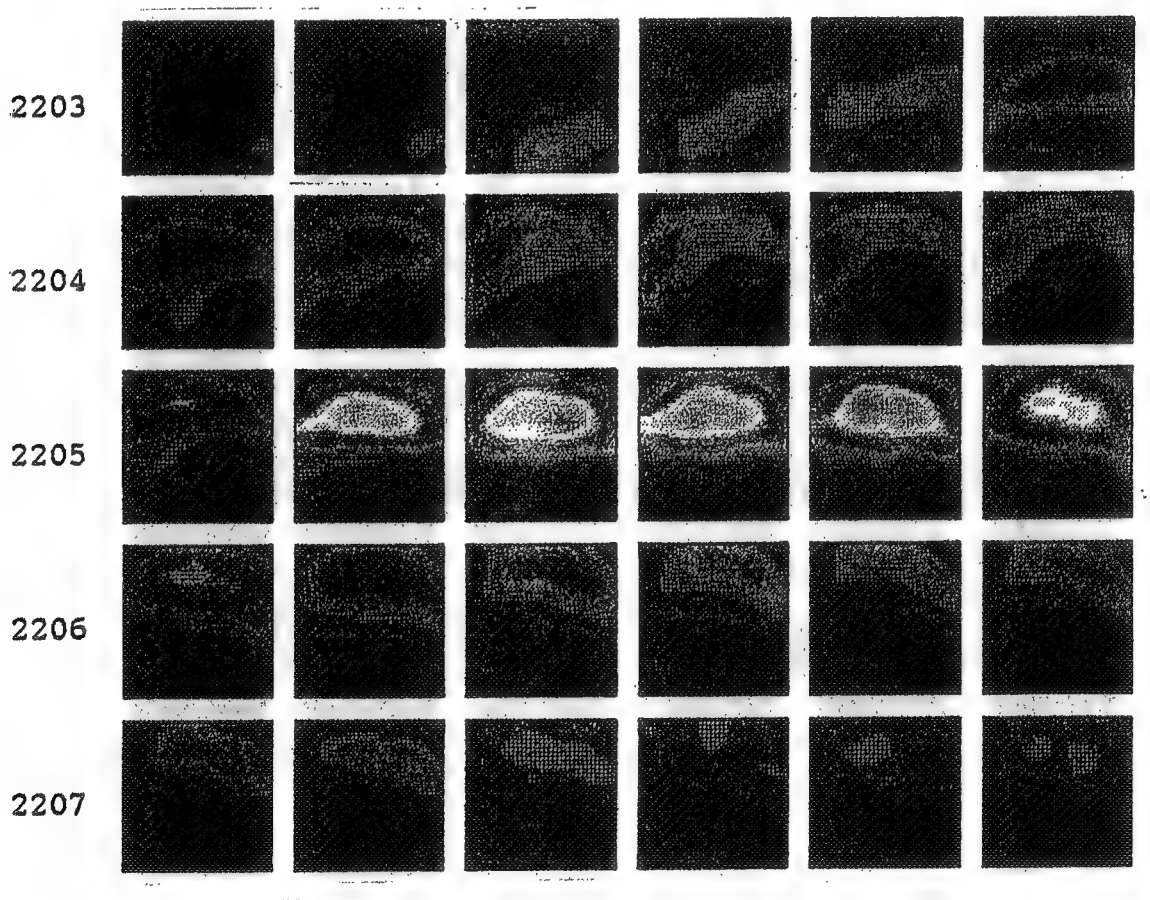

Figure 80 - A 5-minute summary of 10-second samples from the IRIS array during the absorption event in Figure 79.

That figure gives 5-minutes of images, 10 s apart, with the south magnetic pole at the top, the magnetic equator toward the bottom, 0east to the right and west to the left as the ionosphere is viewed from below. The brightest images during 2205 UTC correspond to 10 dB of absorption while fainter patches amount to about 2 dB.

In any event, the absorption region moves, more in latitude than in longitude during that simple, smooth event. But far more structure is found in long-duration, spiky events like that shown in **Figure 77**. Given these remarks, interpretation of auroral satellite maps should be done with care. While the maps suggest electron bombardment throughout the entire auroral zone, it is clear that structure exists when it comes to absorbing regions and they may not be as impervious to low-band signals as they appear.

Now going back to **Figure 70**, it is seen that a storm event with an Ap value of 190 is not an everyday event in solar cycles. So the magnetic excursions are smaller for more typical events, termed auroral substorms, and the same true for the ionospheric absorption. thus, common values would be more like 100-200 nT and 1-2 dB. This may be seen in **Figure 81:**

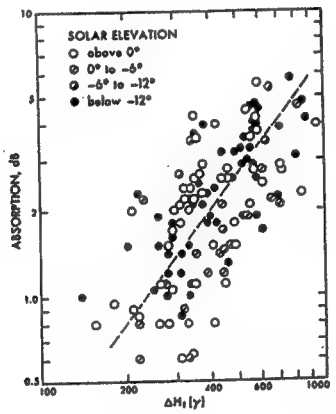

Figure 81 - Absorption vs magnetic disturbance during magnetic bays with current systems centered overhead.

That figure is for a number of sub-storms during Cycle 19 that were selected for their current systems being centered overhead, as mentioned earlier. The study (Brown and Barcus, 1963) was directed at examining whether auroral absorption events showed a day/night ratio like solar proton events but for the moment, it serves our purposes here by providing values of magnetic field and absorption changes that are more typical of activity at auroral latitudes.

In connection with low-band propagation, auroral morphology is one of the most important aspects to consider. Akasofu (1964) has

given a detailed discussion of the development of aurora during sub-storms, from quiet arcs before midnight, to the active, break-up phase around midnight, to the diffuse, pulsating phase in the morning hours, shown in **Figure 82:**

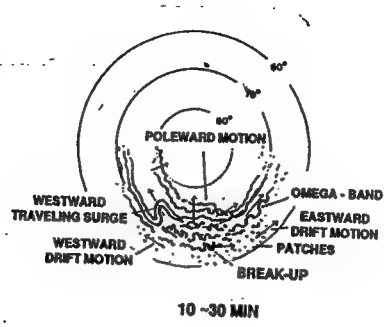

Figure 82 - Auroral forms around break-up at magnetic midnight.

The observations on which that summary was based were obtained with all-sky cameras, another imaging technique. Since all-sky cameras only respond to light emission, they tend to give emphasis to the precipitation of lower energy electrons. Another imaging technique using photometers can give both spatial resolution and, by their placement, also insights (Brown, 2000) into how the bombardment by electrons begins in the magnetotail.

As discussed earlier, this is all the result of electric fields, an unfamiliar subject to low-band DXers, and has the greatest effects in the midnight region. Of course, all these matters are in proportion to the level of disturbance, auroral bombardment moving to lower latitudes and farther into both the evening and morning hours with major disturbances. But for most of the time, those regions are open on occasions to trans-polar propagation, as will be seen in connection with long-path propagation.

Long Path -

On HF Bands -

Long-path propagation on the higher bands is fairly simple to discuss - it is quite common at times of high solar activity as MUFs on paths rise to high levels then. And articles have been written about long-path experiences on the higher bands, Carl Luetzelschwab, K9LA, dealing with long-path to Japan and Australia (Luetzelschwab, 1997) on 10 meters and Jack Emerson, WA4JTE, added his recent work (Emerson, 2002) on 15 meters to the information available. For my part, I did a year-long study on 20 meters, using a total of 1,687 long-path contacts to analyze (Brown, 1992) details of the mode, such as types of paths and the effects of magnetic and solar activity on propagation. On the other HF bands, the information that I am familiar with is more anecdotal in nature, not formally summarized in publications.

Of course, on the higher bands, the definition of long-path is fairly straight-forward - a contact between point A and point B in which the signals go the long way around the earth, more than 20,000 km. At the top of the HF bands, great-circle paths are derived from spherical trigonometry and used to represent actual radio paths, whether short- or long-paths.

Skewing -

At lower frequencies, lateral deviation or skewing of paths by horizontal gradients of ionization becomes important. That is the case as refraction, like absorption, varies as the square of the wavelength, making path deviations on 40 meters some 16 times greater than on 10 meters for a given gradient, etc. The question then comes down to the source of the horizontal gradient, whether solar radiation along the terminator, the sunrise/sunset line, or auroral activity.

The terminator is always present somewhere on the earth's surface so a long-path connection could be affected by it, even aided by taking advantage of propagation along the gray line, the darkness next to the terminator to reduce ionospheric absorption on the path. But auroral activity is a sporadic thing and could rise to the point that auroral ionization is capable of reflecting or refracting signals. In considering the two possible sources, it should be noted that the terminator is not only stable in time but also of a large physical scale. Neither of those attributes can always be used with regard to the aurora.

Auroral ionization is quite variable in time and of variable

spatial structure, particularly in the width and depth of rayed forms. Thus, a broad auroral curtain could be so heavily ionized that it could reflect signals almost like a metal sheet, without appreciable penetration of the curtain, or so lightly ionized that it would allow signals to penetrate it and undergo both refraction and absorption. So it comes down to electron density and scale-size relative to the wavelength of the radiation to choose between the two.

On the transition bands, where both MUFs and absorption are important, long-path connections may fail because signals are skewed away from the desired path or loss of ionization in the F-region. The latter would be due to magnetospheric effects, ionization on field lines lost by being carried back into the magnetotail as field lines on the front of the magnetosphere are eroded away by the solar wind. But it is fairly easy to distinguish between the two causes of a failure; the loss of ionization usually involves several days with little, if any, long-path propagation and the F-region slowly recovers as it refills by photo-ionization while auroral effects are more local, usually of short duration.

On the Low-Bands -

On the low-bands, loss of F-region ionization could be a source of failure of long-path on 7 MHz during intense magnetic activity. That is the case particularly here in North America where the locations determine that a majority of long-paths of interest go across high latitudes. By way of illustration, the long-path study conducted here in the Northwest in '90-'91 had only one sub-auroral path of interest, to South Africa (ZS); all the rest of the long-paths went along the auroral zone, up to 70 S mag lat, or across the polar cap, above 70 S mag lat.

Long-path propagation on 7 and 3.5 MHz are well-known and regarded as a "winter sport" by many DXers. I must admit my own experience on those two bands is very limited, mainly to when I had a high dipole up on a bluff, at about 75 ft above salt water and a clear view toward Europe and Africa. I had my share of long-path contacts but nothing like my experience on 20 meters.

I got into 160 meter long-path questions the hard way, moving down the bands ever so slowly. That was through my interest in HF propagation. It got me into offering advice on propagation to upcoming DXpeditions and when a DXpedition was over, I got to look at all their logs, sort of a reward for my work.

So I worked with Bob Schmeider, KK6EK, and saw first-hand the

results from Peter I, Easter Island and Heard Island. I must say the Heard Island logs had a wealth of information in them, the "dead zone" mentioned earlier and considerable data on long-path propagation on 3.5 and 7.0 MHz. All that was squeezed into a period between two magnetic storms, one a week before the start of the DXpedition and one starting on the very last day of operation.

Then Jeorg Puchstein came along with his DXpeditions, VK9XY, VK9XC, S21XX, P29VXX and ZL7DK. So I got to look atalot of 160 meter logs in what I would call "high activity" situations, where the entire world was looking for a station, such as VK0IR. But look through the logs as I might, I never found a single 160 meter long-path contact, NOT ONE!

After the VK0IR experience with that huge dead zone from ionospheric absorption on 1.8 MHz, Iwas starting to think that long-path was a lost cause on 160 meters. Thus, it looked like 1.8 MHz signals were trapped in the dark hemisphere, unable to refract their way out the top with the ample ionization overhead and blocked by the sunlight that lurked beyond the terminator. In short, it didn't appear that long-path was possible on 160 meters; ionospheric absorption effects were just too great for signals to get out of the dark hemisphere.

But I must say there have been claims from time to time of long-path contacts on 1.8 MHz but they were not in the classical direction, opposite to the short path direction. A brief mention of them was found in a SWL publication (Tippett, 1991), with only one contact on 1.8 MHz prior to the date of publication. That was between W0ZV in Colorado and UA9UCO in Siberia on Sept. 29, 1987. The path was assumed to guided by the terminator, as shown in **Figure 83:**

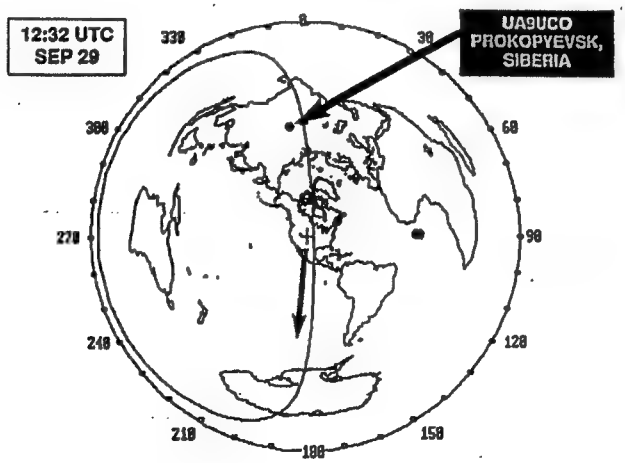

Figure 83 - Azimuthal map with arrow showing the suggested path from W0ZV in Colorado to UA9UCO in Siberia.

Since that time, another seven "long-path" contacts of a similar nature have been claimed, starting with a W0ZV-JJ1VKL/4S7 contact in late 1991 and most recently a N7UA-5B4ADA contact in late 2001. All the dates and times may be found on W4ZV's website:

http://users.vnet.net/btippett/dx_aid_plots.htm

and other such examples are found in a more recent publication (Brown, 2000), an update of my earlier publication on long-path.

As a physicist, that proposed path guided by the terminator did not appeal to either my training and experience nor physical intuition. So, over the years, W4ZV, K1ZM, N4KG and I have gotten into some spirited discussions on the topic. Their arguments came down to defending their observations of signals from the SSW direction at sunrise, as in **Figure 83**, or the SSE directions at sunset. My argument was to the effect that signals would suffer heavy aborption along the terminator and not follow it for long before being refracted into the dark hemisphere and there was no rationale offered as to how signals would reach the far terminus.

Wanting to close the discussion, I wrote up my reasons for not accepting their interpretation and published them in QEX (Brown, 2001). I have said I do not doubt their data but did offer an alternate explanation of their observations, that they were receiving back-scattered short-path signals from those directions. With that, I think I have done all I can do with the problem using the physics of signal refraction.

I have to admit another aspect of that view of long-path propagation came to my attention recently - excessive claims of signal strength on the N7UA-5B4ADA contact. Thus, I was told by N7UA that the "long-path" signals from the SSW direction were S8-S9 here in the Pacific Northwest on December 16, 2001. Again, that went against my intuition since I had recently finished studying signal loss, using the VK6HD-VP9AD contact discussed earlier and shown in **Figure 63**.

The short-path distance for N7UA's contact with Cyprus is 10,000 km and if the contact were "long-path", it would have to be about 25,000 km in length or 15,000 km longer than short-path. That meant the 15,000 km suffered a loss of 6 dB/1000 km for the earth-ionosphere hops in the additional path and 2 dB/1,000 km for any ducted portion of the path. Depending on the mix of modes, that means the S8-S9 long-path signals were 30-90 dB (or 5-15 S- units) WEAKER than the short-path signals. By any standard, that is a conservative estimate and such an awesome signal strength at 10,000 km distance takes the matter out of the realm of a actual reality.

But all the questions about the reality of long-path on 160 meters came to an end with an article by Steve Ireland, VK6VZ, in the March 2001 issue of CQ (Ireland, 2001), even with a QSL for a QSO with the late K1MEM. I carefully checked out all the circumstances of that contact, from Perth, Australia to Sudbury, MA, and came away absolutely convinced it was bonafide long-path contact; except for short distances at the ends, the path was in the dark the rest of the way while the short-path involved almost 20,000 km in sunlight, in **Figure 84**.

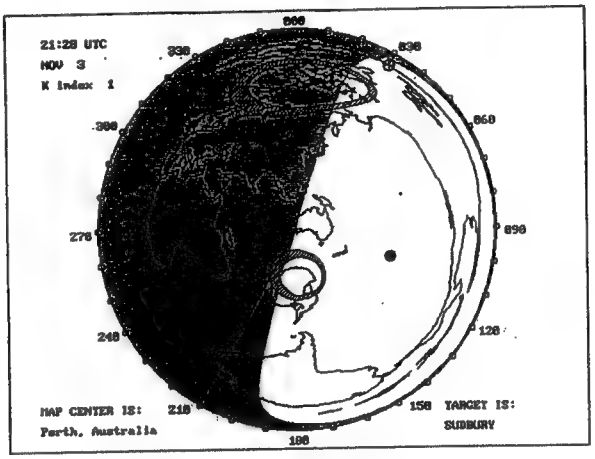

Figure 84 - Azimuthal map showing long-path from VK6VZ to K1MEM.

So I got ahold of Steve and Mike, VK6HD, to learn what other secrets they might be keeping up their sleeves and they kindly provided me with their 160 meter logs for a 20 year period.

It didn't take long to realize that I had an absolute gold mine in my hands; but it was not exactly what I thought, all about long-path contacts (Ireland et al, 2002). It turned out the VK6HD logs contained two types of long-haul DX contacts, the majority with VE1ZZ in Nova Scotia and others with locations in the northeastern part of the USA, like the K1MEM contact by VK6VZ.

The majority of the contacts with VE1ZZ were short-path in the period after the autumn equinox, September to March when the northern polar cap is dark. Those contacts were more than 150 in number but there were also some contacts in the log after the spring equinox, April to September. The northern polar cap is in sunlight then and so those contacts could only be made via the southern polar cap, long-path. So I was looking at equinoctial path-switching (Ireland et al, 2002), a new idea with regard to propagation, especially on 1.8 MHz.

The contacts both VK6s had with northeastern USA proved to be long-path, even between September and March; the difference was due to longitudes and how that influenced the paths. So there it was, finally some long-path on 1.8 MHz but the intriguing thing was how it was there all along; it simply came out in the open from a review of existing log data and no need to make any sort of speculations about it as a possibility. It was true!

But now the question is "how much farther?" The VK6-VE1 experience shows long-path propagation for 1.8 MHz signals out to 22,000 km, a few thousand kilometers into the sunlight beyond the dark hemisphere. Beyond that, there may still be a physical limit to low-band propagation - a distance where ionospheric absorption, noise and receiver sensitivities can no longer come together and still give readable signals. We will need some more long-haul contacts, non-auroral in nature, to finish the analysis. So the next solar minimum should be very interesting.

But Dxpeditions will be the key, particularly if locations are chosen that take into consideration the demographics of the matter. To give an example, around the equinox of 2001, Roger, G3SXW, (personal communication) made a trip to Chatham Island and operated on 3.5 Mhz, dawn and dusk. The results was about 150 long-path contacts with Europe and the U.K. The distribution of the contacts is shown in **Figure 85:**

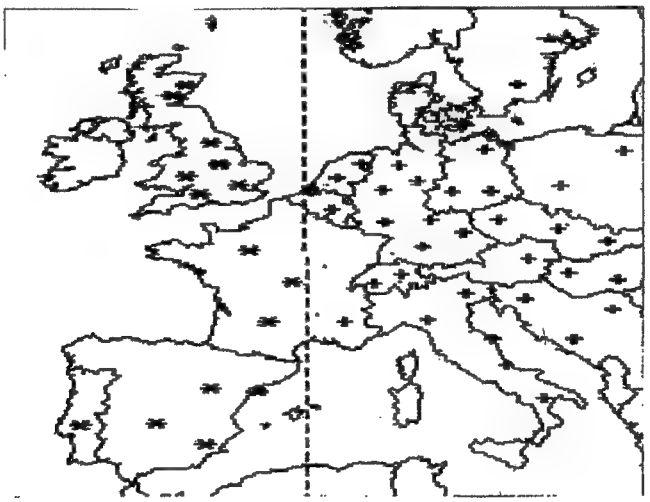

Figue 85 - Long-path contacts on 3.5 MHz from ZL7/G3SXW:
at ZL7 dawn (right "+") and ZL7 dusk (left "*")

By way of contrast, the earlier K5K Dxpedition to Kingman Reef did not work any long-path on that band; it was too close to significant amateur populations and found nothing available at long-path distances.

Chemistry and Low-Band DXing-

Ions, Atoms and Molecules -

Low-band DXing is best done at night during solar minimum. At times like that, the ionosphere is changing slowly, after sunset and before the next sunrise. In the lower ionosphere, where low-band signals are propagated, the main ionospheric reactions at night are related to the recombination of remnants from processes when the sun was up, like photo-ionization and photo-dissociation of the permanent constituents, molecular nitrogen and oxygen, as discussed earlier.

Beyond that, changes in low-band propagation take place on other slow time-scales, changes with the seasons and the solar cycles. Those are astronomical or astrophysical in origin and no great mystery, at least at first glance. But those changes also involve the chemistry of minor constituents, like ozone and water vapor. So the chemistry of the H-N-O atmosphere and the time-scales for its chemical reactions are important as well as how the solar spectrum changes with time and solar cycles.

But the DXer takes most of those changes on faith or long experience, not worrying about how ozone and solar UV affect the ionosphere and low-band DXing, much less the time-scales for all the other important chemical reactions. In that regard, the DXer is lucky in the sense that the relevant reaction rates are all fast compared to those time-scales, so the DXer's atmosphere and ionosphere are going through quasi-equilibrium states in the course of a day, month, year, season or solar cycle.

The DXer takes the solar spectrum on faith too, knowing that it will produce the atmosphere and ionosphere relied on for DXing, day in and day out. Lost in the process are the details, that it takes solar photons of less energy to break up molecules like ozone and molecular oxygen (<11,000 A and <2,422 A, resp.) than molecular nitrogen (<1,270 A), where 10 A = 1 nanometer. In addition, it takes solar photons of much greater energy to ionize molecules, say those of nitrogen and oxygen (<796 A and <1,026 A, resp.) and nitric oxide and atomic oxygen (<1,340 A and 911 A, resp.) than to break up molecules into their constituent atoms.

But time-scales of chemical processes and the energy of solar photons become important when changes take place faster than those slow astronomical events that DXers are used to, say if a solar eclipse blocks solar radiation for a brief period or if a major solar flare takes place with energetic solar Xrays wiping out signals by ionizing the sunlit half of the earth. Then more ozone

is formed in the dark of a solar eclipse by a three-body combination process:

$$O + O_2 + M \text{ ----> } O_3 + M,$$

with M a neutral particle (N_2 or O_2), or the major constituents of the ionosphere are ionized:

$$N_2 + \text{photon } (<796 \text{ A}) \text{ ------> } N_2^+ + e^-$$
$$O_2 + \text{photon } (<1,026 \text{ A}) \text{ ----> } O_2^+ + e^-$$

by bursts of solar UV and Xrays.

When that is the case, the time-rate of gain of products like O3 and ions created are then determined by looking at both their rate of production, as given above, and the rate of loss from destruction reactions, e.g., the loss of ozone by collisions with atomic oxygen and dissociation by infra-red photons:

$$O_3 + O \text{ ----> } 2\ O_2$$
$$O_3 + \text{photon } (<11,000 \text{ A}) \text{ ---->} O_2 + O$$

and the loss of positive ions by recombination with electrons:

$$e^- + N_2^+ \text{ ----> } N + N$$
$$e^- + O_2^+ \text{ ----> } O + O$$

Then, all that is needed is a simple equation saying that:

rate of gain = rate of production - rate of loss.

Ionospheric Modification -

If one goes to the current literature, say Davies' book on Ionospheric Radio (1990), there are a number of other things that can change the properties of the ionosphere, some are of natural origin - auroral activity, solar proton events (like those of November 2001), and ash from volcanic activity - that propagate up to or across ionospheric altitudes to affect the ionization layers or block the solar radiation which creates the ionosphere..

Auroral activity frequently affects the distribution and level of ionization, raising the electron density in the narrow range of auroral latitudes and, in turn, will increase absorption and give rise to wave skewing or reflections. Those modifications have a "signature", a decrease in the magnetic field at the earth's surface, easily recognized in the records of auroral zone magnetometers.

Solar proton events, on the other hand, can disturb entire polar caps, putting ionization down deep in the D-region, and stifle propagation by increasing absorption by HUGE amounts. Moreover, solar proton events may last for days on end, instead of just an hour or so, as with auroral events. Their "signature" is found as a complete shut-down of propagation across polar caps.

Much less apparent to us are the shifts or tilts of the ionospheric layers due to weather effects coming up from below; the problem there is we just have no wind measurements at those altitudes to tell us what is going on. That is part of the unpredictable aspects of low-band propagation (Brown, 2001).

But what about changes of man-made origin that persist in time; that's another matter. There, we're usually dealing with some large-scale event, like a chemical or nuclear explosion, atmospheric pollution or the launching of a major space vehicle in the middle of a DX contest. But the first man-made modification was a day and night affair, the Luxembourg Effect in the 1930s when a powerful radio signal modulated the ionosphere which was carrying another signal from A to B.

Thus, a powerful broadcast station (200 kW on 252 kHz) in Luxembourg was heard by cross-modulation of signals going from Switzerland to Holland on 650 kHz. That modulation was at audio frequencies and just about everybody in ham radio has heard about that effect! Less well-known is that analysis shows it involved changes in index of refraction of the ionosphere from electron heating by the electric field of the Luxembourg signal.

The days of powerful broadcast stations like WLW's 500 kW in Cincinatti are gone now. But electric fields at frequencies below the broadcast range give another type of ionospheric heating, from powerful VLF stations operated by governments at sites across the globe which serve their military communications needs. A recent theoretical investigation (Rodriguez and Inan, 1994) of that question has even shown the extent of the region above a VLF station that produces electron heating or enhancement of the electron-neutral collision frequency in the ionosphere .

For example, transmitters like NAA (1,000 kW) at Cutler, ME, or NLK (850 kW) here at Jim Creek, WA heat patches of the overhead ionosphere which are conical in shape, doubling the collision frequency between electrons and neutral constituents at 87 km. The collision frequency then drops back to ambient values at greater altitudes and out at around 200 km from the center of the transmitting antenna.

Electron heating of a part of the ionosphere changes the ion chemistry there. For VLF heating, the D-region is affected, giving rise to a reduction in electron density. The mechanism is due to increased electron loss by negative ion formation from three-body attachment of electrons with molecular oxygen:

$$e^- + O_2 + M \longrightarrow O_2^- + M$$

(where M is O_2 or N_2) in competition with collisional detachment by atomic oxygen:

$$O_2^- + O \longrightarrow O_3 + e^-$$

Electron heating increases the rate of electron collisions with neutrals, thus increasing the rate of three-body attachment. But the rate of collisional detachment by neutral atomic oxygen is not affected by electric fields so the electron density decreases due to the greater rate of formation of negative ions. Electron heating itself is very rapid but the time-constant for electron attachment and changes in the chemical composition of the region is close to 100 seconds so that is the time-scale for electron density reduction when the VLF E-field is turned ON.

For the 1,000 kW transmitter at Cutler, ME, the E-fields above the transmitter reach 50-100 mV/meter and the electron density loss is about 25% in a steady-state. The extent of the heated region over NAA is shown with respect to a 2,000 km path in the northeast region of North America in **Figure 86.** With ON/OFF transmisions to Gander, NF, heating effects on the amplitude and phase of 21.4 kHz signals from NSS were observed in 1992.

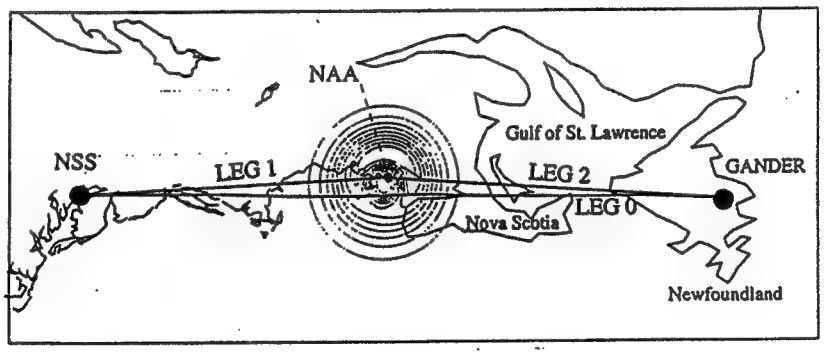

Figure 86 - VLF heated region over the NAA transmitter.

Auroral modification-

Equally well-known are the auroral modifications, electron

density increases from auroral bombardment, cited above. But much less familiar are the decreases in electron density which may result from the heating of positive ions by auroral E-fields. Those E-fields, reaching 50-100 mV/meter and comparable in magnitude to those above megawatt VLF transmitters, extend beyond regions of high electron influx and impart energy to O+ ions between collisions with neutrals above the E-region.

That increases their effective ion temperatures up to 1,500 K or so and as far as chemical interactions are concerned, that leads to a huge increase in the exchange of charge with nitrogen and oxygen molecules and increases in molecular ion densities:

$$O^+ + N_2 \text{ ----> } NO^+ + N$$
$$O^+ + O_2 \text{ ----> } O_2^+ + O$$

Those ions recombine with electrons:

$$e^- + NO^+ \text{ ----> } N + O$$
$$e^- + O_2^+ \text{ ----> } O + O$$

at a rate which is much faster than radiative recombination of electrons with O+. As a result, the enhanced recombination from ion heating may lower the electron density by as much as 25%, producing "polar holes" (Kelley, 1989).

With that, one can understand how d.c. electric fields may reduce the electron densities above the 100 km level in polar regions. That, in turn, raises iso-frequency contours of the plasma frequency in the region, lengthening hops of low-band DXer's signals of a given EVF that are crossing the polar caps and, to some extent, lowers ionospheric absorption there too.

The positive ions are heated more by d.c. rather than a.c. E-fields as they are too massive to respond to fast time-varying E-fields in the VLF part of the radio spectrum. The time-scale for electron density reductions at low-altitudes due to positive ion effects is shown in the lower curve of **Figure 87.**

But at higher altitudes, where collisions with neutrals are far less frequent due to the lower density, electrons do respond to d.c. E-fields and are raised to temperatures around 2,000 K, well above those of positive ions. The electron recombination rates with NO+ and O2+ ions are reduced at higher temperatures, with the result the electron density no longer decreases but, instead of increases at higher altitudes, as shown by the upper curve in **Figure 87.**

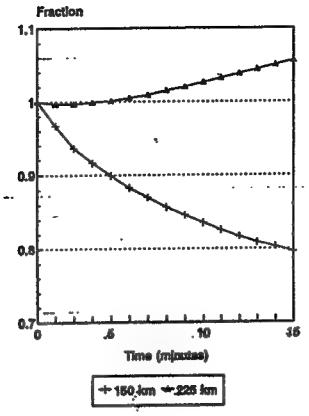

Figure 87 - Electron density variations from auroral E-fields.

The ionospheric "hot spots" due to VLF transmitters are probably too few in number to affect low-band DXing but their detection on VLF circuits gives credence to the lowering of electron densities in the polar caps due to comparable electric fields of auroral origin. But even more powerful support comes from the 160 meter contacts across the polar caps to VE1ZZ by VK6HD and VK6VZ (Brown, 2001); the majority of those contacts were for dawn-to-dusk paths, free of the break-up region in **Figure 82** and not just limited to solar minimum, as shown by **Figure 88:**

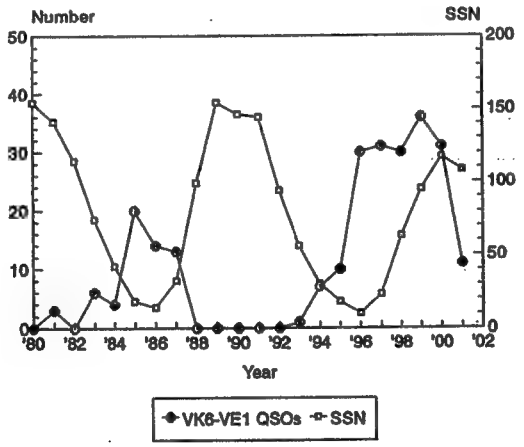

Figure 88 - SSN variations relative to VK6-VE1 QSO dates.

Negative ions -

Ion chemistry is important to low-band propagation not only in the polar regions but also in mid-latitudes, with the effect that negative ion chemistry has on ionospheric absorption. As mentioned earlier, the electron density in the night-time D-region is lowered by formation of negative ions and negative ion-electron ratios may

reach as high as 10-100 before dawn. Those negative ions remove electrons from absorption processes as they are too massive to respond to passing signals. With dawn, the electrons undergo photo-detachment but are bound so tightly as to require UV photons for the process. Thus, the low-band DXer gets a "bump", a delay of 15-30 minutes in the onset of absorption at sunrise, as the electrons remain attached until solar UV rises past the ozone layer, about 40 km above ground level.

Of course, that means ozone chemistry is of importance to the low-band DXer. But the formation of negative ions is not a simple process as it involves other constituents than just oxygen. So minor constituents play a role too but may differ in their origin, some man-made and others natural. Those of man-made origin will be quite variable in concentration and their distribution may subject to the vagaries of transport by weather systems. As a result, there may be "bottlenecks" along the reaction chain, affecting the formation of negative ions (Brown, 1999), as shown by the reaction scheme in **Figure 89:**

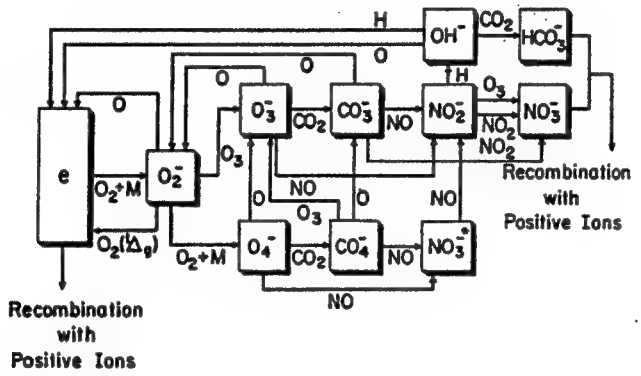

Figure 89 - Negative ion reaction chain during darkness.

The negative ion formation considered thus far was in the night-time D-region and photo-detachment was attributed to UV from the sun rising above the ozone layer. That was not always understood, particularly when it came to solar proton events, and efforts to use visible radiation to detach electrons ended in failure. Thus, UV became important when solar protons deposit large amounts of ionization in the D-region. But until UV gets to the D-region, electron attachment reduces electron densities by factors of 4-5, resulting in the night-time recoveries in absorption shown in **Figure 67**. In that regard, negative ion formation during solar proton events is to the advantage of the low-band DXer and depends on the strong electron affinity of some constituents in the D-region.

Auroral events are another way in which a natural source may deposit ionization in the ionosphere and affect low-band DXing. But the particles are different, electrons vs protons, and the altitudes where the ionization is deposited, E-region vs D-region, each have their own chemistry. Thus, electrons deposit ionization above the 100 km level, a region rich in atomic oxygen.

Going back to the reaction scheme in **Figure 89**, it is clear that atomic oxygen works against the formation of negative ions. And that was found to be the case (Brown and Barcus, 1963), the data given in **Figure 81** showing no day/night effect when it came to auroral absorption. Thus, in contrast to solar proton events, there is no reduction in electron density in auroral events due to negative ion formation as that is something that happens only at lower altitudes, in the D-region, a region lacking in large amounts of atomic oxygen.

Positive ions -

Positive ions are found throughout the lower ionosphere but like negative ions, they undergo a change in composition in nature in the D-region. Thus, instead of always showing up as ions of O2, N2 or NO, below 80 km they appear as water-cluster ions, H+(H20)n. That result came as a total surprise in 1965 but our knowledge has progressed to where they are included in reference ionospheres now.

The production of those ions start with reactions like

$$H_2O^+ + H_2O \text{ ----> } H^+(H_2O) + OH$$

and followed by clustering with other water molecules. Water vapor ions are not a major constituent ion the lower so reactions with O2+ are important too (Reid, 1978) and can also lead to cluster ions. In addition to formation reactions, the recombination rates of cluster ions have been studied and found roughly a factor of 20 times greater than rates for molecular ions, O2+, N2+ and NO+.

For low-band DXers, the formation of negative ions and greater electron recombination rates of water cluster ions at the lower altitudes in quiet times would serve to reduce the electron density, to the low- band DXers benefit. But the target abundance of major constituents is several orders of magnitude greater than that of water vapor. As a result, in non-equilibrium situations such as solar proton events, the rate of ionization of water molecules in the D-region is much smaller than for the major molecules, shifting the transition altitude to cluster ions downward by 10 km or so.

Propagation predictions -

Basic modes -

There are three modes by which radio waves are propagated - refraction, reflection and scattering. Wave refraction by the ionosphere is the mode most commonly used and the best understood, at least in the HF range. Thus, there are a host of propagation programs which take basic input like date, time, sunspot number and path to provide predictions for the user by using rraction. For radio amateurs, that all got started with the MINIMUF program back in '82, went on to the work of Raymond Fricker of the BBC in the mid-80s and then settled down to IONCAP and the derivatives based on it, such as Capman, VOACAP and ICEPAC.

The F-layer algorithm in Fricker's work served as a basis for a number of MUF programs, including MINIPROP, IONSOUND and DXAID. More recently, the CCIR and URSI reference ionospheres from IRI 90 have been used directly in DXAID Version 5.0 and even that will be updated in the near future now that IRI 2001 has been released.

For the HF DXer, the MUF programs are of great help, using global maps of critical frequencies, foE and foF2, and sensible methods based on control points, to predict MUFs on paths. Man-made noise and signal loss are included too and the user HF obtains a reasonable estimate of when paths open and close. But sight must not be lost of the fact that those are statistical predictions, based on median (50%) values of critical frequencies; fluctuations the order of 15-20% may occur. But MUF failure on the high bands can be gotten around at times by using side-scatter of signals.

Of course, MUF programs are not necessary for work on the low-bands so the low-band DXer would seem to be without guidance when it comes to propagation matters. But heavy absorption makes it necessary to operate in night-time hours and the LoProp mapping utility in DXAID makes use of that, allowing the user to see when paths open and close with the advance of darkness. This is done by having the dark hemisphere advance in time, say on an azimuthal map, at a rate chosen by the user; that way the user can see when the path would be open, when it would close because of sunrise and the availability of other paths as well.

In the low-band region, signal propagation breaks down into two basic components, steady or background and variable. The background component results from the reflection or scattering of signals by the fixed structures along paths - mountains, plains, calm oceans and the like. Reflection can be specular, as with a mirror, or diffuse, going in all directions from a rough surface,

and close to scattering. But with close to 80% of the earth's surface covered by water, those reflections and scattering play a large part in low-band DXing.

The variable component takes place more at ionospheric heights but includes reflection and scattering along with refraction. But ionospheric reflection and scattering are both sporadic in time and chaotic in nature - from the ionization during rayed aurora and ionospheric irregularities due to auroral heating during strong magnetic storms; what little prospect there is for making predictions comes down to aspects of refraction.

For that, the ionosphere has to be electrically neutral with the same positive ion density as electron density; but the positive ions are outnumbered by neutrals by at least a million to one and with a high collision rate between the two, it is simply inescapble that positive ions will follow neutrals in their motions and electrons tag along by Coulomb attraction. So the electron density in the lower ionosphere is meteorological in character or nature, not often at rest nor always parallel to the earth's surface.

Ionospheric refraction can still be viewed as an orderly process so long as the electron density varies slowly over a region that extends at least a wavelength in all directions. On the 1.8 MHz band, the distance is at least 160 meters and is much more demanding on stability of the ionosphere than when the same ideas are applied on the 10 meter band.

Beyond questions of stability, the theoretical approach to refraction on the low-bands must include the geomagnetic field as the operating frequency, particularly on 1.8 MHz, is very close to electron gyro-frequencies in the earth's field. Prediction programs cited above go down to 3 MHz but only deal with waves having linear-polarization and not the elliptical polarzation that comes from effects of the earth's field. But that has been addressed by scientists in the Central Radio Propagation Laboratory (CRPL) in Boulder and their work is now found in the PropLab Pro program (Oler, 1996).

That program is more of an aid, not a prediction tool, that is used in interpreting low-band propagation. With more than enough ionization overhead, MUFs are not a concern on the low- bands and the PropLab program is used to show ray-traces from magneto-ionic propagation and ducting, skewing and calculate signal absorption, as was done earlier with the VK6HD-VP9AD QSO.

Those remarks really point to the idea that low-band propagation is unpredictable because, at the moment, we lack the

knowledge of the variables which describe the atmospheric motions at the altitudes where low-band signals are refracted. But predictions look forward in time and it is possible to do a bit of that with the solar/terrestrial conditions which have an influence on the ionosphere, from the result of impacts of the solar wind on the magnetosphere.

Nowcasting -

To see that, we have to turn to magnetic activity and the K-indices used to describe it. Values of those indices from the Kp network are considered to give a measure of the energy input to the auroral regions from the solar wind. But the solar wind reaches the earth's orbit by following an Archimede's Spiral of interplanetary field lines rooted on the sun, as in **Figure 90**, and the sun sweeps those field lines past the earth as it rotates with a period of about 27-days. The streaming of the solar wind along such structures is termed the "garden hose" effect and as the solar wind varies in speed and density, the energy input to the earth shows increases and decreases with the rotation of the sun.

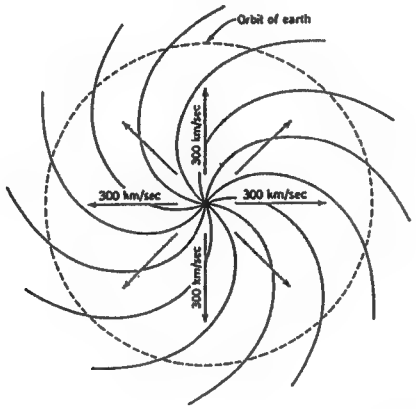

Figure 90 - Archimede's Spiral of interplanetary field lines.

But solar streams are not always short-lived so recurrences do develop in the records of magnetic activity and can be used to predict high and low levels of disturbance on the earth. The recurrences are associated with solar streams that come from coronal holes on the sun and tend to be more frequent in the declining phases of a solar cycle. But they can occur at other times, as may be noted from the current data.

That brings up the idea of "nowcasting", working with short series of current data points, instead of trying to "forecast" from a much larger collections of observations. Thus, using short series of K-sums or A-values from an auroral magnetometer, one

could look to use recurrence tendencies to predict just when ionospheric disturbances of magnetic/auroral origin would be at a minimum for low-band DXing on paths across high latitudes.

Success of predictions with short series of data points improves with any reorganization of the data analysis that takes advantage of even a suggestion of recurrence already in the short record. An example is given below which looks at the distribution of planetary values, Ap, for magnetic activity and illustrates that aspect of the method for the '01-'02 DX season on 160 meters.

The DX season on 160 meters begins with the fall equinox. Using Ap-indices from high latitude records, one can look at three levels of ionospheric disturbance: low (Ap<10), fair to poor (10<Ap<50) and high (Ap>50). With a superposed epoch analysis on a 27-day basis, the levels of activity during the first three rotations of the season may be distinguished symbolically by using "X" for Ap>50, "x" for Ap>25, "o" for values in between 10 and 25 and "-" for Ap<10.

For the first three 27-day solar rotations in '01, we have:

```
          Oct 28 xooox--oXooooo---oooooxo-oox
'01     - Oct 1  xxxxoo-ooooxoooo--ooxxo-o-o
          Sep 4  ooo-o--ooooxoooo--oxooxooxo
                 |+++|++++|++++|++++|++++|++
           Day # 1   5    10   15   20   25
```

The short display shows a recurrence of quiet on two days, #7 and #17. But the geophysical effects at high latitudes result from the impact of the solar wind on the front of the magnetosphere. That may vary from the effect of solar wind speed on the garden- hose angle of the solar wind or the solar latitude of origin as rotation speed varies, from 24-days at low solar latitudes and up to 33-days at 75 degrees. So for completeness, superposed epoch displays are shown for solar rotations of 26, 27 and 28 days:

```
          Oct 25 -oxooox--oXooooo---oooooxo-
26-days   Sep 30 oxxxxoo-ooooxoooo--ooxxo-o
          Sep 4  ooo-o--ooooxoooo--oxooxoox
                 |+++|++++|++++|++++|++++|+
           Day # 1   5    10   15   20   25

          Oct 28 xooox--oXooooo---oooooxo-oox
27-days   Oct 1  xxxxoo-ooooxoooo--ooxxo-o-o
          Sep 4  ooo-o--ooooxoooo--oxooxooxo
                 |+++|++++|++++|++++|++++|++
           Day # 1   5    10   15   20   25
```

```
            Oct 30 oox--oXooooo---ooooxo-ooxo--
28-days     Oct 2  xxxoo-oooooxoooo--ooxxo-o-oxo
            Sep 4  ooo-o--ooooxoooo--oxooxooxox
                   |+++|++++|++++|++++|++++|+++
             Day # 1   5   10   15   20   25
```

After three of the 27-day rotations, there is a good show of recurrence tendency, with expectations of magnetic or ionospheric quiet to occur on the next rotation around day #7 (Nov 27) or around day #18 (Dec 7). On the other hand, the 26-day record gives a "nowcast" that is a bit better in early December than the late days of November:

```
            Nov 20 ooxo-----oooooooo---o--ooo
            Oct 25 -oxooox--oXooooo---ooooxo-
            Sep 30 oxxxxoo-oooooxoooo--ooxxo-o
            Sep 4  ooo-o--ooooxoooo--oxooxoox
                   |+++|++++|++++|++++|++++|+
             Day # 1   5   10   15   20   25
```

For the 160 meter DX contest season, from early December to late January, the Day 18 recurrence did continue being a bit more consistent when data was organized on a 26-day basis:

```
            Mar 4  oxxo--oooo----oo----x-o---     '02
            Feb 6  xooooooo---oooooo-ooooxooo
            Jan 11 xooooooooooooo-oooo--oox-ox
            Dec 17 ooo-oooxooooooxooo----oo-ox
            Nov 20 ooxo-----oooooooo---o--ooo
            Oct 25 -oxooox--oXooooo---ooooxo-
            Sep 30 oxxxxoo-ooooxoooo--ooxxo-o
     '01    Sep 4  ooo-o--ooooxoooo--oxooxoox
                   |+++|++++|++++|++++|++++|+
             Day # 1   5   10   15   20   25
```

than on a 27-day basis:

```
            Mar 13 o----oo----x-o---oo????????    '02
            Feb 14 ---oooooo-ooooxooooxxo--ooo
            Jan 18 oooooo-oooo--oox-oxxoooooooo
            Dec 22 ooxooooooxooo----oo-oxxooooo
            Nov 25 o-----oooooooo---o--ooooo-o
            Oct 28 xoooox--oXooooo---ooooxo-oox
            Oct 1  xxxxoo-ooooxoooo--ooxxo-o-o
     '01    Sep 4  ooo-o--ooooxoooo--oxooxooxo
                   |+++|++++|++++|++++|++++|++
             Day # 1   5   10   15   20   25
```

Beyond that, for the entire '01-'02 DX season, organizing the Ap data on both 26-day and 27-day bases shows that Day 18 recurrence did continue on for 8 solar rotations while the quiet for Day 7 essentially died out after 4 rotations.

That was predictions of magnetic/auroral quiet at high latitudes, where the solar wind makes its impact on the magnetosphere. On the HF bands, the technique of looking for recurrence tendencies can be used to find times of high critical frequencies, simply by plotting up 10.7 cm solar noise from active regions as they rotate across the solar disk. The physical basis for that is different, EUV from the sun and not the solar wind, so superposed epoch analysis method cannot be used as 10.7 cm data is more open-ended, flux values ranging from 65 to 300. But recurrences are still a good way in looking for days with high MUFs.

Satellite studies -

Another approach to looking at magnetic/auroral activity involves getting estimates of energy input to high latitudes from NOAA satellite data of electron influx instead of qualitatively from Kp data. In that regard, satellites like NOAA 14 carry instruments sensitive to the electron energy range that gives rise to the aurora, up to about 20 keV. Individual passes of the detectors across the both polar caps can be seen but statistical results from thousands of passes are more helpful in regard to understanding of the level of activity, as in **Figure 91:**

Figure 91 - NOAA 14 satellite pass across the northern polar cap.

That shows the detector data for a pass across the polar cap from Novaya Zemlya to Nova Scotia. The dotted lines to the left of the satellite track give a measure of the energy of the electrons recorded by the detector at that point while the solid line to the right of the track gives a measure of the amount of energy flow into the atmosphere at the moment. The pass in that figure had a power input of 75 GW.

From the statistics of thousands of polar passes, the data is converted to an estimate of the total power (in Gigawatts) that is deposited by the particles in the entire auroral region; that, in turn, is converted to an activity index, from 1 to 10, and related to the Kp-index:

Power (in GW)	Activity index	Kp-index
4-6	3	1+
10-16	5	2+
24-69	7	3+
61-96	9	5-

That particular pass was at 1150 UTC and with the sun up over western Europe, the satellite pass across the polar cap was from dawn to dusk and the greatest auroral energy input is over western Canada and Alaska.

The reader may see current passes by going to:

http://sec.noaa.gov/pmap

and selecting which hemisphere to view. In addition, there is background material available to explain how the auroral activity patterns are created.

But one note of caution; the PMAP auroral patterns are of a statistical nature, predicting the power input to the auroral zone, even the energy input for auroral particles, from 0 to 10 erg/sq.cm. But probabilities are just that, averages, and do not reveal actual auroral structure at a given time, seen by the eye and imaging techniques, such as all-sky cameras, photometers and riometer arrays.

So the solid colors in PMAP patterns are somewhat misleading. They are not impenetrable; there are openings in the "auroral curtains" and signals can get through. The best example I can point to, supporting that idea, is the 200+ dawn-to-dusk contacts across the auroral ovals that VK6s had with Nova Scotia over a 20-year period, with K-indices averaging 2 but ranging up to 4.

Lower latitudes -

The discussion thus far has dealt primarily with high latitudes. Low-band propagation across lower latitudes may be disturbed but not to the same extent as at high latitudes since field lines containing ionization are deeper in the magnetosphere and more immune to effects of the solar wind. That can be said another way: auroral activity results from sub-storms which are initiated by the solar wind when the magnetic field it brings to the front of the magnetosphere points south.

On the other hand, disturbances reaching lower latitudes 104 result from major geomagnetic storms which are triggered by shock waves in the solar wind. Then, instead of starting gradually, the storm begins with a sudden impulsive change or commencement in the earth's horizontal field, typically a positive increase in the horizontal component, seen around the world and lasting for five minutes or so.

When that happens, particles in the Van Allen radiation belts are precipitated (Brown et al, 1961) into the atmosphere in a ring-like pattern. That is brief and not really noted by low-band DXers but, in addition, the auroral zones move more toward the equator and signal skewing is observed from the inner edge of the auroral zone, now more at lower latitudes.

A good example of this is in the report by W0ZV (Tippett, 1991) in connection with a contact with SM6CPY in 1988. On that occasion the Ap-index was 103 and at the time of the contact the Kp index was 5+, shortly to reach 7+. For W0ZV, signals from Sweden were skewed to 110 degrees, instead of the usual bearing toward 30 degrees, and for SM6CPY, signals from USA were coming from the direction of South America. Clearly, the Swedish station was then located inside the polar cap, not on the equatorward edge of the auroral zone, and reflections instead of refraction were taking place there.

Conclusion -

First thoughts -

On reviewing the preceding chapters, it'd almost seem that a case has been made, not for a "Guide to Low-Band Propagation" but just the opposite, for the "mob scene" scenario mentioned in the Preface. Thus, when one's operating frequency goes below the critical frequency for the ionosphere overhead, the "Guide" for HF DXing offered by MUFs and all that goes with them are lost and low-band operations are cast adrift in the dark sea of noise, with little else to guide the way. That is a very pessimistic view, one not shared at this QTH as progress is being made in our understanding of what lies behind propagation, even on low-bands where the physics is far more complex. Let me give some recent examples, starting with my Australian friends, VK6VZ and VK6HD.

With their help, long-path on 1.8 MHz means a lot more than before 2001 and their logs provided the data that revealed something new and different (Ireland et al, 2002), equinoctial and diurnal path-switching. So we are still learning new things about low-band propagation, even at this late date. But better tools help. In that regard, when I found path-switching in their logs, I kidded Steve that he and Mike had been "flying blind", using sunrise/sunset tables and not enjoying the benefits of a good mapping utility. I put them in touch with Peter Oldfield and he fixed them up with copies of DXAID. Now they're much happier, seeing the DX Universe before them more clearly.

But that wasn't the first time I got help from "Down Under". Just recently, on Tuesday, March 5, 2002 I celebrated the 40th anniversary of one of the most exciting days in my scientific career, March 5, 1962. On that day my research group was on Macquarie Island (VK0), busy flying high altitude balloons carrying radiation detectors. At the same time, the research group of my colleague, Prof. Kinsey Anderson of UC Berkeley, was in Alaska (KL7) doing the same thing. Our hope was to observe simultaneous electron bombardment (Anderson et al, 1963) in the auroral regions of both hemispheres.

In spite of terrible weather conditions on the ground, our balloons got off without incident and promptly ran into a huge auroral event at both locations, different ends of the magnetic lines of force that went up from Macquarie Island, crossed the equatorial plane at about 5.2 earth radii and went down to Alaska. While the radiation effects we observed were exciting to us, allowing us to lay one plot of auroral Xray fluxes right on top of the other and see close agreement in the two hemispheres, there were

other exciting features of the event too.

In that regard, the observations of the event by riometers at both Macquarie Island and Kotzebue, Alaska, shown in **Figure 92**, 106 are meaningful to low-band DXers too:

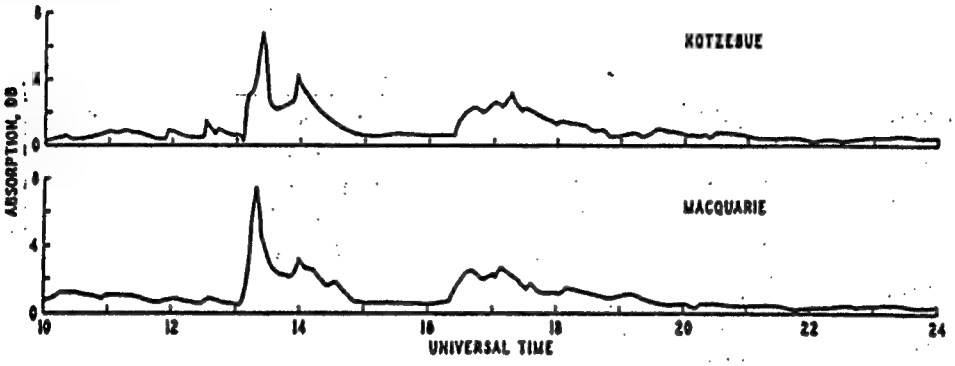

Figure 92 - Absorption records of riometers located at conjugate points in the geomagnetic field.

The riometer records show the low-band DXer that auroral radiation effects which bear on propagation across high latitudes actually originate in a source at the equatorial region, far out in the magnetosphere, and the auroral electrons come roaring down field lines in both directions, as in **Figure 93:**

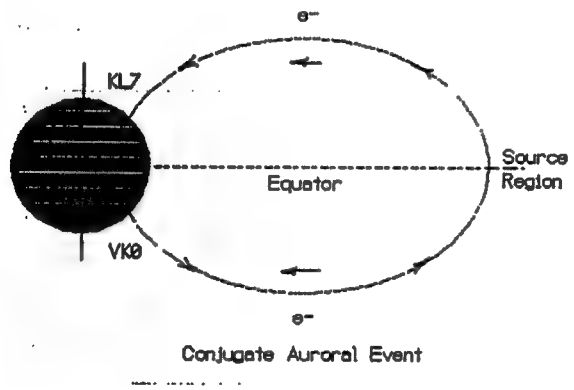

Figure 93 - Diagram showing a line of force going S to N and with an electron source region sending particles down into the atmosphere at conjugate points.

That was "news" 40 years ago and still news to some people even now.

But my Canadian friends, VE3OSZ and VE7DXR, provided some

"news" for low-band DXers just a couple months ago. Thus, while monitoring some 3.3 MHz signals from South Africa, they observed (Kavanagh et al, 2002) simultaneous enhancements of signals at Ottawa, ON and Victoria, BC, at distances of 13,200 km and 16,500 km, respectively, as in **Figure 94:**

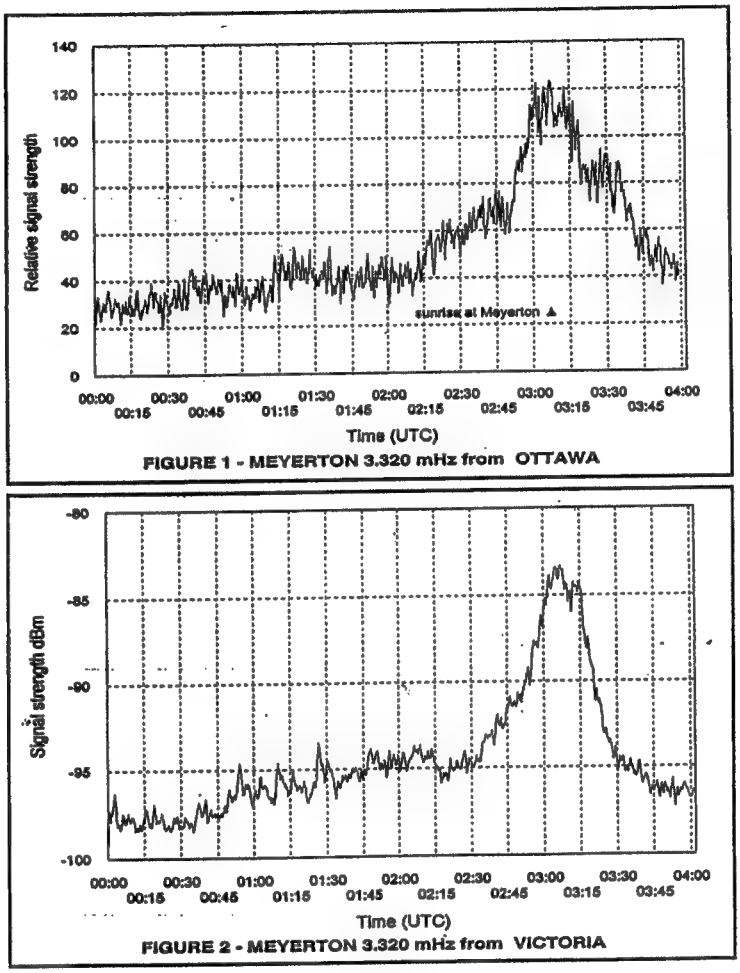

Figure 94 - Simultaneous signal enhancements observed at both Ottawa and Victoria, Canada.

Propagation conditions were such that 3.3 MHz signals were enhanced at dawn in the source region near the transmitter in Africa and propagated outward from there. That's the only way the simultaneity of observatiops could be realized at separate locations some 3,300 km apart.

There is another type of dawn enhancement of magneto-ionic origin (Hall-Patch, 1999) rather than ionospheric origin, as was the case with the ZS signals. Those other enhancements occur at dawn for a receiving site and there is no simultaneity involved. They are

due to ducted signals being brought back to ground by the downward tilt of the ionosphere at dawn and can serve to propagate signals efficiently over great distances without any intermediate ground losses.

Last thoughts -

So new results are still coming forth as far as low-band propagation is concerned. As I have suggested, the meteorological aspects of low-band propagation remain to be untangled but there seems little doubt they are there.

But what are the best ways to look for the new effects? The use of high-profile DXpeditions is one way; that certainly paid dividends in the case of VK0IR. The logs were a treasure trove, no doubt about it, sampling propagation in every direction. Another way involves beacons, either using broadcast stations in that way as VE3OSZ and VE7DXR have done or setting up some sort of low-band beacon network.

In that regard, there were a lot of "folk tales" in the early days of radio about hearing broadcast stations from afar during unusual weather conditions, particularly in the Arctic. Those stories cannot be disregarded and should be looked into again, now with better radio and meteorological recording systems.

But if you need any more encouragement, let me suggest you read the ARRL publication, "200 Meters and Down", by Clinton B. DeSoto, particularly the sections about the early days of Amateur Radio. It tells how Amateur Radio rushed past the low-bands into the VHF region and from CW to AM, leaving propagation studies in the lurch for decades.

But now DXers are back operating just below 200 meters and getting excited when there's good propagation into Europe on the low-bands, like in the old days. But they share the joy by using the Top Band Reflector instead of swapping telegrams. And while the G's were contacting "the Antipodes" with low power and very rudimentary gear in those days, we're trying to do it now with full legal power and 4-square antenna systems.

But after about 75 years, we still have not "figured it out". At best, we do know that low magnetic and auroral activity, found on days with low K-indices, is an aid to trans-polar propagation. But those indices don't help when it comes to trans-continental propagation; for the life of us, we cannot tell whether there will be good propagation or not on any given day. And it seems trans-equatorial propagation goes on, summer and winter, oblivious of what

the solar wind is doing.

But there are tantalizing hints, like low-band propagation being more favorable for DXing at solar minimum than at maximum. Since the 10.7 cm solar flux is a better index for solar control below the F-region peak than the sunspot number R (Bilitza, 2001) and HF DX propagation correlates better with HIGH values of the flux, perhaps anti-correlation with the 10.7 cm flux and LOW values are better for low-band DXing. So it would seem we would do well by returning to our "SWL roots", listening more for DX and seeing which factors correlate or anti-correlate with better propagation on low-bands and which do not.

In a sense, that is the practical side of low-band Dxing but that depends on having "observables", quantities that relate to the region where low-band signals propagate. Those are in short supply, as I indicated earlier (Brown, 2001) about the unpredictable aspects of 160 meter propagation. But there are theoretical aspects as well and a greater understanding of those would help. In saying that, I am really getting down to the question of what is the ideal mode to hope for when getting on the low-bands and chasing DX; is it the conventional earth-ionosphere hops, only ducted hops or an optimal combination of both?

There's not a lot to say about earth-ionosphere hops. They're what "come naturally" and should be quite reliable, aside from problems with man-made noise, if the ionosphere along the path is calm and level. But calm and level may not be all that easy to realize nor to think it can be expected to last for long periods of time. Ionization can be in motion - either raising, lowering or tilting the ionospheric layers - but it will not disappear entirely by recombination during the hours of darkness as long as it stays in the region where created or in regions where weak night-time sources are operating. So calm, level and "full ionization" should give ideal, normal propagation. But skewing could occur if the layers are tilted and signal loss could occur.

As for ducted hops, any type of wave motion can show ducting - electromagnetic, sound, water waves, you name it. On the low-bands, ducted signals are largely of magneto-ionic origin. While the ducted mode is not readily detectable, at least without antennas which are sensitive to changes in signal polarization, its presence becomes rather apparent on very long contacts where losses would be a problem for earth-ionosphere hops, say more than 15,000 km.

Realization of the presence of a ducted mode would depend on having some experience with a propagation that is sensitive to the earth's field, like PropLab Pro. That program can use either the

CCIR or URSI reference ionospheres and represent average ionospheric conditions, the best one can expect from a ionospheric database. In that regard, the user should note the fact that radiation angles for the ducted mode are many-valued, in contrast to the single value for ionospheric ducting (Kavanagh et al, 2002) at the angle for Pederden Rays. In addition, the user should note that both quasi-longitudinal and quasi-transverse modes may occur, making the magnetic dip angle (IGRF, 1996) at both transmitter and receiver variables of interest.

Given the above discussion, one can see that long-haul DXing may be the wave of the future, at least for our theoretical understanding. That should be music to the ears of low-band DXers, another reason for hitting the bands harder. So log the indices, both magnetic and solar flux, note the magnetic dip for any long-haul contacts, keep good records and compare notes with other interested parties; sooner or later, something will give and another page will be turned, marking more progress in untangling the "Mystery of Low-Band Radio".

References

Anderson, K.A., C.D. Anger, R.R. Brown and D.S. Evans, Simultaneous Electron Precipitation in the Northern and Southern Auroral Zones, J, Geophys. Res. Vol. 68, No. 9, 1963.

Bhavsar, P.D., Gamma rays from the solar-cosmic-ray produced nuclear reactions in the earth's atmosphere and the lower limit of the energy of solar protons observed at Minneapolis, J. Geophys. Res. 67, p. 2627, 1962.

Bilitza, D., International Reference Ionosphere, Goddard Space Flight Center, NASA, 2001.

Brekke, A., Physics of the Upper Polar Atmosphere, Wiley-Praxis Series on Atmospheric Physics, 1997.

Brown, R.R., The Superposition of Cosmic-Ray Effects on February 23, 1956, J. Geophys. Res., Vol. 62, No. 1, 1957.

Brown, R.R., T.R. Hartz, B. Landmark, H. Leinbach and J. Ortner, Large-Scale Electron Bombardment of the Atmosphere at the Sudden Commencement of a Geomagnetic Storm, J. Geophys. Res., Vol. 66, No. 4, 1961.

Brown, R.R., On the relationship between polar-glow aurora and solar cosmic ray fluxes, J. Atm. Terr. Phys., Vol. 26, p. 805, 1964

Brown, R.R., Long-Path Propagation, private publication, 1992.

Brown, R.R., Demography, DXpeditions and Magneto-Ionic Theory, p. 44, The DX Magazine, March/April 1998.

Brown, R.R., Signal Ducting on the 160 Meter Band, p. 65, Communications Quarterly, Spring 1998.

Brown, R.R., Negative Ion Basics, Low Band Monitor, February 1999.

Brown, R.R., Power Coupling on 160 Meters, Communications Quarterly, p. 95, Spring 1999.

Brown, R.R., On the South-Southwest Path and 160 Meter Propagation, QEX, December, 2000.

Brown, R.R., On the Plasma Sheet of the Magnetosphere and Low-Band DXing, The Low Band Monitor, January 2000.

Brown, R. R., Long-Path Propagation: Revisited in Year 2000, private publication, 2000.

Brown, R.R., Crossing the Polar Cap on 160 Meters, The Low Band Monitor, June, 2001.

Brown, R. R., Equinoctial Path-Switching on 160 Meters, CQ Magazine, February and March issues, 2002.

Campbell, W.H., Introduction to Geomagnetic Fields, Cambridge University Press, 1997.

Davies, K., Ionospheric Radio, Peter Perigrinus Ltd, London, 1990.

Hall-Patch, N., Some thoughts on sunrise enhancements of MF Trans-Pacific signals, Low-Band Monitor, November, 1999.

Hargreaves, J. K., The Solar-Terrestrial Environment, Cambridge University Press, 1992.

IGRF, International Geomagnetic Reference Field, Utility Programs for Geomagnetic Fields, National Geophysical Data Center, Boulder, CO. 1995.

International Reference Ionosphere (IRI 90), D. Biilitza, Editor, National Space Data Center, Greenbelt, MD, 1990.

Ireland, Steve, Go Surf the Grey and Dark Lines, CQ Magazine, March 2001.

Kavanagh, R., N. Hall-Patch and R. R. Brown, Dawn Enhancement of Signals from South Africa, Low-Band Monitor, Jan. 2002.

Kelley, M. C., The Earth's Ionosphere, Academic Press, 1989.

Luetzelschwab, R.C., An Investigation into Propagation Modes and Absorption on 160 m., Appendix in Long-Path Propagation: Revisited in Year 2000, by R.R. Brown, private publication.

Oler, C., PropLab Pro, A High Frequency Radio Propagation Laboratory, Solar Terrestrial Dispatch, Canada, 1994.

Philips, G.J. and P. Knight, Effects of polarization on medium frequency sky-wave service, Proc. I.E.E., Vol. 112, Jan. 1965

Reid, G.C., Ion chemistry in the D region, Advances in Atomic and Molecuilaar Physics, Vol. 12, p. 375, 1976.

Rodriguez, J.V., and U.S. Inan, Electron density changes in the night-time D-region dueto heating by very-low-frequency transmitters, Geophys. Res. Lett., 21, 93-96, 1994.

Rosenberg, T.J., D.L. Detrick, D. Venkatesan and G. Van Bavel, A Comparative Study of Imaging and Broad-Beam Riometer Measurements: The Effect of Spatial Structure on the Frequency Dependence of Auroral Absorption, J. Geophys. Res. Vol. 96, No. A10, p. 17,793, Oct. 1991.

Taylor, K., Earth's Grand Light Show, National Geographic, p. 48, Nov. 2001.

Terman, F.E., Radio Engineer's Handbook, McGraw-Hill, 1943.

Tippett, B., Long Path and Skewed Path Propagation on the lower Frequencies, Proceedings of Fine Tuning, 1991.